Università degli Studi di Siena

Genetics, Oncology and Clinical Medicine

XXXIII Cycle

Identifying antagonist drugs for TRPM8 ion channel as candidates for repurposing

By

Farhad Jahanfar

PhD candidate

Tutor: Professor A. Arcangeli

October 2021

Outline

List of figures ..... **V**

List of tables ..... **VIII**

List of abbreviations ..... **IX**

Abstract **1**

Introduction **3**

1.1 Ion channels as target **4**

1.1.1 TRP ion channels as promising targets **6**

1.1.2 TRPM8 ..... **8**

1.1.3 Physiological functions of TRPM8 ..... **9**

1.1.4 Modifications and modulations of TRPM8 ..... **11**

1.1.5 Structure of TRPM8 ..... **13**

1.1.6 Channelopathies of TRPM8 ..... **14**

1.1.7 TRPM8 -Disease association network **17**

1.1.8 TRPM8 agonists **20**

1.1.9 TRPM8 antagonists **20**

1.2 Drug discovery **22**

1.2.1 Drug repurposing **23**

1.2.2 Drug repurposing vs rare diseases **24**

1.2.3 Repurposing drug based on polypharmacology 26

1.2.4 Virtual screening for efficient screening 31

1.2.5 Automated vs manual electrophysiology 32

1.2.6 Automated electrophysiology with IonFlux 16 34

Material and Methods 37

2.1 Operating IonFlux 16 Platform 38

2.1.1 Experiment Setup 39

2.1.2 Procedure of experiment 45

2.1.3 Recording protocols and analysis of results 46

2.2 Virtual screening 50

2.3 Cell culture for WST-1 assay 51

2.4 WST-1 assay 51

2.5 Manual Patch-clamp experiments 51

2.6 Western blot 52

2.7 Chemicals 53

2.8 Molecular docking study 53

2.8.1 Autodock vina 53

2.8.2 SwissDock 54

2.8.3 Analyzing and visualizing docking results 54

2.9 Data analysis 55

Results 57

3.1 Evaluating TRPM8 via IonFlux 16 ..... **58**

3.2 Screening sodium channel blockers **63**

3.3 Virtual screening **66**

3.4 Screening beta blockers **70**

3. 5 Manual patch clamp electrophysiology **73**

3.6 Western blot **75**

3.7 WST-1 Cell Cytotoxicity Assay **76**

3.8 Molecular docking **78**

3.8.1 Autodock vina **78**

3.8.2 SwissDock **82**

Discussion **86**

4.1 Automated patch clamp vs manual patch clamp **87**

4.2 Impact of virtual screening **89**

4.3 Identified drugs **90**

4.3.1 Nebivolol **90**

4.3.2 Carvedilol **90**

4.3.3 Propafenone **91**

4.3.4 Propranolol **91**

4.4 Possible mechanism for blocking effect **92**

4.4.1 Direct binding to antagonist binding site **92**

4.4.2 Drug membrane interactions **93**

4.5 Effect of drugs on cells viability **96**

Conclusion **100**

Acknowledgment **101**

Research integrity **102**

References **103**

List of figures

Figure 1. The physiological functions of TRPM8 ion channel **10**

Figure 2. Network representation of the Gene-Disease associations **19**

Figure 3. Menthol, rotundifolone, and eucalyptol are natural **21**

Figure 4. A representation of differences between traditional **24**

Figure 5. The drug-target networks for carbamazepine **28**

Figure 6. Ionflux 16 uses specific plates. A) microfluidic **35**

Figure 7. Overview of 96-well Plate used for IonFlux **40**

Figure 8. Prime window in IonFlux software first phase **47**

Figure 9. The overview of negative and positive pressure **48**

Figure 10. Break protocol: increasing pulses from 4 to 11 Hg **49**

Figure 11. program for compound addition in data acquisition **49**

Figure 12. Voltage command for outward current of TRPM8 ..... **50**

Figure 13. The outward current elicited by activating **58**

Figure 14. Concentration response curve for menthol **59**

Figure 15. High stability of TRPM8 currents activated **60**

Figure 16. Steady activation of TRPM8 by 300 μM menthol **60**

Figure 17. Time and concentration dependence inhibition **61**

Figure 18. Currents elicited by a voltage ramp protocol **62**

Figure 19. Concentration–response relationship for AMTB **62**

Figure 20. Raw data of current traces recorded **63**

Figure 21. 75 µM phenytoin only had around 38% **64**

Figure 22. TRPM8 currents evoked by applying 300 µM **64**

Figure 23. Outward and inward TRPM8 currents in stable **65**

Figure 24. concentration–response curve relationship for **65**

Figure 25. Submission page, the query molecule could **66**

Figure 26. Example of an output page obtained **67**

Figure 27. Selected drugs from beta blockers to screen **69**

Figure 28. Concentration–response curve for propranolol **70**

Figure 29. Concentration–response curve for carvedilol **71**

Figure 30. Concentration–response curve relationship **71**

Figure 31. Time and concentration dependence inhibition **72**

Figure 32. Concentration–response curve for Menthol **73**

Figure 33. Concentration–response curve for nebivolol **74**

Figure 34. Effect of 300 µM menthol on outward 74

Figure 35. TRPM8 expression in pancreatic cancer **75**

Figure 36. Concentration and time dependent changes in viability **76**

Figure 37. Concentration and time dependent changes in viability **77**

Figure 38. A) Structure of TRPM8, black circle shows **79**

Figure 39. A) 2D depiction of the intermolecular interactions for **80**

Figure 40. 2D depiction of the intermolecular interactions for **81**

Figure 41. Docking results from SwissDock **83**

Figure 42. Docking results from SwissDock for propafenone **84**

Figure 43. Membrane proteins like ion channels require **94**

Figure 44. The drug-target networks for carvedilol **98**

List of tables

Table 1. List of drugs and their properties **29**

Table 2. Part of virtual screening outputs for different **68**

Table 3. Comparing docking results from two methods **92**

List of abbreviations:

PDAC:	Pancreatic Ductal Adenocarcinoma Cell
GPCR:	G-Protein Coupled Receptors
TRP:	Transient Receptor Potential
TRPM8:	Transient Receptor Potential Melastatin 8
TRPA:	Transient Receptor Potential Ankyrin
TRPV:	Transient Receptor Potential Vanilloid
TRPC:	Transient Receptor Potential Canonical
TRPML:	Transient Receptor Potential Mucolipin
TRPP:	Transient Receptor Potential Polycystin
TRPM:	Transient Receptor Potential Melastatin
CGRP:	Calcitonin gene-related peptide
IL:	Interleukin
SLN:	Superior laryngeal nerve
OPRM1:	Opioid Receptor Mu 1 ()
PIRT:	Phosphoinositide-Binding Protein
5-HT_{1B}:	5-hydroxytryptamine 1B
PIP_2:	Phospholipid phosphatidylinositol 4,5-bisphosphate
LPL:	Lysophospholipids

List of abbreviations

PLA_2:	Phospholipase A_2
NADA:	N-arachidonoyl dopamine
FDA:	Food and Drug Administration ()
HTS:	High-throughput screening
SOSA:	Selective Optimization of Side Activities
DRG:	Dorsal root ganglia
CHO - SFM II medium:	Serum free medium for suspension CHO cells
DMEM:	Dulbecco's modified Eagle medium or
FBS:	Fetal Bovine Serum
PBS:	Phosphate Buffered Saline

Abstract

Even though it is confirmed that ion channels are at the centre of many diseases, approved drugs are only available for small percentage of these proteins, and yet many pathologically important ion channels like transient receptor potential (TRP) cation channels remain without approved drugs. One reason could be the time-consuming and expensive process in drug discovery. Which has high possibility of failure in any step even after approval and marketing. Therefore, repurposing approved drugs might be considered as a solution and may offer an accelerated procedure in finding new treatments for patients.

For the present research we selected TRPM8 ion channel as a neglected target despite growing number of studies regarding its association with numerous diseases. In this project we have first identified potent antagonists for TRPM8 ion channel among approved drugs, by using mainly the automated patch clamp device IonFlux 16. Such device allowed us to screen blocking potency of drugs against TRPM8 ion channel in time efficient way. Our approach consisted of using ligand-based virtual screening method, to optimize our screening by identifying candidates for further screening. We also studied possible interactions of identified drugs with antagonist binding site on TRPM8 channel by molecular docking. Furthermore, we have evaluated the effects of identified antagonists against different types of pancreatic ductal adenocarcinoma (PDAC) cells.

We were able to identify four drugs with IC_{50} lower than 50 µM including propranolol, propafenone, carvedilol and nebivolol. Among them nebivolol with IC_{50} = 0.97± 0.15 µM and carvedilol with IC_{50} = 9.1 ± 0.6 µM were the most potent blockers. Studying the interactions of identified drugs with known binding site of TRPM8 by molecular docking, revealed high possibility of direct binding of nebivolol to binding site of TRPM8. Nebivolol

was the most cytotoxic drug against PDACs, but it was also toxic against non-cancerous HEK-293 cells. While carvedilol had cytotoxic against PDACs, interestingly it wasn't cytotoxic against HEK-293 cells.

Result of these study will provide promising candidates for drug repurposing and will propose promising lead compound in drug discovery for new antagonists of TRPM8 ion channel. Also, our method of approach for identifying candidate drugs as agonist or antagonist could be applied for other ion channels.

Introduction

1.1 Ion channels as target

Ion channels are proteins located at cellular membrane, they act as pathway for the movement of ions across the membrane. In human genome more than 400 genes encode ion channel proteins(Camerino, Tricarico, and Desaphy 2007). They are involved in almost any biological process. Accordingly, they are valuable targets and important off targets in drug discovery.

In fact, next to G-Protein Coupled Receptors (GPCR), ion channels are the most common drug targets. Studies show increasing number of diseases associated with different types of ion channels. These kind of disorders that related to dysfunctions of ion channels are classified as channelopathies, dysfunction might arise from ion channel subunits or the proteins that regulate the ion channels(Kaczorowski et al. 2008).

Channelopathies of the cardiovascular system (e.g., Brugada syndrome, long QT and short QT syndrome, and catecholaminergic polymorphic ventricular tachycardia), could turn to chronic condition or it could cause sudden death (Fernández-Falgueras et al. 2017). Cardiovascular channelopathies are responsible for almost half of fatalities caused by sudden arrhythmic death syndrome(Behr et al. 2008). Several Mutations have been identified in association with different of cardiac arrhythmic disorders on calcium, potassium, sodium, and TRP ion channels genes, and numerous polymorphisms related to ion channels have been considered to be risk factors (Abriel and Zaklyazminskaya 2013).

Introduction

Ion channels are essential part of neuronal signalling, growing number of studies demonstrate association of nervous system disorders with ion channels, for instance channelopathies such as neuropathic pain, episodic ataxia, generalized epilepsy with febrile seizures plus, hypokalemic and hyperkalemic periodic paralysis, familial hemiplegic migraine (Kullmann 2010).

Other identified channelopathies affects the respiratory system (cystic fibrosis (Planells-Cases and Jentsch 2009)), the immune system (myasthenia gravis, neuromyelitis optica, Isaac syndrome, and anti-NMDA [N-methyl-D-aspartate] receptor encephalitis (Vaeth and Feske 2018)), the urinary system (bartter syndrome, nephrogenic diabetes insipidus, autosomal-dominant polycystic kidney disease, and hypomagnesemia with secondary hypocalcaemia (Kim 2014)), the endocrine system (neonatal diabetes mellitus, familial hyperinsulinemic hypoglycaemia, thyrotoxic hypokalemic periodic paralysis, and familial hyperaldosteronism(Rolim et al. 2010)).

Although diseases such as various types of cancer not yet been considered as channelopathy, but growing number of evidences indicate association of mutations, aberrant expression, malfunction of ion channels and transporters with well-known cancer hallmarks such as independence in growth signals, insensitivity to antigrowth signals, limitless replicative potential, evasion of programmed cell death (apoptosis), continuous angiogenesis, tissue invasion and metastasis(Prevarskaya, Skryma, and Shuba 2010).

Proliferative cells need to constantly polarize and depolarize the membrane potential during cell cycle progression, such changes demand participation of different ion channels. Studies indicate that potassium channels play a critical role in the initial steps of the cell cycle and controlling cell volume during cell proliferation(Wang 2004). Also, potassium channels can regulate the phenotypic transition of cells from an epithelial to a mesenchymal state, this

transition leads to enhanced invasive and migratory abilities(Restrepo-Angulo, Sanchez-Torres, and Camacho 2011). It appears the expression of voltage-gated sodium channels accelerates migration, invasion, and metastasis through enhancing depolarization with the following more swift and stronger activation of potassium channels. For instance, expression of Nav1.5α subunit is linked with poor prognosis of breast cancer(Brackenbury 2012).

Cytosolic level of Ca^{2+} is vital for regulating cell cycle, mostly in controlling S and M phases(J. T. Taylor et al. 2008). Ion channels associated with alteration Ca^{2+} signalling in cancer cells comprise Ca^{2+}-permeable cation channels of the melastatin, vanilloid and canonical families of transient receptor potential channels(Venkatachalam and Montell 2007). However, lasting increase in cytosolic Ca^{2+} may result in apoptosis, but Ca^{2+} entry via TRP channels may prevent apoptosis this might be resulted due to the stimulation of NF-κB(Thippegowda et al. 2010). TRPC1 is essential for cytokinesis during proliferation and migration in glioma cells(Cuddapah, Turner, and Sontheimer 2013). TRPM8 activates calcium sensitive potassium channels (KCa1.1) through Ca^{2+} influx, which contribute with migration(Wondergem et al. 2008).

1.1.1 TRP ion channels as promising targets

Even though it is confirmed that ion channels are at the centre of many diseases, approved drugs are only for a small percentage of this proteins, and yet many pathologically important ion channels like transient receptor potential (TRP) cation channels remain without approved drugs(Kaczorowski et al. 2008). In mammalian genome there is six different subgroups of TRP channels based on their sequence homology: TRP ankyrin (TRPA), vanilloid (TRPV), canonical (TRPC), mucolipin (TRPML), polycystin (TRPP), and melastatin (TRPM). In

addition to their role in regular physiological processes such as signal transmission, TRP channels are known to act as cellular sensors by involving in nociception, thermosensation, taste perception, mechanosensory and osmolarity sensing. TRP channels help cells in detecting and responding to changes in the cellular environment, like temperature, chemicals, stretch/pressure, osmolarity, oxidation/reduction and pH in both acidic and basic range(Venkatachalam and Montell 2007).

TRP channels are also receptor for some natural products, which some has therapeutic potential. For instance, capsaicin an active component of chili peppers activates and subsequently desensitize TRPV1, it is used to treat minor aches and pains of the muscles and joints, or menthol as main compound of peppermint oil is a prototypical TRPM8 agonist which is used to treat minor sore throat pain, or mouth irritation caused by a canker sore(Vetter and Lewis 2011).

Mutations in genes encoding TRP channels are the cause of numerous inherited diseases (TRP channelopathies) that affect the cardiovascular, renal, nervous and skeletal systems(Nilius and Owsianik 2010). Nociceptive neurons were the early focus of research on TRP channels. There are some potent, small-molecule antagonists for TRPV3, TRPV1, and TRPA1 that are already in clinical trials as new analgesic compounds. However, in 2008, clinical trials of AMG-517, a highly selective TRPV1 antagonist was cancelled due to the occurrence of hyperthermia(Gavva et al. 2008) .

Not surprisingly, dysfunction of these channels was reported in several disease ranging from chronic pain and overactive bladder (TRPV1 and TRPM8), through obesity (TRPV4 and TRPM5), diabetes (TRPV1, TRPM4), chronic cough and asthma (TRPA1, TRPM8, TRPV1), neuropathic pain (TRPV1, TRPA1, TRPM8), chronic obstructive pulmonary disease (TRPM8 and TRPV4), cardiac hypertrophy (TRPC6), familial Alzheimer's disease (TRPM7),

dermatological disorders (TRPV3) and cancer (TRPC6, TRPV2 and TRPM8)(Kaneko and Szallasi 2014).

Both gain of function and loss of function mutations in genes encoding TRP channels have been linked to diseases, for example gain of function mutation in TRPA1 ion channel was reported in familial episodic pain syndrome(Kremeyer et al. 2010), and loss of function mutation of TRPML1 associated with type-IV mucolipidosis(Dong et al. 2008). TRP ion channels became interesting targets in disease areas such as cancer(Prevarskaya, Zhang, and Barritt 2007), respiratory disorders(Grace et al. 2014), psychiatric disorders(Chahl 2011), migraine(Benemei et al. 2013), cardiovascular(Inoue et al. 2006) and as well as metabolic disorders and obesity(Tabur et al. 2015).

1.1.2 TRPM8

Transient Receptor Potential Melastatin 8 (TRPM8) is from the melastatin TRP channel subfamily, initially it was identified in the prostate and testis tissue. In human TRPM8 gene is located on region 2q37.1 of chromosome 2 translates to a 1,104 amino acid protein(Tsavaler et al. 2001). localization of TRPM8 is not only in the plasma membrane, but it also found in the endoplasmic reticulum(Valero et al. 2011). TRPM8 channel is non-selective Ca^{2+}-permeable channels with permeability ratio $P_{Ca}{}^{2+}/P_{Na}{}^{+}$~3, which is known as sensor for cold temperatures. It has multimodal gating which can get activated by cold temprature (<28 °C), depolarization, cooling compounds like menthol and icilin, and changes in osmolality(McKemy, Neuhausser, and Julius 2002).

TRPM8 channels are essential for thermoregulation, responding to innocuous cool and wetness, cold hypersensitivity, noxious cold, and cooling-mediated analgesia. Both menthol

and low temperature increase probability of the open form of TRPM8, and both have synergistic effect on the activation of TRPM8(Knowlton et al. 2011). TRPM8 was initially detected in the testis and prostate tissue(Tsavaler et al. 2001), and it has high expression in a subpopulation of primary sensory neurons located within the dorsal root ganglia (DRG) and trigeminal (McKemy, Neuhausser, and Julius 2002), it is also detected in other tissues like vascular smooth muscle, lung, uterus, placenta, skin, eye, liver, the bladder urothelium and male urogenital tract(Stein et al. 2004).

1.1.3 Physiological functions of TRPM8

The wide pattern of TRPM8 expression suggests the broad physiological functions this channel has (Fig. 1). Beside cold perception, TRPM8 acts as a metabolic sensor to control serum insulin(McCoy et al. 2013), and a crucial sensor to induce thermoregulation. Activation of TRPM8 induces thermogenesis without effect on heat diffusion(Masamoto, Kawabata, and Fushiki 2009). TRPM8 is also part of the mechanical pain perception in the mouse colon, but it is restricted to signals of highly noxious pressure. Unlike from TRPV4-/- and TRPA1-/- mice, TRPM8 null mice displayed the different decrease of colonic calcitonin gene-related peptide (CGRP) release induced by distension at only 150 mmHg(Mueller-Tribbensee et al. 2015).

TRPM8 channels in the genitourinary system, participate in bladder contraction and bladder mechano-sensation. Vesical administration of icilin and menthol as TRPM8 agonists, improved contractions of the isolated whole pig bladder induced by carbachol(Vahabi et al. 2013). In normal bladder, activation of the afferent pathway is accompanying with the TRPM8 channels, and least partially mechanosensitive C-fibres mediate this effect(Ito et al.

2016). TRPM8 also has an essential role in prostate, like controlling cell proliferation, apoptosis, and secretion of ion and protein from prostate epithelial cells(L. Zhang and Barritt 2004). Furthermore, TRPM8 activation initiates the reaction of acrosome in sperm(De Blas et al. 2009).

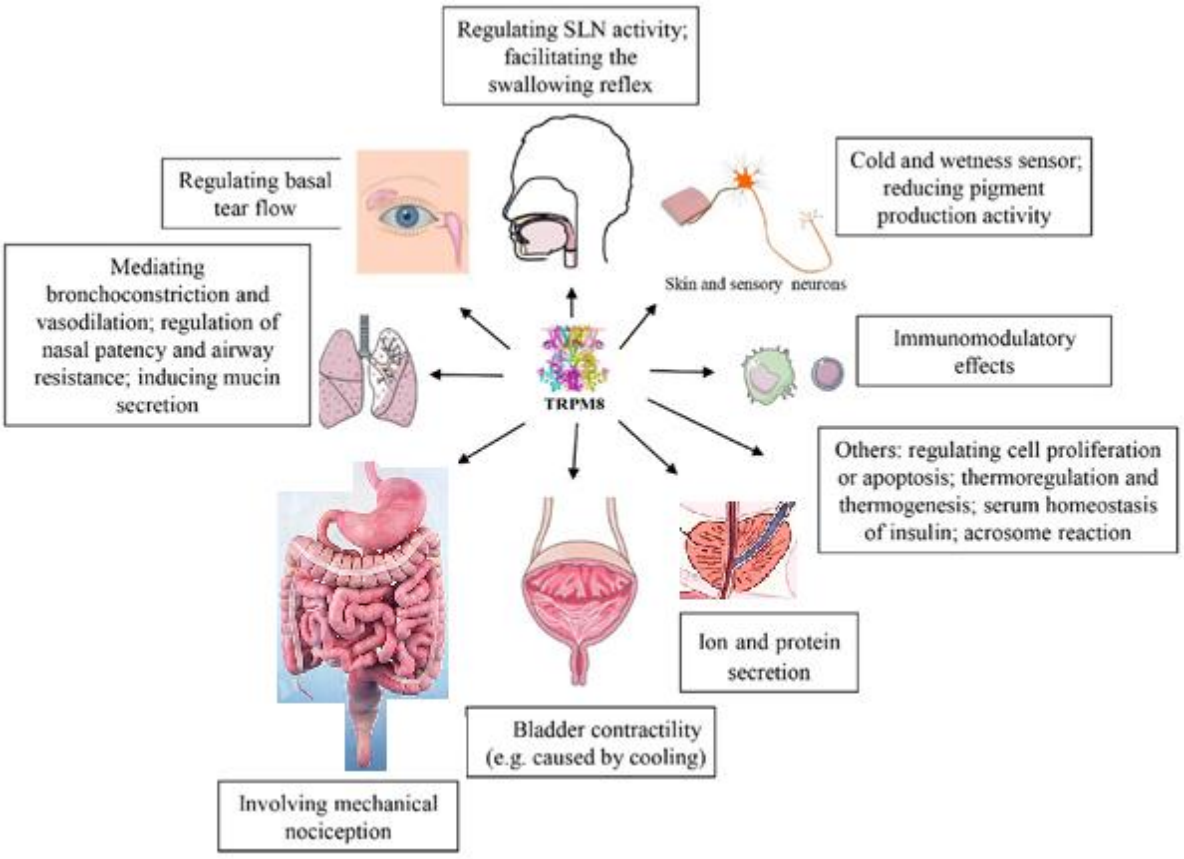

Figure 1. The physiological functions of TRPM8 ion channel.

Cold activates respiratory responses in the TRPM8-dependent mechanism, by cough, airway contraction and mucosal secretion(Li et al. 2011) . TRPM8 also act in modulation of the immune response. TRPM8 null murine peritoneal macrophages showed defective phagocytosis. TRPM8 in macrophages determined as both anti- and pro-inflammatory by regulating the production of interleukin (IL)-10 and TNF-α, respectively(Khalil et al. 2016). Additionally, blocking TRPM8 suppresses T-cell activation in murine. The TRPM8 channel antagonist AMTB decreased the production of IL-6 and IL-2 as well as increasing expression of CD25 in activated T cells(Khalil et al. 2016). TRPM8 maintain the basal tear flow(Parra et al. 2010). Activity of TRPM8 in the larynx and related laryngopharyngeal regions controls the superior laryngeal nerve (SLN) activity and helps in swallowing reflexes(Hossain et al. 2018). Also, TRPM8 is contributes in inhibition of pigmentation by reducing the expression of tyrosinase as well as tyrosinase-related protein-1(Guo, Carlson, and Slominski 2012).

1.1.4 Modifications and modulations of TRPM8

Posttranslational modifications of TRPM8 channels affect their function. the *N*-glycosylation happens at residue Asn934 near the pore loop, lack of *N*-glycosylation cause reduction in sensitivity of channel to physical and chemical activators(Pertusa et al. 2012). In addition, glycosylation of TRPM8 could affect interactions of TRPM8 with lipid rafts, by facilitating segregation of TRPM8 into lipid rafts(Pertusa et al. 2012), (Morenilla-Palao et al. 2009). Another posttranslational modification is the complex formed by the polyester poly-(R)-3-hydroxybutyrate (PHB) with TRPM8 ion channel, this posttranslational modification by PHB is required for function of TRPM8(Cao et al. 2013).

Few proteins were identified to have direct interaction with TRPM8. Gαq subunit from G alpha subunits, has inhibitory effect on TRPM8 by forming complex with it(X. Zhang et al. 2012). Another protein is opioid Receptor Mu 1 (OPRM1), after morphine binds to OPRM1 it co internalize with TRPM8, also presence of TRPM8 is essential for Withdrawal syndrome caused by naloxone(Shapovalov et al. 2013). Phosphoinositide-Binding Protein (PIRT) as a membrane protein has specific expression in peripheral nervous system has shown to have positive regulatory effect on TRPV1, also enhances the sensitivity of TRPM8 to cool temperature and menthol(Tang et al. 2013). TRPM8 has reported to form complex with the 5-hydroxytryptamine 1B (5-HT_{1B}) receptor and enhances the analgesic effects for both TRPM8 and 5-HT_{1B} agonists(Vinuela-Fernandez et al. 2014).

Several pathways have been identified to modulate the function of TRPM8, by altering its sensitivity to different activators. However, no putative protein kinase C -phosphorylation sites were identified on the TRPM8 channel, but activation of protein kinase C inhibits TRPM8 activity(Premkumar et al. 2005). In addition, cAMP-dependent protein kinase A cause reduction in sensitivity of TRPM8 to menthol and icilin(De Petrocellis et al. 2007).

Phospholipid phosphatidylinositol 4,5-bisphosphate (PIP_2) is known as main regulator of TRPM8, it activates TRPM8 channel even without chemical and thermal stimulation and enhances sensitivity of TRPM8 to cold temperature and menthol (Sarria et al. 2011). The inhibitory effect of ethanol is known to be caused by weakening the interaction of PIP_2 with TRPM8(Benedikt et al. 2007). In addition, it is reported that PLC-mediated PIP_2 hydrolysis eliminates TRPM8 activity(Rohács et al. 2005).

Polyunsaturated fatty acids (PUFA) and Lysophospholipids (LPL) both are downstream products of phospholipase A_2 (PLA_2) activation(Bavencoffe et al. 2011). PUFA reduce the sensitivity of TRPM8 channel to the cold, menthol and icilin, but LPL activates TRPM8

channel. In general inhibition of PLA_2 cause suppression of TRPM8 function(Andersson, Nash, and Bevan 2007). Although phosphoinositide PIP_2 is a main regulator of TRPM8, growing number of studies have indicated the inhibitory role of testosterone in nanomolar concentrations on TRPM8 channels, which might explain gender differences in cold perception(Asuthkar et al. 2015).

Localization of TRPM8 into lipid rafts is another aspect of modulation for TRPM8 activity, which is due to its association with lipid raft by intramembrane lateral mobility(Veliz et al. 2010). For instance, reduction of cholesterol disrupts lipid rafts and produces a significant increase of TRPM8 responses to cold and menthol(Morenilla-Palao et al. 2009). Endocannabinoid like N-arachidonoyl dopamine (NADA) and endovanilloid anandamide inhibit TRPM8 activity(De Petrocellis et al. 2007). As well as plant-derived cannabinoids like cannabidiol acid, cannabidiol, Δ9-tetrahydrocannabinol, cannabigerol, and Δ9-tetrahydrocannabinol acid also can inhibit TRPM8 activity with sub micromolar IC_{50}(De Petrocellis et al. 2008).

1.1.5 Structure of TRPM8

The TRPM8 channel is a homotetramer protein, which means it is made of four identical subunits. Like other TRP channels, TRPM8 has six transmembrane spanning domains (S1–S6), which S5 and S6 are the pore-forming loop and S1-S4 act as act as the voltage sensor and has binding site for icilin, menthol and other similar agonists, also both –NH2 and –COOH ends are in intracellular. Until just recently, the knowledge about the structure of TRPM8 channels were came from experiments of mutagenesis and molecular modelling. The most significant finding from mutagenesis experiments was the identifying Y745, situated in

the middle of supposed transmembrane segment 2, as a critical residue for menthol binding and activation(Bandell et al. 2006).

The structure of TRPM8 in calcium-bound, ligand-free, and antagonist-bound forms were studied recently via cryo-electron microscopy. It was noticed both antagonists AMTB and TC-I 2014 share same binding site located at the lower half of the S1-S4 domain, close to the membrane-cytosol interface which is embedded at membrane. Same as agonists, the antagonists AMTB and TC-I 2014 bind in the S1-4 cavity. But instead, they prevent conformational changes required to open the channel and the stabilize TRPM8 in a resting-state-like, closed conformation. Both antagonists bind with different orientations, which is eased by complementary rearrangement of the side chains that form the cavity(Diver, Cheng, and Julius 2019).

1.1.6 Channelopathies of TRPM8

In the normal tissues with low expression of TRPM8, it has found to be highly enriched in the related tumours to those tissues. Study by Tsavaler and colleagues found that TRPM8 is noticeably upregulated in prostate cancer and other cancers(Tsavaler et al. 2001). several other reports also confirming increased expression of TRPM8 in prostate cancer and prostate cancer cell lines(Bidaux et al. 2005), (Valero et al. 2011). It is reported that mRNA of TRPM8 can be detected in men's body fluids, and they increase meaningfully in patients during metastatic stage, which could be considered as diagnostic method for distinguishing these two stages of disease(Bai et al. 2010).

In other malignancies like pancreatic cancer(Yee 2016), breast adenocarcinoma(Jinxin Liu et al. 2014), melanoma(Yamamura et al. 2008), the increased expression of TRPM8 was

noticed. Activation of TRPM8 channels by menthol in melanoma cells, cause sustained calcium influx and reduction in cell viability(Yamamura et al. 2008). But in neuroendocrine pancreatic tumour, activation of TRPM8 elevates neurotensin secretion or in human glioblastoma, TRPM8 has secondary effect on cell migration after changes in Ca^{2+}-activated potassium channels activity(Wondergem and Bartley 2009).

TRPM8 has been related to some health issues in the urogenital tract, like the overactive bladder syndrome and bladder pain syndrome, are also linked to TRPM8 via hypersensitive afferent input from the bladder wall. TRPM8 channels in hypersensitive afferent input originate from the bladder wall is thought to be involved in these conditions. In patients diagnosed with the overactive bladder syndrome, the expression of TRPM8 protein in bladder wall afferents was increased(Mukerji et al. 2006). AMTB, a selective TRPM8 antagonist, can reduce the occurrence of rat bladder contractions and the visceromotor reply to bladder expansion(Lashinger et al. 2008).

A decline in skin temperature from 34 to 2°C evokes cold pain in a monotonic increase, with a threshold between 14–10°C for humans(Harrison and Davis 1999). Several studies indicate the probable involvement of TRPM8 channels in regular and pathological noxious cold sensations(M Knowlton and D McKemy 2011), (Fernández-Peña and Viana 2013). Remarkably, in the neuropathic pain of animal models, cold allodynia is meaningfully decreased by capsazepine, known as TRPM8 blocker(Zuo et al. 2013).

Oxaliplatin is an anticancer drug used for the treatment of colorectal cancer and development of peripheral neuropathic pain with cold hypersensitivity is a recurrent side effect of oxaliplatin. In animal models, cold pain induced by oxaliplatin is associated with upregulation of TRPM8(Gauchan et al. 2009)(Kawashiri et al. 2012). These results highlight the potentials of TRPM8 modulators in the therapeutic use for treating cold-evoked pain.

Though, cold is also have analgesic effects on some types of pain and TRPM8 agonists can use as analgesic in certain neuropathic cases(Proudfoot et al. 2006).

Studying transgenic mouses null for TRPM8 for evaluation of the temperature sensation, inflammation, thermo regulation and pain provided supportive results about the multiple roles of TRPM8 like thermoregulation, anti-inflammatory role, cool temperature discrimination, cold-induced analgesia, and noxious cold sensing. Mice without functional TRPM8 channels show a significantly reduced discrimination of innocuous cold temperatures(Dhaka et al. 2007)(Colburn et al. 2007).

Primary headache and migraine without aura were other diseases that linked to TRPM8. It was reported that TRPM8 could be activated in meninges and this might cause headaches, like headache caused by ice cream and migraine started by cold temperature(Prince et al. 2004). Two different genome-wide association studies have found a strong association between genetic markers near or in the TRPM8 gene and probability to a primary headache of neurovascular origin known as migraine without aura(Chasman et al. 2011)(Freilinger et al. 2012). However, the role of TRPM8 channels in the pathogenesis of migraine remain unknown.

Moisture of the ocular surface by tears originated from lacrimal glands, plays a significant protective role of the cornea. It has found activation of TRPM8 channels in corneal afferents are part of the tear secretion mechanism(Madrid et al. 2006). TRPM8 ion channel seems to be the first ion channels to be activated after dryness of the ocular surface, this activation regulates tear secretion by detection eye wetness. It is known, heating the cornea in humans also reduce tearing rate. Hence, modulation of TRPM8 may be applicable for the pathophysiology and treatment of dry eye syndrome(Parra et al. 2010).

During respiration, the airways and the mouth can be exposed to noticeable fluctuations in temperature, cold sensitive afferents detect these changes(Hensel and Zotterman 1951). TRPM8 has expression in nasal trigeminal sensory afferents, which are mainly around blood vessels(Keh et al. 2011). TRPM8 gene has been related to the occurrence of chronic obstructive pulmonary disease and pulmonary hypertension in chronic obstructive pulmonary disease(Xiong et al. 2016). Increased expression of TRPM8 gene on bronchial epithelial cells was observed in chronic obstructive pulmonary disease patients and linked to extra production of mucus in airway, causing in cold-induced chronic obstructive pulmonary disease aggravation(Li et al. 2011). The rs11562975 Polymorphism in TRPM8 gene is associated with the progress of cold-induced airway hyperresponsiveness in patients with bronchial asthma(Naumov et al. 2015).

1.1.7 TRPM8 -Disease association network

Publicly accessible databases on disease and genes association are important advantage in evaluating validity of target. Furthermore, increasing number of literature demands using computational tools to have overall picture of current knowledge. Multiple bioinformatic tools are available to gather and analyse information. Among them we used DisGeNET(Piñero et al. 2016) to gather and compile current information on gene-disease association for TRPM8 and visualised using Cytoscape(Saito et al. 2012). Searching on the DisGeNET database provides 127 diseases associated with TRPM8 gene, which from 127 diseases, 50 of them related to neoplasm and 24 of them belongs to nervous system diseases (Figure 2). Hence, the TRPM8 is valuable therapeutic target to discover and develop new

active pharmacological compounds as agonists and antagonists for above mentioned pathologies.

Introduction

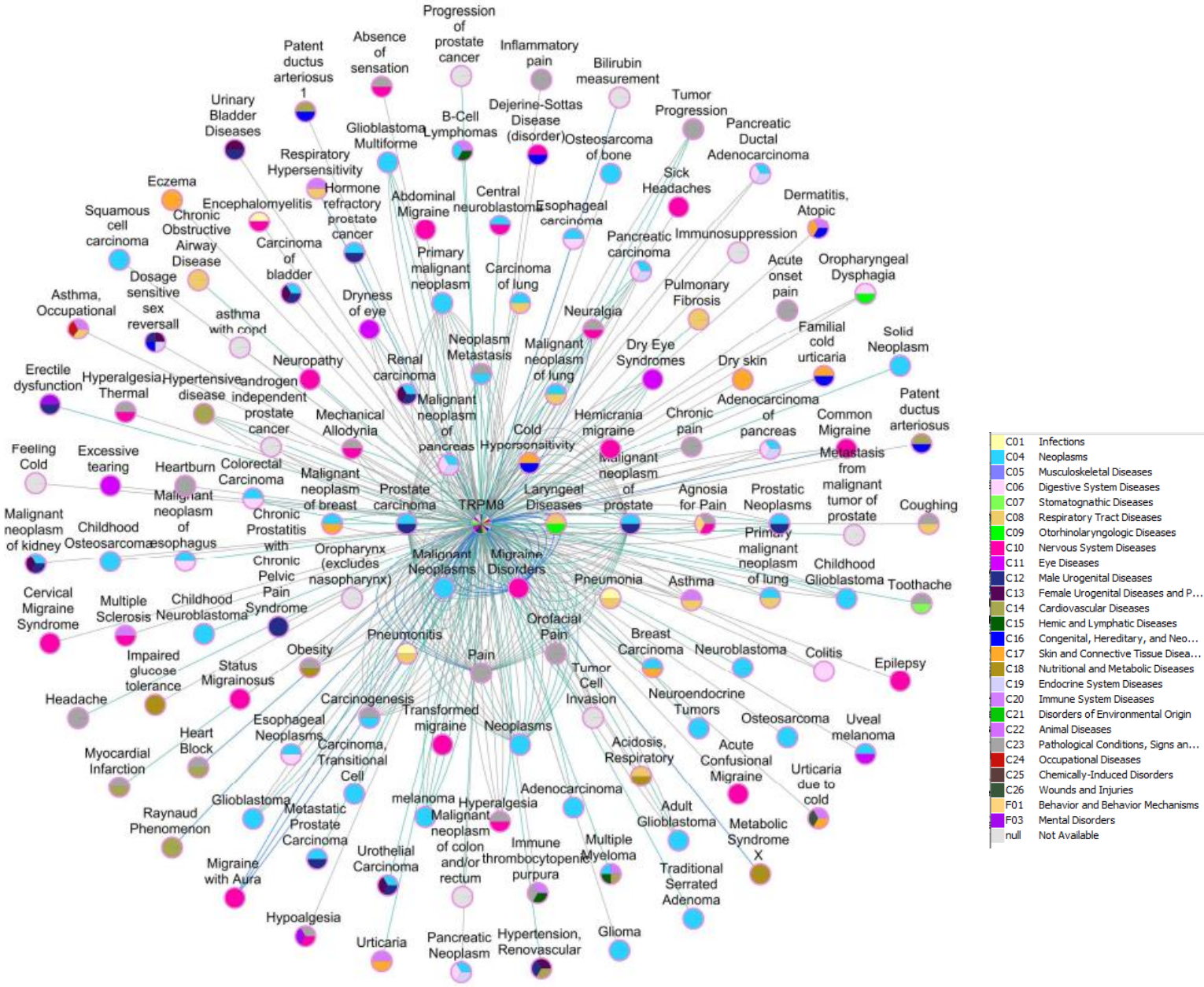

Figure 2. Network representation of the Gene-Disease associations for TRPM8 obtained with DisGeNET all sources on Cytoscape platform. The node in centre represents TRPM8 gene, and other nodes are associated diseases with colours representing class of disease. The edges between nodes represent the association types: blue: genetic variation; green: altered expression; grey: biomarker. Also, length of edge indicates strength of association of disease to gene, shorter edges indicate stronger association. From 127 diseases, 50 related to neoplasm and 24 of them belongs to nervous system diseases.

1.1.8 TRPM8 agonists

In addition to menthol and cold temperature Variety of Natural and synthetic compounds are available as agonist for TRPM8, like icilin, eucalyptol and an abundance of menthol derivatives(Viana 2011)(Behrendt et al. 2004). However, some agonists in high concentrations could affect other TRP channels, for instance camphor can activate TRPV1, TRPV3, and TRPM8(Selescu et al. 2013). Natural monoterpene like rotundifolone which is found in different species of the genus *Mentha L*, and eucalyptol as another monoterpenoid found in Eucalyptus plant. Both compounds show analgesic effects, while anti-inflammatory effect was noticed for eucalyptol, and both compounds activate TRPM8 ion channel(Silva et al. 2015)(Caceres et al. 2017). Praziquantel the anthelminthic drug and Tacrolimus an immunosuppressive drug, were reported to activate the TRPM8 channels, due to relative selectivity of praziquantel it is suggested for drug repurposing as agonist for TRPM8(Babes et al. 2017)(Arcas et al. 2019).

1.1.9 TRPM8 antagonists

Initial Investigations for potent TRPM8 antagonists identified drugs like phenanthroline and capsazepine (Behrendt et al. 2004)(Weil et al. 2005). However, there are also many patents regarding TRPM8 antagonists(Malkia, Morenilla-Palao, and Viana 2011). Several studies were conducted to synthesis antagonists for TRPM8, as result β-lactam derivatives(de la

Torre-Martínez et al. 2017), naphthyl derivatives(Beccari et al. 2017) and tryptophan-based compounds(Bertamino et al. 2018) were found to be potent antagonists for TRPM8 channel.

Among numerous synthetic and natural antagonists that were discovered, only three compounds have started clinical trials, AMG-333, PF-05105679, and Cannabidivarin, however AMG-333 didn't pass the phase 1 studies(González-Muñiz et al. 2019)(Gaston and Friedman 2017).

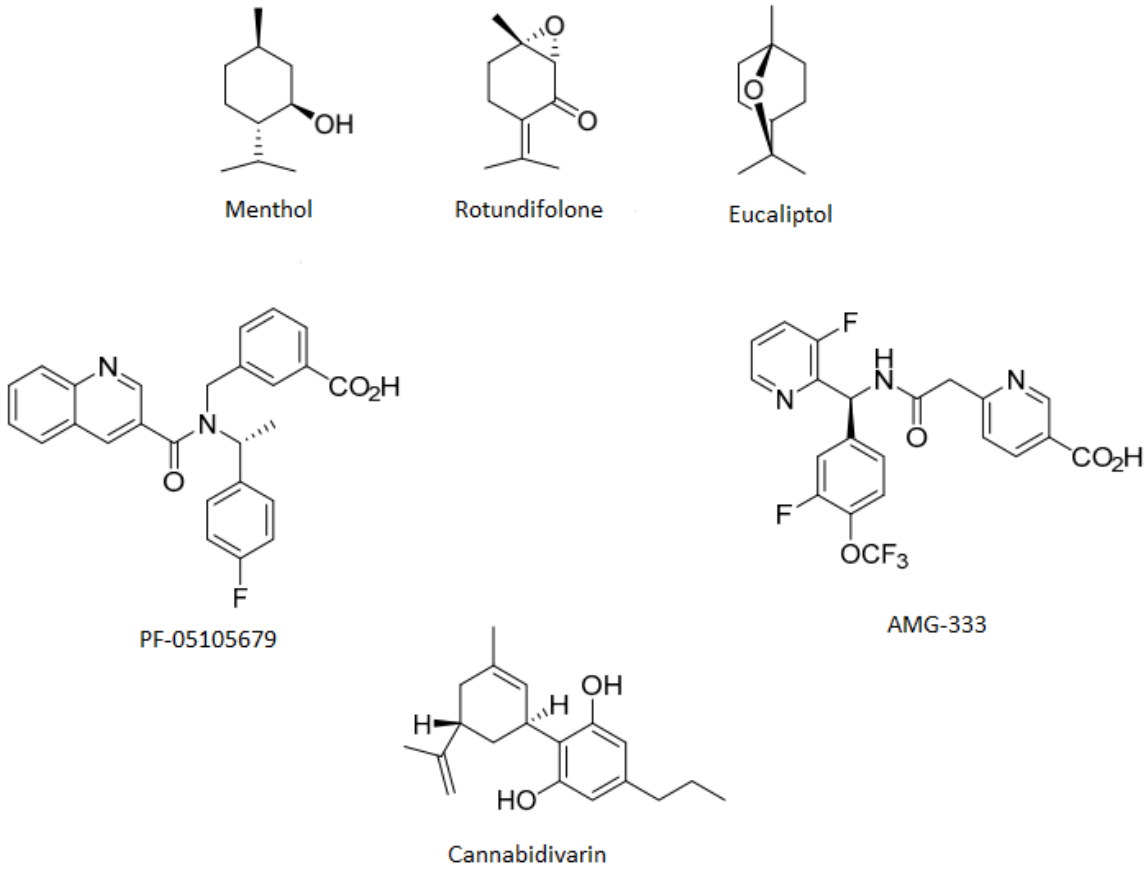

Figure 3. Menthol, rotundifolone, and eucalyptol are natural agonists of TRPM8. PF-O5105679, AMG-333, and cannabidivarin are selective antagonists of TRPM8.

1.2 Drug discovery

Despite availability of commercial agonists for TRPM8, yet there is no drug as antagonist for this ion channel. One reason could be the time-consuming and expensive process in traditional drug discovery approach which has high possibility of failure in any step even after approval. In fact, the general development and approval procedure is complex and includes lot of time as per each demand of Food and Drug Administration (FDA) guidelines. The progress for a new compound from synthesis to receiving marketing approval could take an estimated average of 8 to 12 years(Moridani and Harirforoosh 2014).

Additionally, regulatory requirements and obligations have increased gradually over time and this caused a surge in both the trial scale and the duration, as result an increase in the general cost of the development procedure happened(Morgan et al. 2011). Furthermore, recently there has been an increase in the amount of safety recalls of earlier approved drugs, like Valdecoxib which was removed from market due to possible increased risk of serious cardiovascular adverse events, and higher risk for serious skin reactions(Atukorala and Hunter 2013). As result, the number of drugs approved for marketing has declined to an all-time low.

Drug discovery in the neuroscience is much more challenging, and some pharmaceutical companies are stepping away from drug development for nervous system due to high failure occurrence and demand for large financial investments. Animal models for instance, often do not resemble an entire disorder or disease of nervous system and it results in translational failures due to using animal models(O'Donnell et al. 2019).

One of early stages in drug discovery after the procedure of target validation, is the hit identification and lead compound discovery, which is during process that compound

screening assays are developed. A ‘hit’ compound could be defined as a molecule which has the desired effects in a screening procedure and lead compound is a compound that has desirable pharmacological or biological activity and very likely to be therapeutically valuable, nevertheless lead compound might require some structural optimizations to fit better to the target. Generally, a drug–target interaction is not always considered clinically and biologically applicable if its effect is equal or higher than 1 μM or pAct ≥6, where “p” is the negative logarithm of pharmacological or biochemical in vitro assay values like IC_{50} and EC_{50}(Hughes et al. 2011).

A diverse amount of screening methods exists to discover hit molecules. High throughput screening includes the screening of the total compound library against the drug target. However, High-throughput screening (HTS) is main method in hit generation for drug discovery, despite HTS enabled pharmaceutical companies to screen massive scale of compounds in a short time. But this method is expensive approach due to amount of required resources, and it is unable to provide data about toxicity and bioavailability of compounds(Posner 2005).

1.2.1 Drug repurposing

Repurposing approved drugs might be considered as a solution and may offer an accelerated way to identifying new treatments for patients. Repurposing, also termed repositioning, rediscovering, or reprofiling, refers to the idea or procedure of taking a drug that is developed for one disease and applying it to another one. Existing information of pharmacological properties and safety profiles of repurposed drugs can accelerate early phases of clinical development, considerably cuts research and development costs, shorten drug development

timelines, and reduce failure rates due to pharmacokinetic and safety problems(Pushpakom et al. 2019).

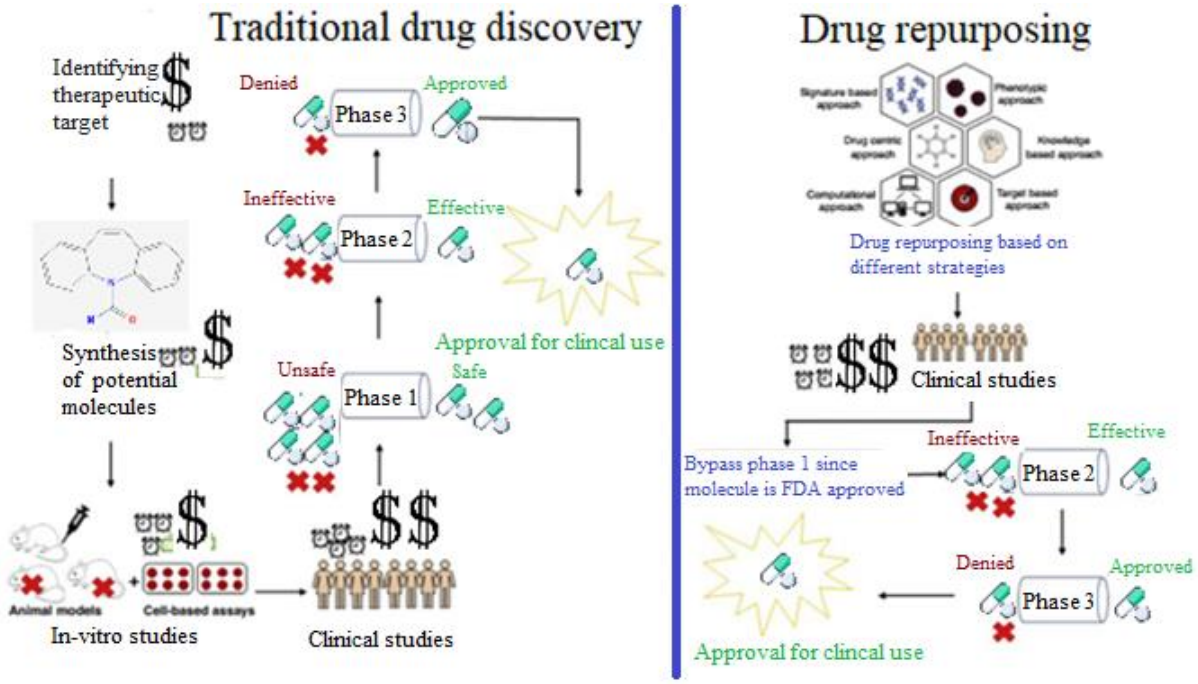

Figure 4. A representation of differences between traditional drug discovery process against drug repurposing. The repurposing drug process is saving time, effort, and money.

1.2.2 Drug repurposing vs rare diseases

About 7000 rare diseases have been identified, but approved treatment is available only for around 6% of these rare diseases. Therefore, drug repurposing is a main attractive approach for neglected and rare conditions, where the investments for developing a new drug are not sufficient(Wakap et al. 2020). For example, Muckle-Wells syndrome is an autoinflammatory illness resulted by increased interleukin-1. Canakinumab, a drug used to treat rheumatoid arthritis, is a monoclonal antibody that has selective and constant blockage of IL-1β. Several clinical studies proposed that canakinumab has a sustained control of disease activity and a

quick reduction of related symptoms in Muckle-Wells syndrome patients. In 2009 canakinumab was approved by the FDA and by the European Commission treat Muckle-Wells syndrome(Tran 2017).

The candidate drugs for repurposing could be from different stages of drug discovery procedure like drugs failed to show effectiveness in last stage of clinical trials and were without safety issues, drugs in clinical development phase, Marketed drugs for which patents are close to expire or already are generic, drugs that delayed in development for commercial reasons, or were discovered in another geographical markets(Sleigh and Barton 2010). However, most of the well-known and successful drug repurposing cases (e.g. sildenafil, minoxidil, aspirin, carbamazepine, valproic acid) were emerged due to serendipitous observations or from unorganized finding procedures, often based on the already recognised pharmacology of a drug like off-target, polypharmacology, or adverse effect(Jourdan et al. 2020).

There are two main approaches to identify drug candidates, experimental and computational. Experimental method includes phenotypic screening methods and binding assays that can be used to find lead compounds from big compound libraries and find binding interactions of ligands to assay components. Computational methods are generally classified into target-mechanism-based, pathway- or network-based, text mining approach, signature-based, and target-based approaches(Parvathaneni et al. 2019).

In drug repurposing the identifying interactions between drugs and novel targets are one of the initial steps in evaluating the possibility of repurposing. Most drugs act on several targets which results in ‘off target’ effects, enabling to pursue a new purpose where the other targets are relevant(Palve et al. 2020). For instance, thalidomide originally was an sedative or tranquiliser drug but due to its devastating side effects it was withdrawn(McBride 1961), after

its withdrawal, further investigations on the mechanism of drug have shown that thalidomide could be effective as an immunomodulator and antiangiogenic(Singhal et al. 1999), currently it is used for treatment of multiple myeloma patients(Palumbo et al. 2008).

1.2.3 Repurposing drug based on polypharmacology

As it is said by Sir James Black, Nobel Laureate 1988 in Physiology and Medicine: 'The most fruitful basis for the discovery of a new drug is to start with an old drug'. Screening drugs not only used for identifying candidate for repurposing, it also could be used to identify and optimize the lead compound. The Selective Optimization of Side Activities, known as SOSA approach, is based on side activity or polypharmacology of drug. It represents a precise alternative to high throughput screening, by generating drug-like hits. SOSA is a method to identify new lead compound displaying acceptable bioavailability and low toxicity since in fact that compound is already approved drug. Identified structure could be used as start point for further optimization to increase its affinity for new target(Wermuth 2006).

Drugs expected to be selective on one target, but usually a drug can interact with more than one target, this phenomenon known as polypharmacology can cause the adverse effects of drug by interacting with nontherapeutic targets, it can also be a promising opportunity for the much efficient drug discovery. For instance, polypharmacological drugs are supposed to avoid drug resistance by interacting with several targets. Such drug resistance is expected in infectious diseases or in different types of cancer(de Castro and Camarasa 2018). Possibility of repurposing for another disease, is additional aspect of polypharmacological drugs(Peters 2013).

For instance, carbamazepine is a sodium channel blocker and is example for polypharmalcology of a drug, it was initially marketed to treat epilepsy but also was discovered to be effective for trigeminal neuralgia(J. C. Taylor, Brauer, and Espir 1981). Its antipsychotic effect was identified later and was suggested for treatment of bipolar disorder(Greil et al. 1997). Recently there are some studies regarding repurposing carbamazepine for some rare diseases such as metaphyseal chondrodysplasia type Schmid and amyotrophic lateral sclerosis(Forouhan, Sonntag, and Boot-Handford 2018)(J. Zhang et al. 2018).

Searching on the STITCH database(Szklarczyk et al. 2016) (http://stitch.embl.de/), we can construct the drug-target network for carbamazepine. Only interactions with high confidence ≥0.7 were considered. According to network after Cytochrome P450 proteins, Sodium ion transport-associated proteins are the main interacting proteins with carbamazepine, but there are other proteins interacting with different affinities (Figure 5).

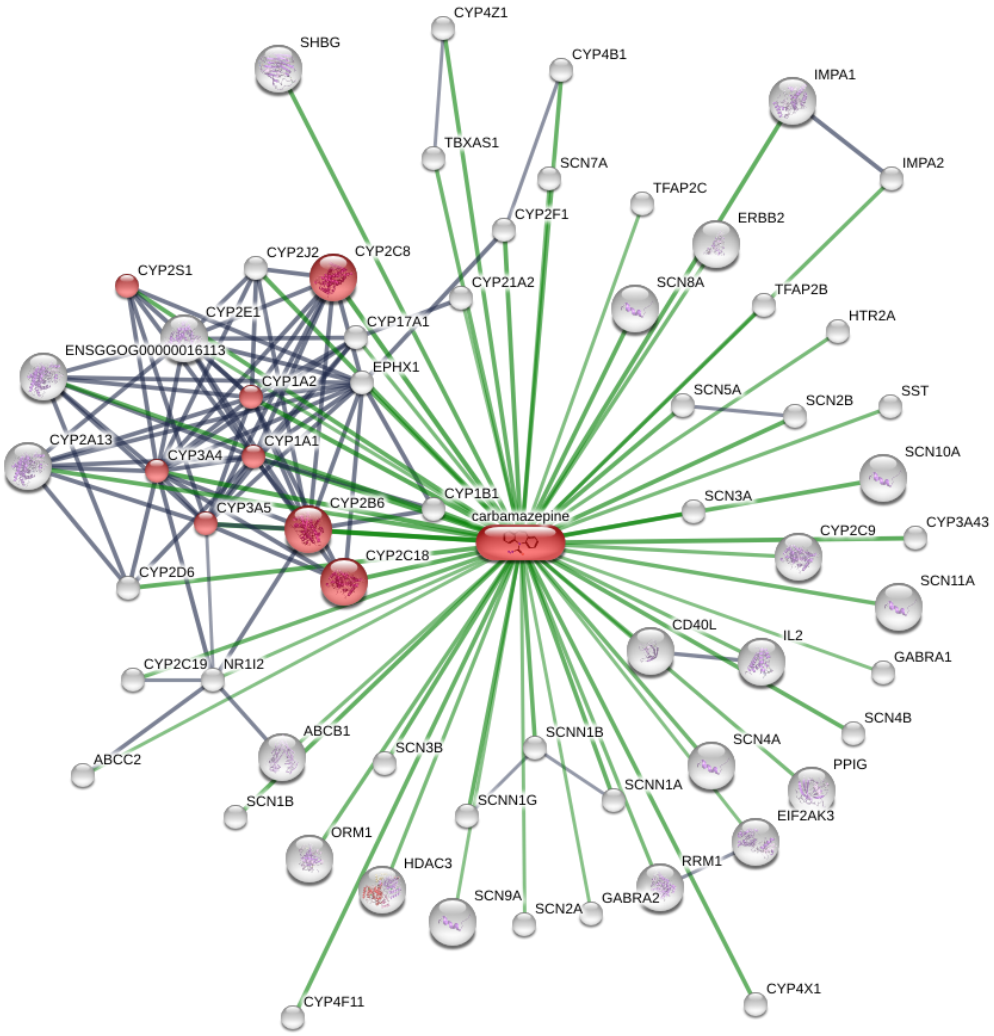

Figure 5. The drug-target networks for carbamazepine constructed by the STITCH database.

Riluzole as another sodium channel blocker, is neuroprotective drug and is used for treatment of amyotrophic lateral sclerosis(Miller, Mitchell, and Moore 2012). It is reported that, riluzole suppresses increase of the menthol sensitive cells induced by oxalate, in the cultured DRG neurons. Additionally, in oxaliplatin treated rats, riluzole reduced cold allodynia and increase of TRPM8 mRNA levels was prevented(Yamamoto et al. 2018).

Lamotrigine, gabapentin, and lidocaine were known to be sodium channel antagonists are prescribed to manage cold allodynia(Coderre et al. 2007). As it was mentioned TRPM8

channel has strong association with cold induced pain(Xing et al. 2007). In fact, sodium channel blockers have diverse chemical structure. Some of them are flexible molecules that contain a polar group in the middle an aromatic moiety at the one end, and a protonatable amino group at the opposite end. Classical examples are lidocaine, mexiletine, tetracaine, and bupivacaine. Some other sodium channel blocking drugs such as phenytoin, carbamazepine, and lamotrigine are electroneutral molecules. They contain aromatic moiety at one end of the molecule and a nonionizable polar groups at the other end. Much complex structure like ranolazine also could block Sodium channels such molecules resemble two aromatic moiety bridged by a moiety with an ionizable amino group (G. Liu et al. 2003)(Tikhonov and Zhorov 2017).

There is high potential for this class of drug to repurposed for other diseases(Matthews and Hanna 2014)(Bugan et al. 2019). Therefore, due to the structural variety and affordable cost, our initial library of compounds for screening on TRPM8 ion channel includes sodium channel blockers. List of drugs with their description from drugbank database(Wishart et al. 2018) are represented in Table 1.

Table 1. List of drugs and their properties based on drugbank database.

Drug	**2D-Chemical Structure**	**Category**	**Main Targets**	**Lipophilicity (logP)**
Mexiletine	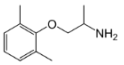	antiarrhythmic agent (Class Ib)	Voltage-gated sodium channel, Aryl hydrocarbon receptor.	2.17

Tetracaine	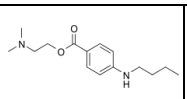	local anaesthetic	Ryanodine receptor 1, Ryanodine receptor 2, Voltage-gated sodium channel.	3.54
Ranolazine	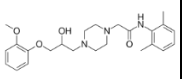	anti-anginal	Voltage-gated sodium channel, Inward rectifier potassium channel, Voltage-gated calcium channel, Alpha-1 adrenergic receptors, Beta-1 adrenergic receptor.	2.08
Rufinamide	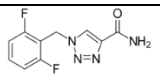	anticonvulsant	Metabotropic glutamate receptor 5, Sodium channel protein type 9 subunit alpha	0.95
Propafenone	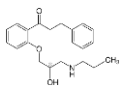	antiarrhythmic agent (Class IC)	Sodium channel protein type 5 subunit alpha, Potassium voltage-gated channel subfamily H member 2, Beta-1 adrenergic receptor, Beta-2 adrenergic receptor.	3.1
Flecainide	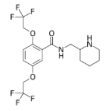	antiarrhythmic agent (Class IC)	Sodium channel protein type 5 subunit alpha, Sodium channel protein type 4 subunit alpha, Potassium voltage-gated channel subfamily H member 2, Ryanodine receptor 2.	2.98
Phenytoin	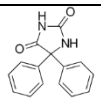	Anticonvulsants	Voltage-gated sodium channel, nuclear receptor subfamily 1 group I member 2, Potassium voltage-gated channel subfamily H member 2, Voltage-gated calcium channel,	2.26
Oxcarbazepine	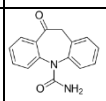	Anticonvulsants	Voltage-gated sodium channel.	1.76
Lamotrigine	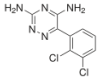	Anticonvulsants	Voltage-dependent R-type calcium channel subunit alpha-1E, Voltage-dependent R-type calcium channel subunit alpha-1E,	1.87

			Adenosine receptor A1.	
Riluzole	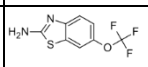	Anticonvulsants	Sodium channel protein type 5 subunit alpha, Cystine/glutamate transporter	2.83
Carbamazepine	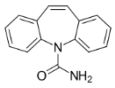	Anticonvulsants	Voltage-gated sodium channel, Neuronal acetylcholine receptor subunit alpha-4, Nuclear receptor subfamily 1 group I member 2.	2.77
Gabapentin		Anticonvulsants	Voltage-gated sodium channel, Voltage-gated calcium channel, Adenosine receptor A, Voltage-gated potassium channel.	1.25

1.2.4 Virtual screening for efficient screening

There are several useful tools and databases for enhance drug repurposing procedure such as PubChem, ChEMBL, ZINC and KEGG drug databases combine various information such as molecular mechanisms, experiments, and drug targets(Tanoli et al. 2021). SwissSimilarity is one of online resources from the Swiss Institute of Bioinformatics, which is a web tool for fast ligand-based virtual screening from different types and sizes of small molecules libraries. For academic settings or small companies generally lacking high throughput screening capabilities, virtual screening of publicly available chemical databases is the most affordable method to generate virtual drug candidates.

SwissSimilarity can screen from diverse chemical libraries like approved drugs, bioactive and commercial molecules, and 205 million of virtual compounds. Screenings can be carried out

using different computational methods, including 2D molecular fingerprints, 3D superimpositions, and efficient nonsuperpositional shape-based techniques(Zoete et al. 2016). This method will be used to optimize our screening library based on initial experimental results by searching for drugs with similar structure to the most potent compound.

1.2.5 Automated vs manual electrophysiology

After Identifying the target, the assay development is another crucial step in drug discovery. Normally, cell-based assays were used to evaluate targets such as membrane receptors, and nuclear receptors and ion channels, and biochemical based assays are recommended for enzymes and receptors(Michelini et al. 2010).

For TRPM8, we use the patch clamp technique. The patch-clamp technique was developed by Neher and Sakmann in the 1970s(Neher, Sakmann, and Steinbach 1978), for which it was awarded the Prize Nobel in Physiology and Medicine in 1991. Which it was an adaptation of the initial technique of voltage-clamp that allowed Hodgkin and Huxley to carry out a study model on the generation of the action potential(Hodgkin, Huxley, and Katz 1952) and was awarded the Nobel Prize in Physiology and Medicine in 1963. This was possible thanks to the first observations in electrophysiology, which led Cole and Curtis in 1938 to propose the excitable cell membranes as similar as electrical circuits that are ruled by the Ohm's Law(Curtis and Cole 1938).

This technique essentially consists of pressing the tip of a glass micropipette containing electrolyte solution against the cell membrane and after applying negative pressure through the pipette, achieve a tight seal or high resistance seal with resistance of giga ohms, known as giga seal. Since micropipette through an electrode attached to amplifier and another

electrode is placed in a bath surrounding the cell as a reference ground electrode, an electrical circuit forms between the recording electrode and ground electrode with the cell in between.

However, manual patch clamp considered as gold standard for studying ion channels, but in comparison to automated version of patch clamp, this method requires extensive manual labour and has a low throughput progress, and it demands longer duration of training for staff to perform the experiments. Technologies of automated patch-clamp electrophysiology have been progressively advancing since late 1990s and is available commercially since 1999(Bell and Dallas 2018), three major automated patch clamp systems based on method of patching are in vivo(Kodandaramaiah et al. 2012), in suspension(Jones et al. 2009), and in culture(Martinez et al. 2010).

IonFlux 16 was introduced in 2009 and suspension of cells is used for this system. The technology of IonFlux 16 provides high quality and physiologically relevant data of ion channel function, and for pharmacological testing of compounds. It offers an acceptable quality for measuring the potency of compound in modulating ion channel, this automation has broad applications in the ion channel drug discovery process(Golden et al. 2011).

Although the manual patch-clamp provides a direct, high detail with real-time method to study the channel function, but manual patch clamp electrophysiology causes a significant bottleneck effect in the drug discovery for ion channels, and it is not appropriate for screening large number of compounds. The automation of patch clamp electrophysiology systems critically simplifies the process of electrophysiology experiments and significantly increases compound screening throughput. Nevertheless, the manual patch clamp electrophysiology technique is still necessary, and it is not replaceable by the automated patch clamp systems due to its exceptional features of high quality of data and flexibility to patch different types of cells(Yajuan, Xin, and Zhiyuan 2012).

1.2.6 Automated electrophysiology with IonFlux 16

The description and general protocols for the use of the Ionflux system are widely detailed on the Fluxion - Molecular Devices website, therefore we will give a brief description for each part of experiment here and in material method section.

Since a large part of this doctoral thesis is development of an assay for screening drugs on TRPM8, we will explain in the results chapter all the steps in detail. Only in this section we briefly indicate the protocols used to carry out our experiments. The Ionflux system is based on the electrophysiological patch-clamp technique that allows the recording of ionic currents through very small areas of cell membranes or patches.

In comparison to manual Patch clamp, The IonFux system allows faster screening of compounds. The system consists of a combination of a screening device, a connected computer, a software and special 96 well plates with the bottom of wells replaced by microfluidics arrays (Figure 6).

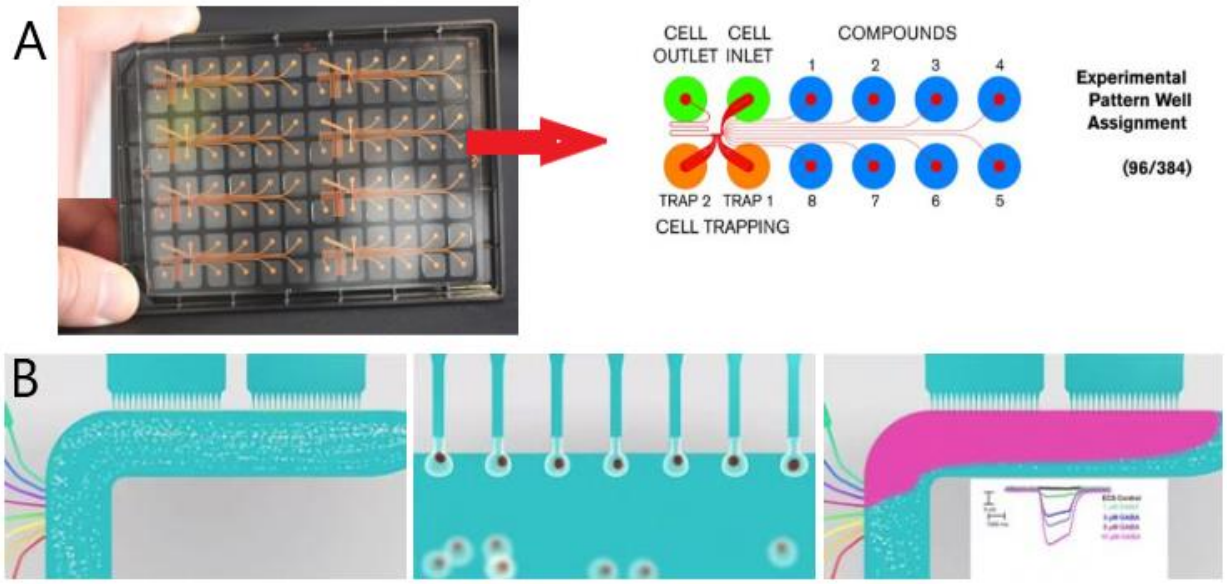

Figure 6. Ionflux 16 uses specific plates. A) microfluidic plate and scheme of a pattern of a plate "assembly" B) Representation of the main channel, the microchannels and the traps with the trapped cells

Wells contain cell suspension, intracellular and extracellular solutions, and compounds to be tested. The system works with 20 cells per amplifier to improve data consistency and success rate.

Once plate is ready and inserted to device, the plate sealed by inserting the electrodes into the wells. The instrument uses air pressure that controls the flow of fluids, and formation of whole-cell patch clamp.

The software controls: channel filling, cell sealing, cell membrane rupture, and the voltage / pressure / fluid protocol during data acquisition. This program also allows compensation of parameters such as membrane capacitance, series resistance and leakage currents. Finally, the software allows the analysis of data, as well as export results to analyse on Excel and clampfit.

In this study, we will try to find a potent antagonist for TRPM8 ion channel among approved drugs, mainly using automated patch clamp device IonFlux 16 to screen blocking potency of drugs against TRPM8 ion channel and by ligand-based virtual screening method we will optimize our screening list. By performing molecular docking, we will analyse the possible interactions between drugs and antagonist binding site on TRPM8 channel. Furthermore, we will evaluate effect of identified antagonists against different types of cancer cells. Result of this study will provide possible insights for drug repurposing and will propose promising lead compound in searching for new antagonists for TRPM8 ion channel.

Material and Methods

2.1 Operating IonFlux 16 Platform

The system contains an electrical and pneumatic interface and 16 patch amplifiers. Device needs external source of pressure and vacuum, which in our case provided by a cylinder of nitrogen and a vacuum pump.

The working plates for the IonFlux 16 are based on standard 96-well plates. The lower part of the board has been replaced by a network of interconnected microchannels. Each plate is divided into 2 individual experimental work zones, and each zone consists of 4 patterns, with 12 wells for each pattern). Each pattern includes 8 wells for compounds, one well for cell suspension (INlet), a well to discard excess fluids (OUTlet), and two wells where they will insert the measuring electrodes, called traps. Traps contain the micropipettes that will allow to trap the cells and break the membrane to enter whole-cell mode, with providing two independent patch clamp registration points (Figure 7).

There are two varieties of plates; the “Ensemble” or ensemble plates, in which there are 20 micropipettes per trap that record a summation of current of all the trapped cells, increasing the success rate, and the average resistance generated by the 20 pipettes (usually not reaching GΩ), and “Single” or single cell plates, in which there is only one pipette per trap, and recording current and resistance is due to a single seal (usually Giga seals).

The plates are sterile, packed with a hydrogen peroxide solution and individually vacuum sealed to prevent contamination growth in the microchannel network. Each plate is marked with a unique barcode, which will be recognized by a handheld laser reader before the experiment. Both dispensing and storage require refrigeration between 4-7° C and have a shelf life of 3 months from their production.

Software version 4.6 have been used, in this version tool design and execution of the experiment and data collection and analysis are two programs independent. The design and execution software of the experiment offers several control tabs including setup, for the design of the plate and the sequence of the experiment, and runtime, to see the experiment in real time. The runtime data allows to see offline what happened in the experiment.

2.1.1 Experiment Setup

A) Plate design

In this section the work zone of the panel is selected (Zone 1 and / or Zone 2). They can provide data on the type and concentration of cells used, solutions and any information about the experiment that we consider clarifying. In addition, it offers a template presented in which to indicate each well contains which compound or compounds, and their concentrations. It can be written and edited directly on the template or import and export as file in Excel format.

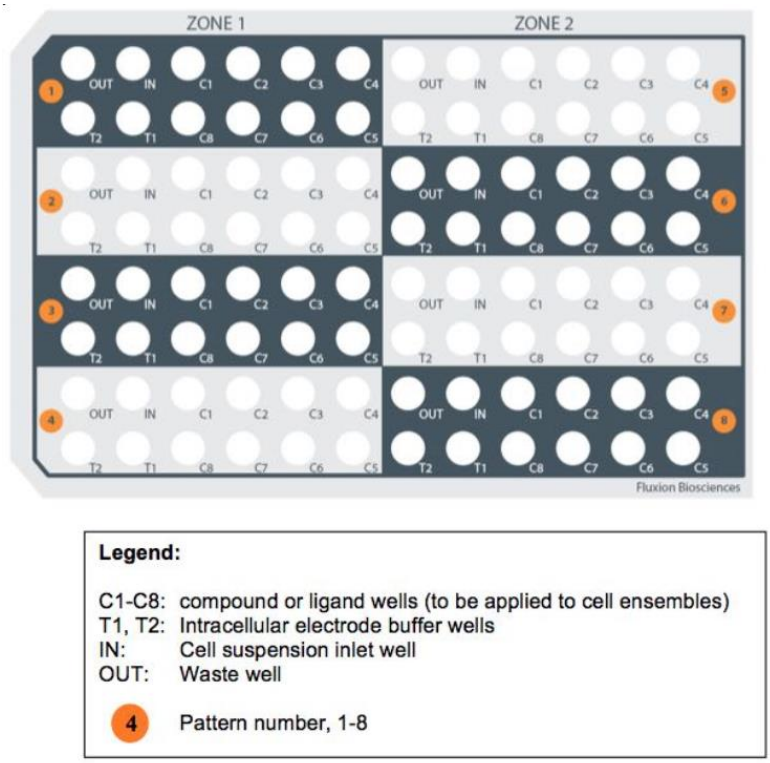

Figure 7. Overview of 96-well Plate used for IonFlux: 2 experimental zones, 4 patterns per zone and 2 recording channels per pattern

B) Design of the experimental protocol

The experiment sequence contains 4 subsections: Prime, Trap, Break and Data acquisition. All of them will be explained later when the procedure is described. Each subsection is divided into 2 windows with different editing commands and design the protocols.

B.1) Pressure editor

Determines the pneumatic pressure exerted on the wells of the plate, which is transferred to the liquid from the microchannels exiting the well. This pressure determines the magnitude and direction of flow. Positive pressure (for Inlet and C1-C8) provides a continuous flow to the discard well (Outlet), and negative or vacuum pressures (for traps only) that allow cells to be trapped in the traps micropipettes and break the membrane to form the whole-cell.

To establish the desired sub-protocol, the sequence items (continuous, pulse, ramp, series) and the times of these sequences are selected, for all appropriate channels or wells. The pressure units used are:

Positive pressures, psi: or pound-force per square inch (1 psi = 6894.5 Pa).

Negative or vacuum pressures, inHg: or inch of mercury, (1 inHg 0˚C = 3386.389 Pa).

B.2) Compound addition

In this section, in the Data acquisition phase, the protocol for compound addition is possible to be designed. A graph and a table allow us to edit the order, when and for how long time that compound will be perfused to the cells. It gives us the option to import / export a spreadsheet in Excel format, which facilitates time calculations. The total time of addition of compounds, must coincide with that established in the pressure protocol.

In addition, this is where we will set the positive pressure exerted on the wells of the compounds, which shows what flow pressure the cells will withstand. This point should be consistent with main channel flow pressure to prevent compounds to be diluted before reaching the cells.

B.3) Voltage Editor

In this section we determine the voltage sequences applied to the cell, as well as the potential of membrane by the amplifier. There is also another software model to perform "current clamp" experiments with current editor. Measurement protocol is designed using the sequence items (continuous, pulse, ramp, series and increasing pulses) and the times of these sequences.

B.4) Cursor editor

Cursors for "R": These are the cursors that will register the resistance of the cell membrane. Placing these cursors in a small voltage pulse allows to adjust the baseline throughout the experiment.

Cursors for "ΔI": One cursor will measure the current of interest and the other the current on the baseline. The system will automatically subtract both values and they will be represented in real time during the experiment on a current trace vs time graph. For the measurement method the system's default is to select a single point but we can select several points, which allows to calculate the minimum, maximum or average of points. The cursors and calculation method can be modified during the experiment and after obtaining the data in the end of the experiment.

Sample rate: Allows us to select the number of records that the amplitude records during the experiment. It is indicated in samples per second, and the number will depend on the type of kinetics of the channel that we are studying. In comparison to manual patch clamp there is no filtering rate, and the recordings will register and analysed in sampling ratio.

B.5) Amplifier controls

These settings are like those made in the manual patch clamp technique. They make it possible to compensate for electrophysiological parameters that affect current measurement and the registers. Some of them are applied automatically, and others, which will appear in the control window, and have the option of automatic or manual.

Fast capacitance or C_{fast} eliminates capacitive current due to amplifier connection to electrode. It also known as pipette capacitance. This value is automatically corrected before starting the experiment. Junction potential or $J_{p,}$ is a potential for diffusion generated by ionic

transfer, once the internal and external solutions come into contact. It is corrected automatically after the prime phase.

Leakage resistance or R_{leak} is the compensation of the leakage currents. Leak current is compensated by applying a current of equal magnitude and opposite to the leak current upstream of the digitizer circuit. The current is calculated based on the leak resistance multiplied with the applied voltage. Slow capacitance or C_{slow}, is the capacitance of the cell membrane or C_m. These capacitive currents, or transients are only observed when the cell has entered the whole-cell and will be compensated for automatically or manually once the seals and currents are stabilized.

This uncompensated part can be eliminated automatically using P/n series of pulses of known voltage. The amplifier registers the artifacts, and these are extrapolated and subtracted from each sweep measured throughout the experiment. Series resistance or R_{series}, is the sum of all the resistances between the amplifier and the cell membrane. And in the same way as C_{slow}, once the seals and currents are stable it is possible to correct it automatically or manually compensate. Amplifier gain or sensitivity of the amplifier is a relationship between the quantity to be measured and the signal that the equipment picks up. It is manually adjustable, and low gain is recommended during the entire experiment.

To run the experiment, a file with an .IET extension must be loaded (Ionflux Experiment Template), which we have designed previously. Once the experiment has started, the 4 subsections automatically will start. the experiment begins by the prime, in which all the microchannels will be filled with their respective liquids, then during the trap, the cell suspension will begin to flow from the “IN” well to the “OUT” passing through the traps and will be trapped in the micropipettes by suction, and in break it will be possible to break the membrane of cells. Finally in the data acquisition, the compounds will be perfused to the

cells in the order and the indicated time. While the designed voltage pulses applying the changes in the intensity of current between the exterior and the interior of the cell.

All the steps can be followed by real time graph in of resistance vs time or current trace vs time. Once the seals are stable, and we see that the current or resistance are consistent, we can modify some amplifier settings, Cslow, P/n and Rseries, as already it was indicated previously.

Once the data of experiment is loaded to data analyzer software, a graph regarding resistance or current vs experiment time will appear, with a colour code linked to related traps. The graph ΔI vs time, is linked to the sweeps performed during the entire experiment, with the designed voltage pulses. These sweeps can be viewed by opening the window of real time sweeps. By using this software, it is possible to carry out the subtraction of the leakage currents using the option of "offline leak subtraction", with adjusting the graphs to the current baseline.

The analysis table will give relevant information such as the event number (C1-C8), the pattern (P1-P8), the name of the compound and the concentration (if it has been indicated in the board setup), the current intensity, and the resistance of trap (T1 or T2). It is possible to create an analysis template in Excel, which remembers the events of interest for future experiments. For further analysis, we can export the data in different formats: Excel, Clampfit and CSV. It is possible to export the data of the desired sweeps or of the cursors of interest.

2.1.2 Procedure of experiment

Cells and Solutions

Stably expressing TRPM8 HEK293 cells were a kind donation from Prof. Alyn Morice (University of Hull, United Kingdom). Cells were cultured in T75 tissue culture flasks using Dulbecco's modified Eagle medium or DMEM (Euroclone) supplemented with 2% L-Glutamine (Euroclone), 10% Fetal Bovine Serum or FBS (Euroclone) plus Genenticin (Gibco) 800 µg/ml at 37° C, in a humidified 5% CO_2 atmosphere. Cells were maintained till they reach 70~80% confluency. For the experiment with IonFlux, cells were washed with 1X Phosphate Buffered Saline or PBS (Euroclone) without Ca^{2+} and Mg^{+}, for two times, to remove all medium and waste substances.

Then we incubate the cells for 5 minutes at 37°C and 5% CO_2 with 5 mL of Accutase (Euroclone). Accutase is a protease solution used as alternative to trypsin, it is more gentle in comparison to trypsin. Accutase was used to avoid affecting membrane proteins like ion channels during detaching. After the time of incubation, the suspension centrifuged at 800 G for 1 minute, and the cell pellet is resuspended with 5 ml of CHO - SFM II medium (Serum free medium for suspension CHO) (Gibco), and single cell suspension was made by gentle pipetting. Then we can keep them in normal agitation to use later.

To prepare the plate for IonFlux, the hydrogen peroxide within the wells and microchannels should be washed with double distilled water by washing protocol that replaces water with hydrogen peroxide in all the microchannels. Once the plate is clean, the corresponding compounds or solutions are added to each well. It worth to mention the plates shouldn’t left to be dried. We also remove the cells from the agitation and after verifying under the microscope that no aggregations are present, they are collected and centrifuged for 1 min at 800G to remove the medium, then we resuspend the pellet in external solution with

concentration of 2-5 million cells/ml. For each well maximum 250 µl or minimum 100 µl of solutions should be added.

The cells should be in the external solution for the shortest time possible between the removal of agitation and before the start of the experiment. It is advisable to have already loaded the file of the necessary protocols (explained in detail later), recording type, the work file of the plate template and the order and time of compound addition. Once the cells are loaded, the plate is inserted in the reader, and proceed to the beginning of the test.

The extracellular solution contained 140 mM NaCl, 4 mM KCl, 1 mM $MgCl_2$, 10 Mm glucose, and 10 mM HEPES, pH 7.4 with NaOH and 310 mOsm, we removed Ca^{2+} from external solution to avoid Ca^{2+}-dependant desensitization of TRPM8. The intracellular solution for the whole-cell voltage clamp contained the following (mM): 60 CsCl, 70 CsF, 5 Na_2ATP, 10 HEPES, and 10 EGTA, pH 7.2 with CSOH and 295 mOsm.

2.1.3 Recording protocols and analysis of results

As has been already said in the description of the software, the 4 phases of the experiment consist of, adjusting the pressure and / or vacuum, and the voltages. In the Prime, Trap and Break phases the values will depend on the cell line but will remain constant regardless of the data acquisition protocol. We will indicate below the sub-protocols used for this doctoral thesis.

Prime: The objective of this phase is to complete the filling of the microchannels with their respective fluids, so positive pressures and a voltage pulse will be applied. Voltage pulses are only to check if the electrodes are connected. Cells are not yet entered to microchannels, so this phase is common regardless of the cell line under study.

The total duration of the Prime will be 55 seconds. We adjusted to a pressure of 5 psi in the wells of compounds and traps for 20 s, 30 s more at 2 psi, and further 2 psi for 5 s only in the traps and 1 psi in the main channel for 30 s and 0.4 psi for the rest 25 s. The voltage pulse will have a baseline at 0 mV for 50 ms, followed by 50 ms at 20 mV, and another baseline at 0 mV for another 50 ms. Monitoring the results of this section is useful for analysing the quality of plates.

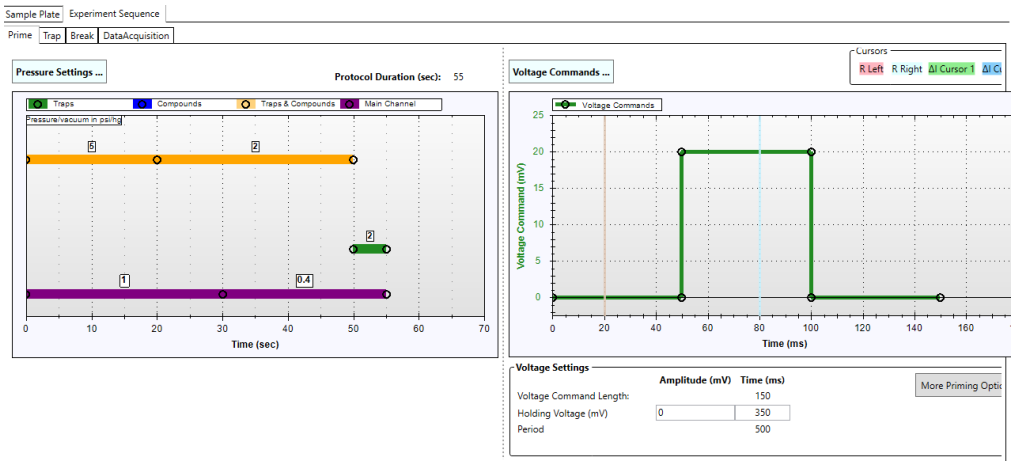

Figure 8. Prime window in IonFlux software first phase during experiment.

Trap: In this second phase, the cell suspension deposited in the "IN" well of the plate is pushed by positive pressure along the main channel into the wells of the traps, where the 40 micropipettes (20 in each trap) are exerting a negative pressure.

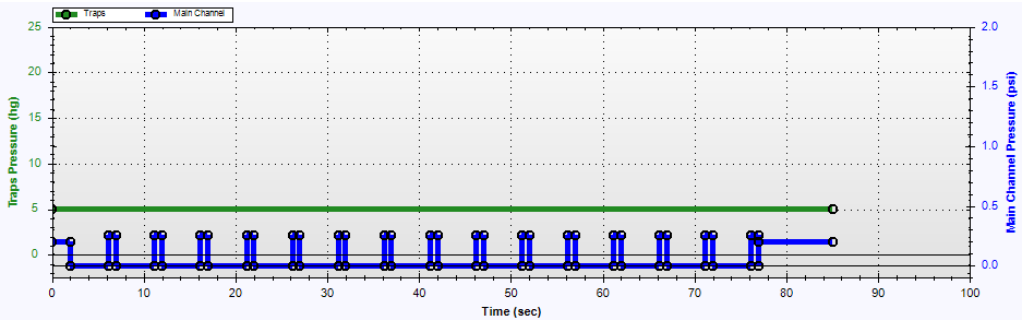

Figure 9. The overview of negative and positive pressure of main channel and micropipettes during trap phase. Green line is the constant negative pressure of traps. And blue line shows pulses of positive pressure for main channel that contain cells.

This phase is already conditioned by the morphology of the cell line used. For instance, for HEK-293 cell lines, cells tend to aggregate easily. The total duration of the Trap is 85 seconds. The traps exert a constant vacuum of 5 Hg during the 85 s, and 25 pulses of 0.25 psi for 0.8 s are applied to the main channel, each pulse had a baseline of 0.0 psi for 4.2 s. With these repeated pulses cells stop when they are passing the micropipettes and this increase possibility of the seal. The pulse voltage carries a holding potential fixed at -90 mV, and with a small jump to -95 mV to monitor changes in seal resistance.

Break: Once the seals have been made, the whole cell is achieved by breaking the patch of the membrane and accessing the cell interior. This is achieved by exerting a negative pressure slightly stronger than the previous phase. The reverse pressure exerted in this phase also depends on the cell line under study. For HEK-293, the sub-protocol lasts 18 s in which series of increasing pulses from 4 to 11 Hg with duration of 0.2 s.

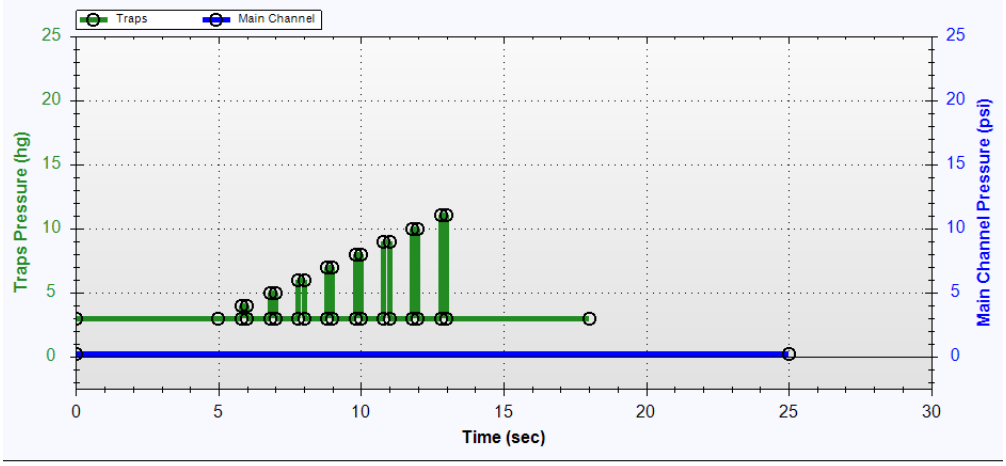

Figure 10. Break protocol: increasing pulses from 4 to 11 Hg with duration of 0.2 s

Data Acquisition: During the last phase, the compounds in the C1-C8 reservoirs immerse the cells in programmed time and order while recording the currents.

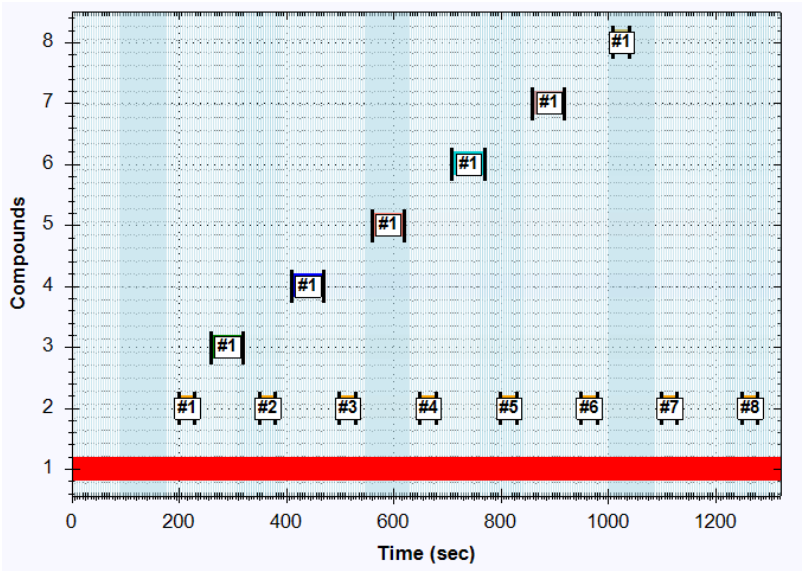

Figure 11. Program for compound addition in data acquisition, compound number 2 with 8 repetitions is 300 µM menthol.

In general, for the HEK-293 cell lines the main channel will have a positive pressure flow of 0.15 psi and in the traps the negative pressure maintained at 3 Hg. In all cases, the positive pressure of the compounds flow was 8 psi.

During data acquisition phase cells were voltage clamped at a holding potential of -60 mV and for ramp protocol stepped to -100 mV and then ramped to +100 mV in 200 mS and finally stepped back to -60 mV. Voltage command was executed each 5 s and currents were recorded with the sampling rate of 5 kHz at 20°C ± 1.

Cells were activated by 300 µM menthol for 30 s then exposed to drugs in different concentrations containing 300 µM menthol for 90 s with 30 s interval between each

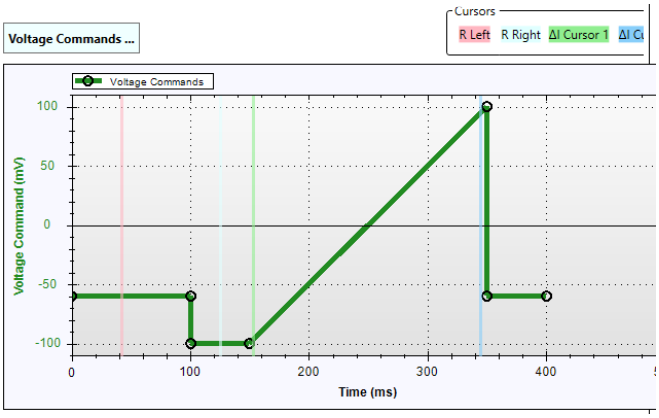

Figure 12. Voltage command for recording outward current of TRPM8

concentration, during intervals cells were under constant perfusion of external solution containing vehicle. In the end of each experiment, full block solution of AMTB 5 µM was applied to reach 100% inhibition. However, the duration of perfusing a compound could be adjusted based on kinetic of drug to reach plateau on effect of that compound.

2.2 Virtual screening

After identifying the most potent blocker drug from first group of drugs, the SwissSimilarity web tool http://www.swisssimilarity.ch (Zoete et al. 2016) were used to identify candidate ligands from approved drug library with similar structure to our most potent drug from the initial screening of sodium channel blockers. The server performs ligand-based virtual

screening with different approaches such as FP2 fingerprints, spectrophores, electroshape and align-IT screenings. Our library of compounds for screening is approved drugs.

2.3 Cell culture for WST-1 assay

MIA PaCa-2, PANC-1 and HEK-293 cell lines were cultured with DMEM (Euroclone) supplemented with 2% L-Glutamine (Euroclone), 10% FBS (Euroclone) and 1% penicillin/streptomycin (Euroclone) in T25 tissue culture flasks at 37° C, in a humidified 5% CO2 atmosphere. For BxPC-3 we used RPMI-1640 medium (Euroclone) instead of DMEM. Cells were maintained till they reach 70~80%. MIA PaCa-2, PANC-1, BxPC-3 and HEK-293 cell lines were obtained from the American Type Culture Collection ATCC (Manassas, VA, USA)

2.4 WST-1 assay

A total of 4 $\times 10^3$ cells/well were seeded into 96-well plates and were cultured for 24, 48, 72 h at 37˚C. 24 h after seeding cells were treated with different concentration of compounds and cellular proliferation was subsequently analysed by adding 10 µL cell proliferation reagent WST-1 (Roche Diagnostics) and incubated for 4 h at 37°C and 5% CO_2 according to the manufacturer's protocol. The absorbance was measured at 440 nm using a multimode plate reader.

2.5 Manual Patch-clamp experiments

Cells were plated on 35 mm cell culture dishes 24 hours before experiment. Whole cell patch clamp experiments were performed at the -60 mV holding potential. Currents were recorded at room temperature (21 ± 1° C). Same ramp protocol that was used in automated patch clamp was used in manual patch clamp for studying TRPM8 currents. And currents were

elicited by 300 μM menthol. Also compounds in different concentration were co applied with 300 μM menthol.

Pipette (Harvard Apparatus) resistances were about 5 MΩ. Cell capacitance and series resistance errors were compensated (85-90%) before each voltage clamp protocol was run to reduce the voltage errors to less than 5% of the protocol pulse. Currents were sampled at 10 kHz (Digidata 1440A), filtered at 3 kHz, amplified with Axopatch 1D, and measured in the whole-cell patch clamp mode (pClamp 9.0).

The extracellular solution contained 140 mM NaCl, 4 mM KCl, 1 mM $MgCl_2$, 10 Mm glucose, and 10 mM HEPES, pH 7.4 with NaOH and 310 mOsm, we removed Ca^{2+} from external solution to avoid Ca^{2+}-dependant desensitization of TRPM8. The intracellular solution for the whole-cell voltage clamp contained the following (mM): 60 CsCl, 70 CsF, 5 Na_2ATP, 10 HEPES, and 10 EGTA, pH 7.2 with CSOH and 295 mOsm.

2.6 Western blot

Total and membrane protein extraction were performed by standard methods using 1× lysis buffer (Cell Signaling Technology). Proteins were electrophoretically separated on 7.5 or 10% SDS-PAGE (Bio-Rad, Hercules, CA) using Tris-glycine sodium dodecyl sulfate (SDS) buffer (Bio-Rad) at a constant voltage of 180 V. The electrophoresis buffer for the native gels did not contain SDS. Protein bands were visualized by staining with Coomassie blue.

For Western blot analysis, protein was transferred onto polyvinylidene fluoride (PVDF) membranes (EMD Millipore). membrane was blocked in 5% non-fat dry milk and incubated overnight at 4 °C with anti-TRPM8 antibody (Abcam-ab109308) and anti-α Tubulin antibody (T3526 Sigma) in 1:1000 concentration. Excess primary antibodies were washed by the

membrane in Tris-buffered saline containing 0.1% Tween 20. For secondary Antibody, anti-Rabbit IgG (A6154 Sigma) were used in 1:10000 concentration for detection. The protein levels of TRPM8 were normalized with those of Tubulin by quantifying the protein levels in the uncompressed images using the National Institutes of Health (NIH) ImageJ 1.6 software.

2.7 Chemicals

All drugs and chemical reagents were purchased from Sigma-Aldrich (St. Louis, MO). Reference compounds were prepared in dimethyl sulfoxide (DMSO) (Sigma) at 10 mM stocks and stocks kept at -20°C. Different concentrations were obtained by serial dilution of the stock solution in extra cellular solution, with final concentration of DMSO was 0.3%.

2.8 Molecular docking study

To have better understanding of possible mechanism of drugs, we performed docking studies using two different methods, site specific and blind docking. For site specific docking we used Autodock vina 1.1.2 software(Trott and Olson 2010), and for blind docking we used SwissDock webserver http://www.swissdock.ch (Grosdidier, Zoete, and Michielin 2011). In site specific docking we restrict ligand to known binding site, while in blind docking ligand has freedom and we don't define a specific site.

2.8.1 Autodock vina

To predict and analyse possible protein-ligand interactions with the known binding site on TRPM8, we performed docking using Autodock vina 1.1.2 software(Trott and Olson 2010).

TRPM8 structure (PDB code: 6O6R)(Diver, Cheng, and Julius 2019) obtained from the RCSB Protein Data Bank (available at http://www.rcsb.org). PDB file for ligands were obtained from DrugBank(Wishart et al. 2018) (https://go.drugbank.com/) and AutoDock tool 1.5.7 software was used to prepare the structure.

All nonprotein molecules were removed from the proteins, polar hydrogen atoms were added, and non-polar hydrogen atoms were merged. We defined flexible residues around binding pocket, and the grid dimension and box based on the binding site. The structure of protein and ligands were converted to pdbqt format.

2.8.2 SwissDock

Blind docking was executed on SwissDock webserver(Grosdidier, Zoete, and Michielin 2011), which is based on EADock DSS engine, we uploaded same PDB file used for Autodock vina on SwissDock webserver. And ligands were uploaded in mol2 format on SwissDock webserver. Flexibility of docking was on 5 angstrom and the type of docking set on accurate.

2.8.3 Analysing and visualising docking results

UCSF-Chimaera software(Pettersen et al. 2004) was used to perform the analyses of all docked poses resulted from two methods, and binding pose with minimum binding energy for each ligand was selected for analysis. Furthermore, the 2D representation of ligand-protein is provided by the program LigPlot+(Laskowski and Swindells 2011).

2.9 Data analysis

Analysis of data for automated patch clamp was carried out using the 'data analyzer 5.0 software' (IonFlux 16 software application), Microsoft Excel-365 and the Prism 9.0 software (GraphPad Software Inc., San Diego, CA, USA) for results manual patch clampfit 9.0 was used along with Microsoft Excel-365 and the Prism 9.0 software.

The average current amplitude of the last 3 recordings for each compound application period was used as the current amplitude for effect of each concentration of compound. Inhibition of drugs on menthol induced currents were normalized to current induced by menthol in 300 µM concentration and currents during washing with vehicle considered as baseline. Percent inhibition of TRPM8 channel current at each compound concentration was determined using Eq. 1.

Eq. 1 $$\% \, Inhibition \, of \, I = 100 \times \left(\frac{I_{control} - I_{drug}}{I_{control}}\right)$$

IC_{50} and EC_{50} were calculated by fitting to 4-parameter Hill equation using GraphPad Prism 9. In the 4-parameter logistic equation, $I_{min} = 0$ and $I_{max} = 100$ (agonist) or $I_{min} = 100$ and $I_{max} = 0$ (antagonist), h is the Hill coefficient, C is the concentration of the agonist or antagonist, and C_{50} is the EC_{50} (agonist) or IC_{50} (antagonist) value. Data are expressed as mean ± standard deviation (SD).

Eq.2: 4-parameter Hill equation: $f(x) = I_{min} + \left(\frac{I_{max} - I_{min}}{1 + \left(\frac{C_{50}}{x} \right)^{h}} \right)$

Significance testing was performed using one-way analysis of variance (ANOVA), followed by post-hoc Tukey test. $P<0.05$ was considered to indicate a statistically significant difference with control.

Results

3.1 Evaluating TRPM8 via IonFlux 16

TRPM8 is known to be a thermosensitive ion channel, activated by cold temperatures (below ~25˚C) and ligands like menthol, and icilin. Since icilin (but not menthol) needs extracellular Ca^{2+} to activate TRPM8, and due to Ca^{2+}-dependent desensitization, icilin is not suitable for repeated activation. We choose menthol as activator to remove Ca^{2+} and Ca^{2+}-dependent desensitization. The outward currents elicited by 50, 100, and 200 µM menthol are shown in Figure 13. The current provoked by menthol is totally reversible upon washing and are dependent on the menthol concentration. The activation by menthol reaches steady state quickly and the time gap between perfusion of menthol and activation of TRPM8 is within seconds. In contrast, no menthol-induced currents were detected in wild type HEK-293 cells (data not shown).

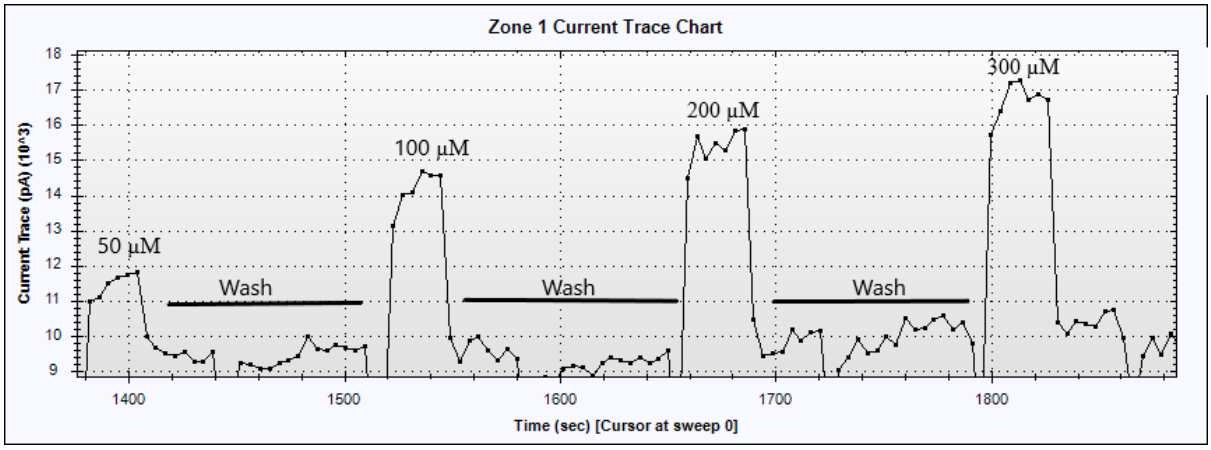

Figure 13. The outward current at +80 mv, elicited by activating HEK-293 cells expressing TRPM8 ion channels with increasing concentrations of menthol 50, 100, and 200 µM Using ramp protocol (-100 mV to +100 mV over 200 ms)

The concentration response relationship obtained for menthol using a voltage ramp protocol is shown in Figure 14. The EC50 = 118.2 ± 14 μM (n ≥ 6; Hill coefficient 1.89).

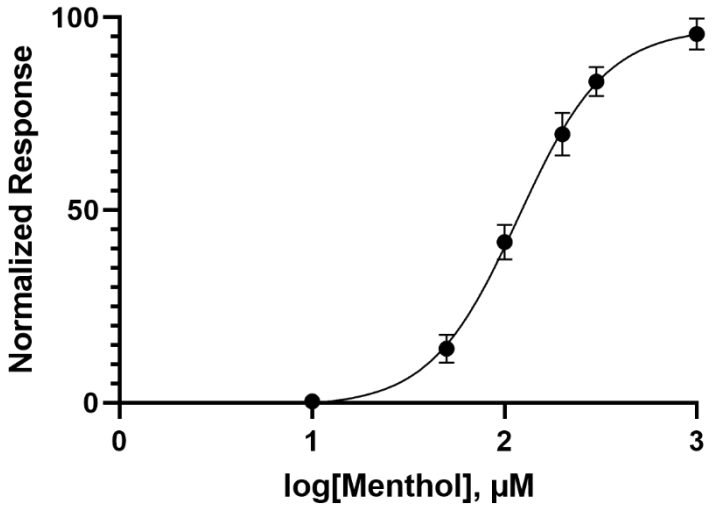

Figure 14. Concentration response curve for menthol using IonFlux 16 system. The EC_{50} for menthol is 118.2 ± 14 μM (n ≥ 6)

A common problem with studying effect of compounds on ion channels is current instability, which could be caused by variations in patch-clamp parameters or properties of channel. After adjusting the parameters, including solutions composition, we have obtained a high stability in recorded currents. Indeed, as we can observe in Figure 15, the TRPM8 current activated by menthol has shown a long-lasting stability even after 25 minutes from the start of the experiment and the frequent cycles of washing. The current amplitude in the presence of menthol remained relatively stable throughout the 22 periods of menthol application. Menthol induced currents showed <5% rundown during 25 minutes recording.

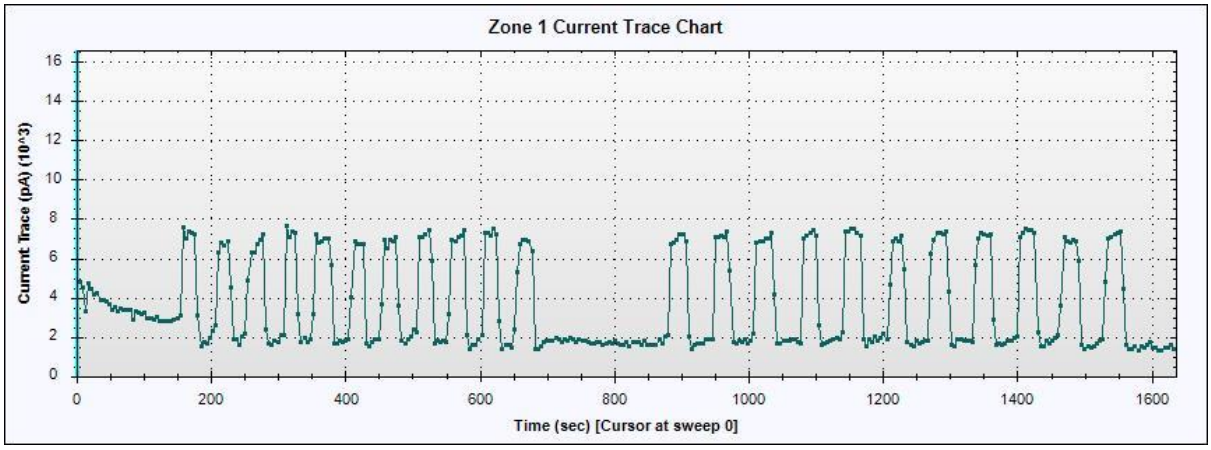

Figure 15. High stability of TRPM8 currents activated by 300 µM menthol at 20° C. In this graph the current density at +80 mv against time is represented.

Steady activation by 300 µM menthol for 200 seconds after 30 minutes, also confirms stability of currents (Figure 16). Stability of current is mostly important for compounds with slower kinetics.

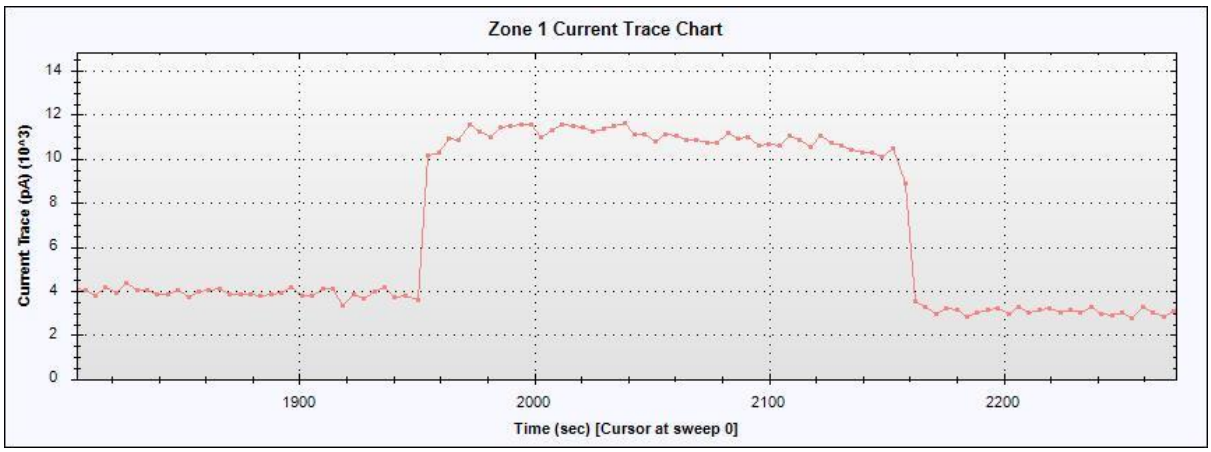

Figure 16. Steady activation of TRPM8 by 300 µM menthol for 200 seconds.

We also tested blocking effect of AMTB a selective antagonist for TRPM8 by co applying with menthol. AMTB is well known antagonist for TRPM8 ion channel, which the 3D structure of bound state for AMTB with TRPM8 is available on RCSB database. The

blocking effect of 500 nM of AMTB on outward current provoked by 300 µM menthol is shown in Figure 17. On average over several recordings, inhibition by 500 nM AMTB reached a steady-state value of ~70% inhibition after 100 seconds of application, whereas rundown in only menthol controls for these experiments remained small (Figure 16).

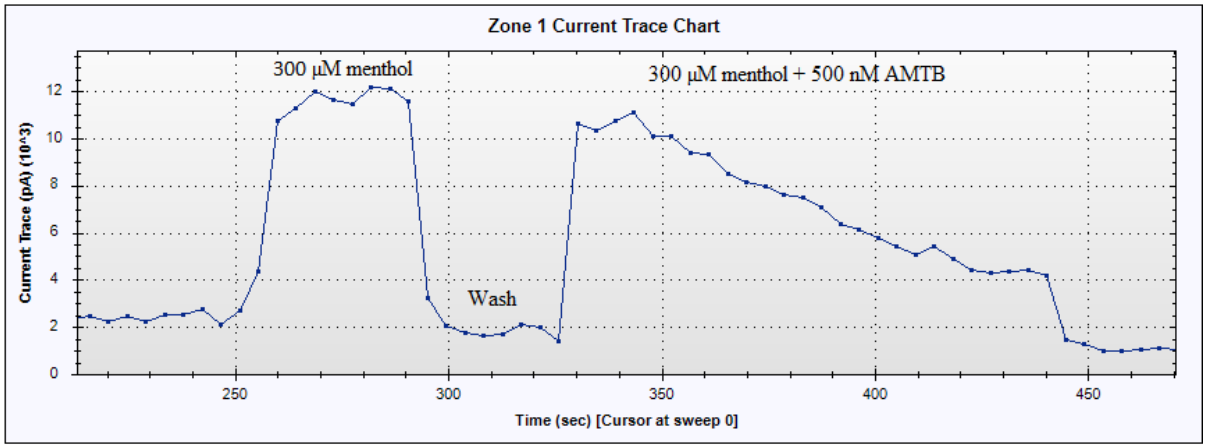

Figure 17. Time and concentration dependence inhibition of 500 nM AMTB on the outward current induced by 300 µM menthol and using ramp protocol (-100 mV to +100 mV over 200 ms). Graph shows current density at +80 mv.

The concentration response relationship obtained for AMTB with using same voltage ramp protocol, and The IC_{50} = 355.5 ± 25 nM (n ≥ 6; Hill coefficient 4.02), which is in agreement with the IC_{50} value previously reported using conventional patch clamp. AMTB was also difficult to wash due to its high affinity to the binding site, which required longer duration of washing.

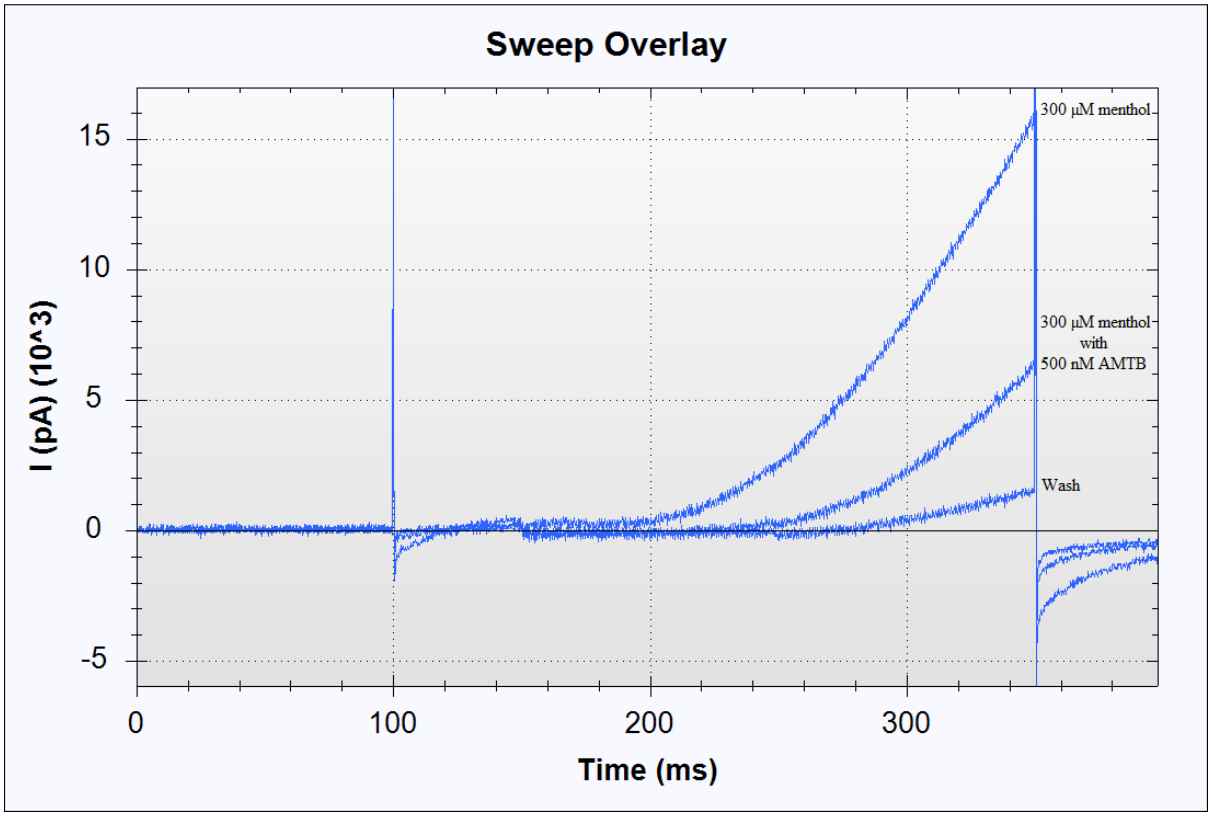

Figure 18. Currents elicited by a voltage ramp protocol from −100 mV to +100 mV in the absence (wash) and presence of 300 µM menthol and inhibitory effect of 500 nM AMTB on activated TRPM8 ion channels by 300 µM menthol.

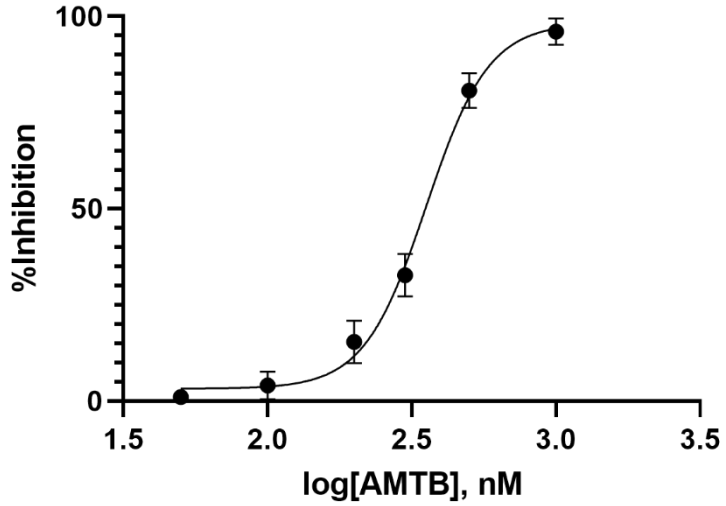

Figure 19. Concentration–response relationship for AMTB obtained using IonFlux 16. The IC_{50} of AMTB is 355.5 ± 25 nM.

3.2 Screening sodium channel blockers

We started by screening a group of sodium channel blockers mentioned in Table 1. Our first library of drugs contains 12 sodium channel blocker drugs: mexiletine, propafenone, ranolazine, carbamazepine, tetracaine, flecainide, rufinamide, gabapentin, oxcarbazepine, lamotrigine, phenytoin, riluzole. In whole plate we could test 2 different concentrations above and below 50 µM with 2 repeats for each drug.

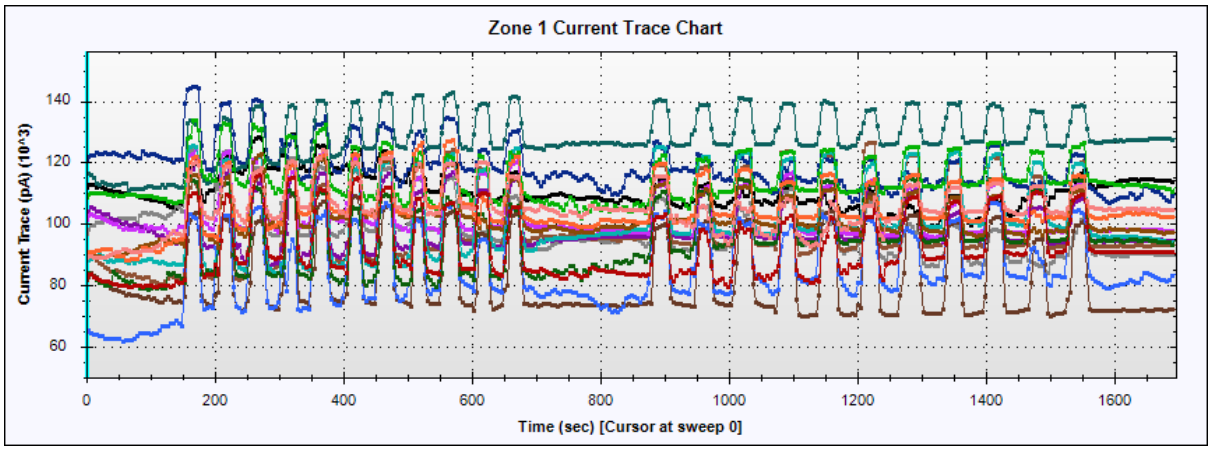

Figure 20. Raw data of currents at +80 mv recorded using whole plate in one experiment. As its shown each compound has repeated after long period of washing, however in second term the duration of perfusion for each concentration is longer.

Most of drugs did not have any blocking effect on outward currents of TRPM8 channel evoked by menthol. Among those drugs only flecainide, phenytoin and propafenone had blocking effect. For flecainide and phenytoin partial blocking was beyond 50 µM, which is high enough to not be considered as potent blocker (Figure 21).

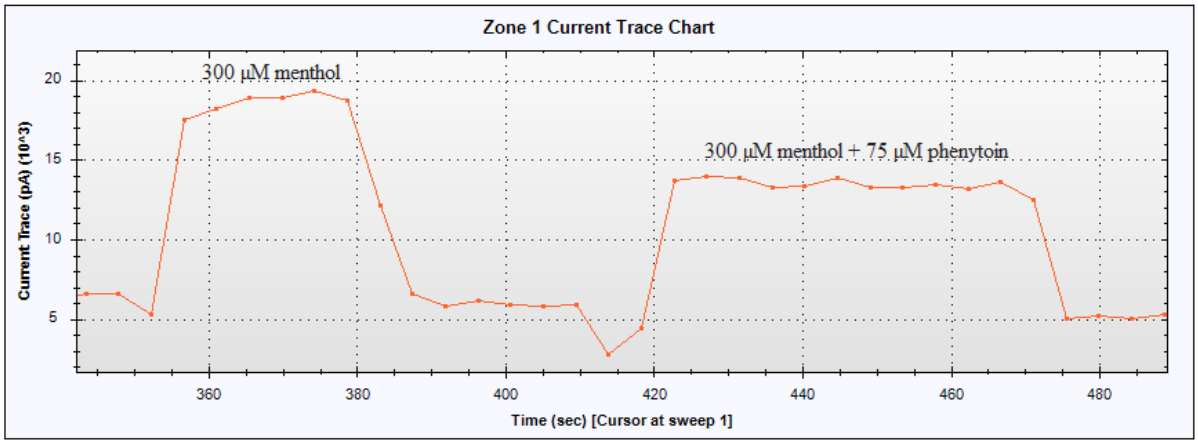

Figure 21. Current density graph at +80 mv shows 75 µM phenytoin only had around 38% blockade on menthol evoked current.

Only propafenone had significant blocking below 50 µM. Hence, we further studied propafenone in different concentrations. In the figure 22, in figure "a" represents effect of 300 µM menthol and b, c, d, e represents effect of 5, 25, 50 and 75 µM propafenone co applied with menthol, respectively. Before and after of each compound, cells were washed for 30 seconds.

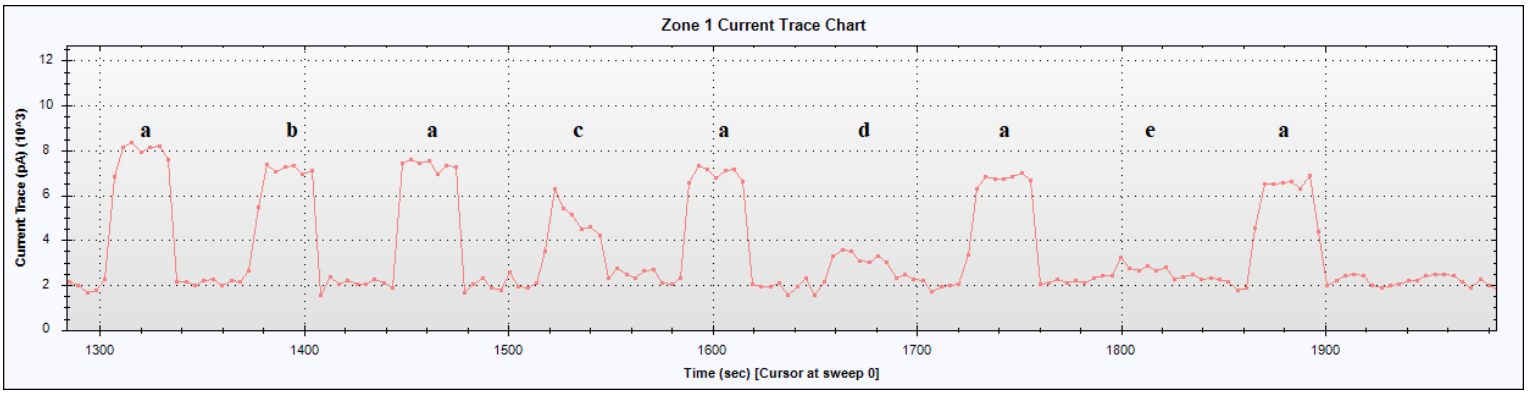

Figure 22. TRPM8 currents at +80 mv from ramp protocol evoked by applying 300 µM menthol alone, and co applied with different concentration of propafenone on stable transfected HEK-293 cells. In this figure "a" represents effect of 300 µM menthol and b, c, d, e represents effect of 5, 25, 50 and 75 µM propafenone co applied with menthol,

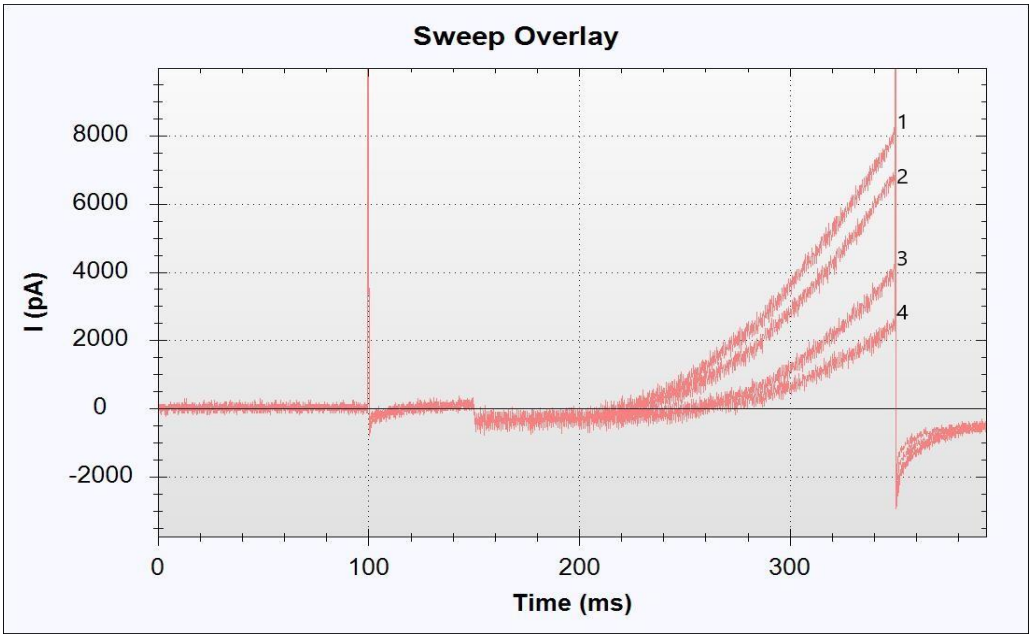

Figure 23. Outward TRPM8 currents in stable transfected HEK293 cells at 20° C evoked by 300 µM menthol (#1). The currents # 2, 3, and 4 are recorded after the addition of 5, 25, and 75 µM propafenone co applied with 300 µM menthol, respectively.

As it shown in figures 22 and 23, 75 µM propafenone blocks more than 90% of currents evoked by 300 µM menthol. The concentration response relationship obtained for propafenone shown in figure 24 and with the IC_{50} = 16.8 ± 5 µM (n ≥ 6; Hill coefficient 1.78).

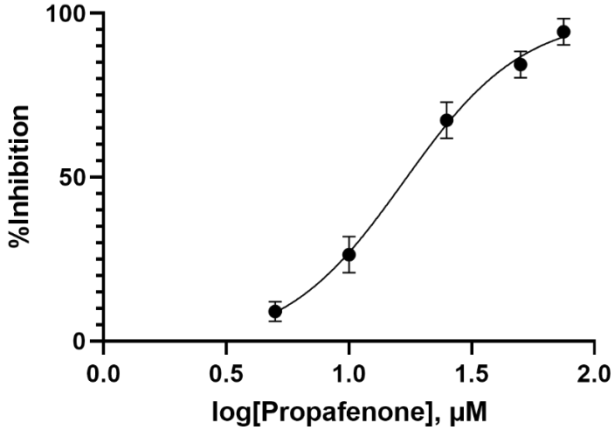

Figure 24. concentration–response curve relationship for propafenone. The solid line represents the best fit for the data with an IC50 value of IC50 = 16.8 ± 5 µM (mean ± SD) and a Hill coefficient of 1.78.

3.3 Virtual screening

To optimize our screening for identifying potent antagonist for TRPM8 ion channel we searched for compounds similar to structure of propafenone. By ligand based virtual screening on the SwissSimilarity platform(Zoete et al. 2016), we are able to identify compounds from FDA approved drugs or other libraries with respect to our reference structure which is propafenone.

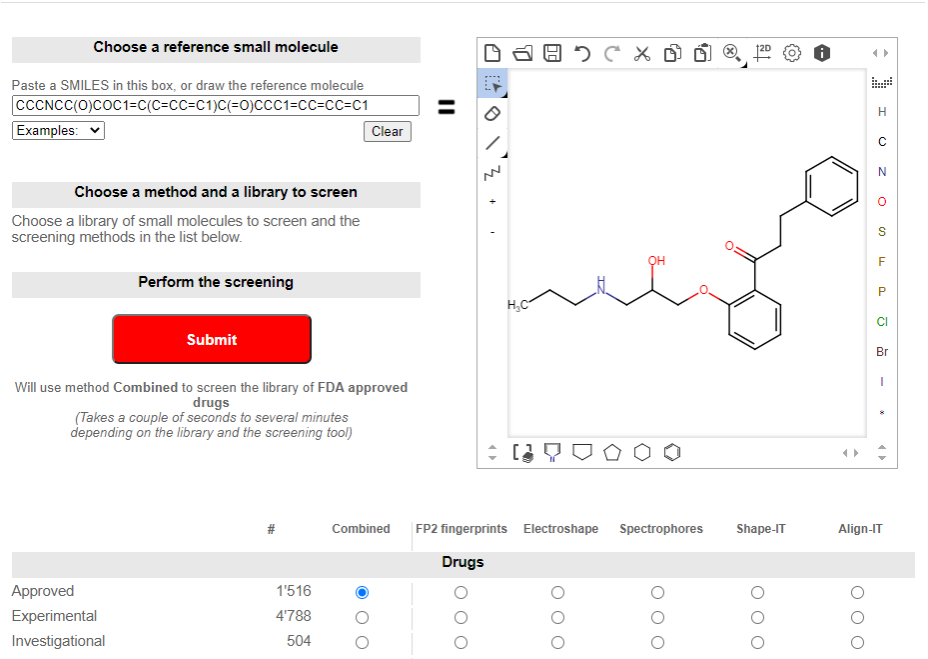

Figure 25. Submission page, the query molecule could be submitted either by drawing it by embedded molecular editor or pasting its SMILES in the dedicated text box. The method of screening and the library of screening can be selected at the submission page.

Our virtual screening library was from FDA approved drugs with 1516 drugs, and among methods of screening only FP2 fingerprint, electroshape, spectrophores and combined

methods had results with 11, 215, 400, 215 drugs, respectively. Propafenone also was one of results in the screening.

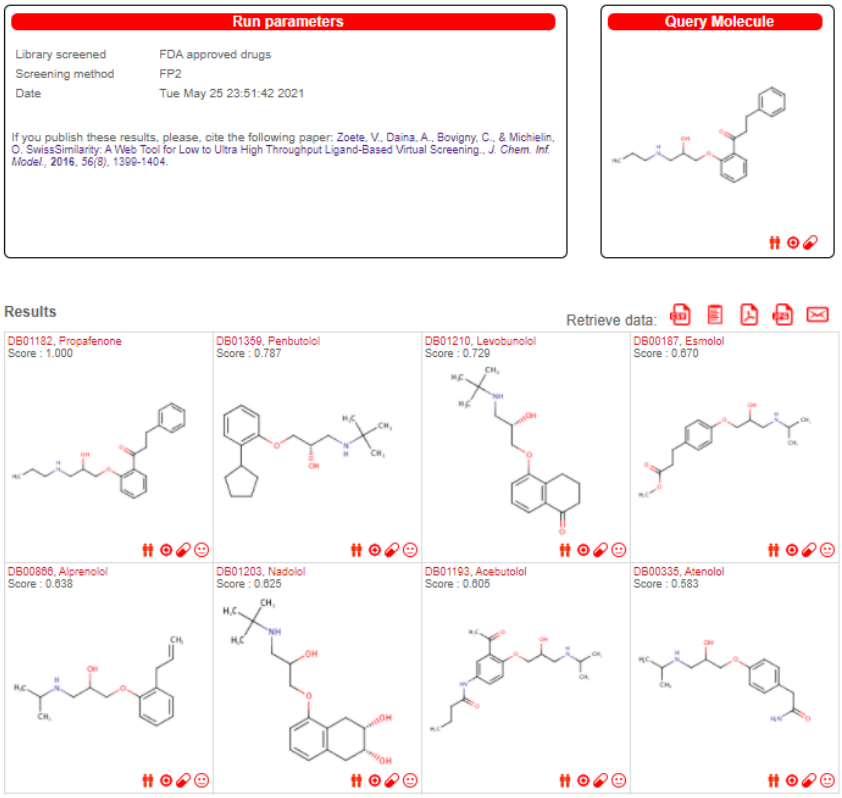

Figure 26. Example of an output page obtained by screening the FDA approved drugs against propafenone as reference ligand with FP2 method. The molecules most similar to the reference molecule are displayed based on the similarity score with links to their databases of origin (e.g., DrugBank, ChEMBL, etc.). As it shown most similar identified structure is propafenone itself.

The screened drugs were ordered based on similarity score values, ranged from 0 to 1. Scores closer to 1 are much similar to reference molecule. Most of the results with highest scores in similarity to propafenone were belong to beta blocker drugs.

Results

Table 2. Part of virtual screening outputs for different screening methods, results are ordered based on the similarity score. As you can notice propafenone is part of results, interestingly in spectrophres method it has less similarity than primaquine.

	FP2 fingerprint	Electroshape	Spectrophores	Combined
1	Propafenone	Propafenone	Primaquine	Propafenone
2	Penbutolol	Atenolol	Propafenone	Penbutolol
3	Levobunolol	Propranolol	Clomipramine	Levobunolol
4	Esmolol	Alprenolol;	Solifenacin	Alprenolol
5	Alprenolol	Metipranolol	Amoxapine	Esmolol
6	Nadolol	Bevantolol	Cloperastine	Atenolol
7	Acebutolol	Sotalol	Azelastine	Metipranolol
8	Atenolol	Bupranolol	Desipramine	Nebivolol
9	Nebivolol	Oxprenolol	Bicalutamide	Acebutolol
10	Metoprolol	Cyclopentolate	Bromfenac	Nadolol
11	Metipranolol	Pindolol	Amlodipine	Metoprolol
12		Levobunolol	Nebivolol	Propranolol
13		Carteolol	Nortriptyline	Bevantolol
14		Homoharringtonine	Levomilnacipran	Sotalol
15		Labetalol	Propranolol	Cyclopentolate
16		Dipivefrin	Penbutolol	Bupranolol
17		Esmolol	Atomoxetine	Oxprenolol
18		Fursultiamine	Carbinoxamine	Pindolol
19		Penbutolol	Loxapine	Carteolol
20		Mirabegron	Clemastine	Homoharringtonine

As it is mentioned in Table 2, most of results are from beta blocker drugs. Based on these results and the availabilty of compounds we selected 7 drugs (Figure 27) from beta blockers for second part of screening with IonFlux 16. Our selection of drugs were based on availability of drugs with structural varity.

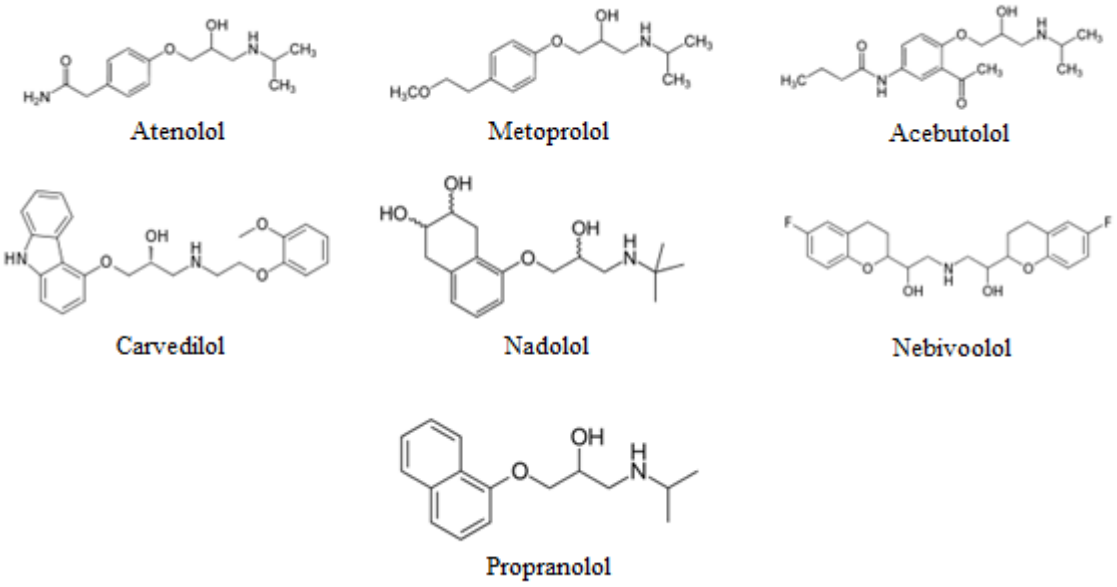

Figure 27. Selected drugs from beta blockers to screen via IonFlux 16

3.4 Screening beta blockers

From selected compounds we identified propranolol, carvedilol and nebivolol with blocking effect on menthol evoked currents of TRPM8 ion channels. Propranolol was not potent blocker as much as propafenone and had IC_{50} equal to 45 ± 7 µM (n ≥ 6; Hill coefficient 1.35).

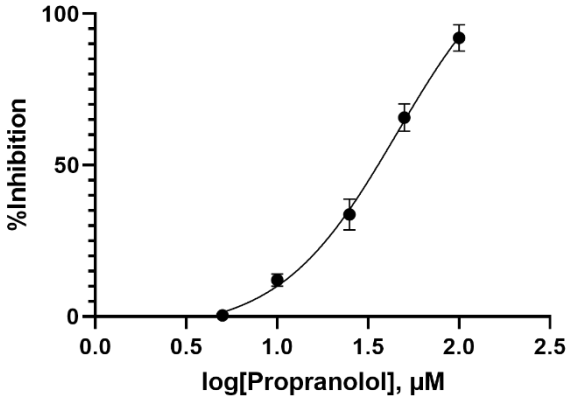

Figure 28. Concentration–response curve for propranolol. The solid line represents the best fit for the data with IC_{50} of 45 ± 7 µM (mean ± SD)

Carvedilol with IC_{50} = 9.1 ± 0.6 µM and hill coefficient of 3.75, is second most effective blocker we identified for TRPM8 ion channel.

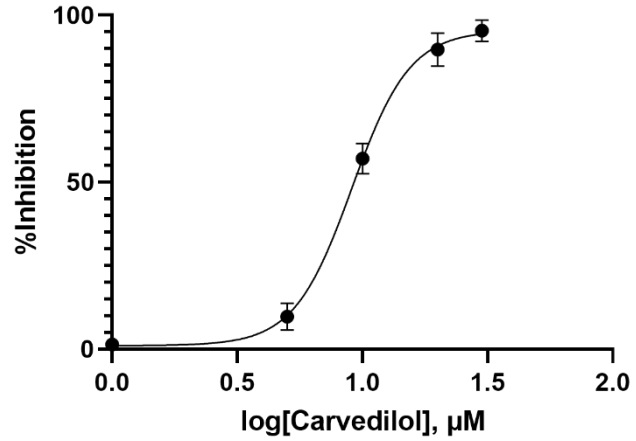

Figure 29. Concentration–response curve for carvedilol, with IC50 = 9.1 ± 0.6 µM.

Nebivolol was the most potent blocker we identified among drugs, with IC_{50} = 0.97± 0.15 µM and hill coefficient of 2.99.

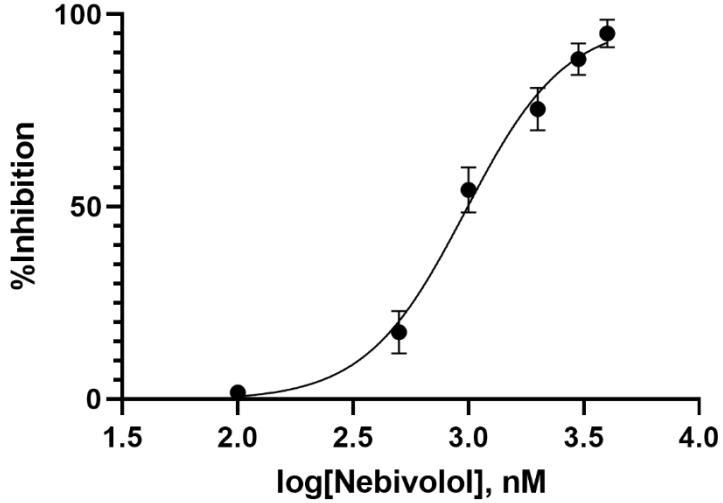

Figure 30. Concentration–response curve relationship for nebivolol, with IC_{50} value of 0.97 ± 0.15 µM (mean ± SD)

Similar to AMTB, both nebivolol and carvedilol were difficult to wash due to their higher affinity, and it required longer duration of washing (Figure 31).

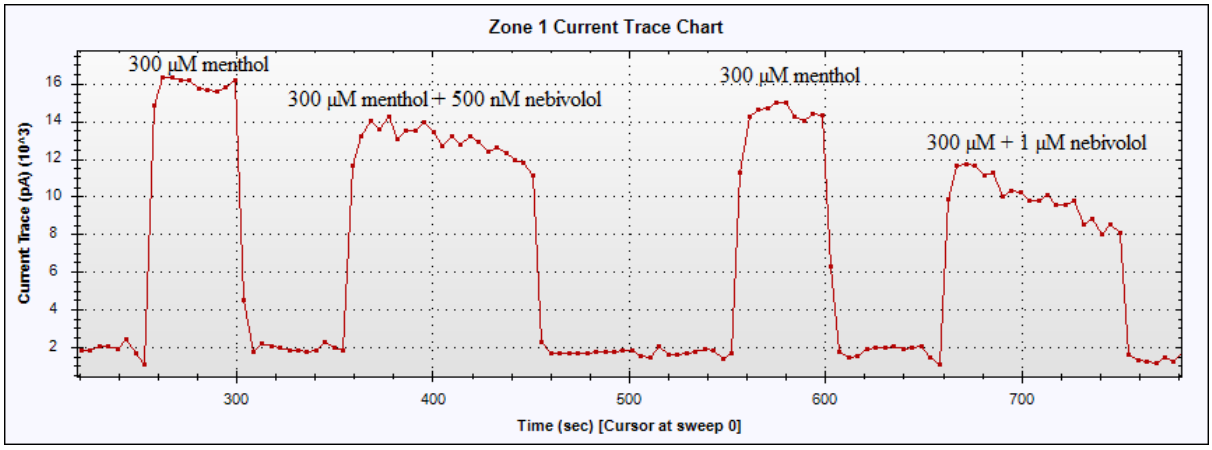

Figure 31. Time and concentration dependence inhibition of 500 nM and 1 µM nebivolol on the outward currents induced by 300 µM menthol and using ramp protocol (-100 mV to +100 mV over 200 ms). Each point in graph is current density at +80 mv.

3. 5 Manual patch clamp electrophysiology

To examine validity of our results from Automated patch clamp system. We had to determine EC_{50} and IC_{50} for menthol and AMTB on TRPM8 with manual patch clamp electrophysiology as gold standard. We used the same protocol and solutions that was used for Automated patch clamp. The EC50 for Menthol was 152± 32 µM And IC_{50} for AMTB was 407 ± 40 nM (Figure 32).

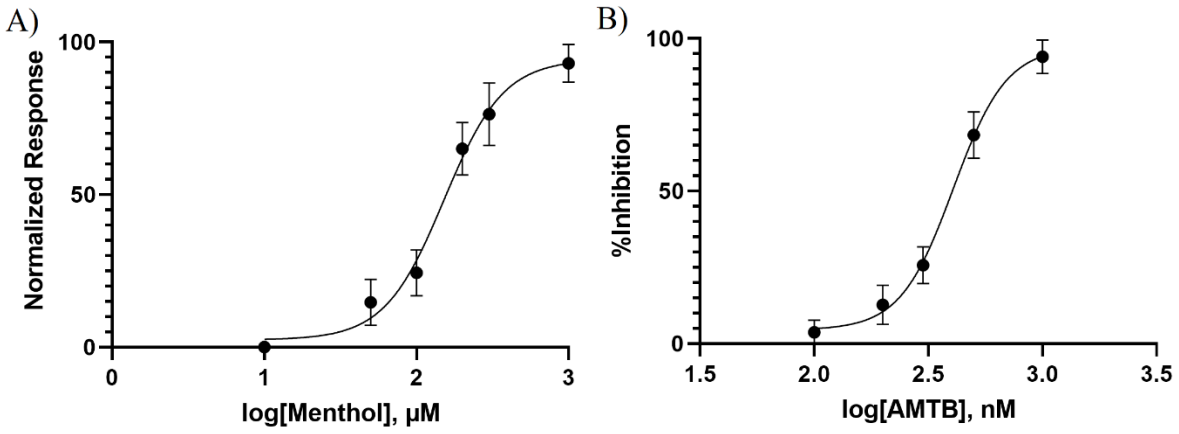

Figure 32. Concentration–response curve for Menthol and AMTB using manual patch clamp, EC50 of menthol is 152 ± 32 µM And IC50 for AMTB was 407 ± 40 nM

We also tested inhibitory effect of nebivolol on TRPM8 ion channel as most potent identified drug with same method used in automated patch clamp. The IC_{50} determined by manual patch clamp for nebivolol was 1.43 ± 0.38 µM (Figure 33).

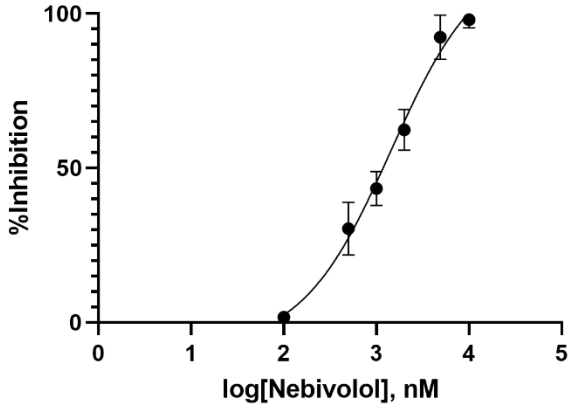

Figure 33. Concentration–response curve for nebivolol determined by manual patch clamp, IC50 is 1.43 ± 0.38 µM.

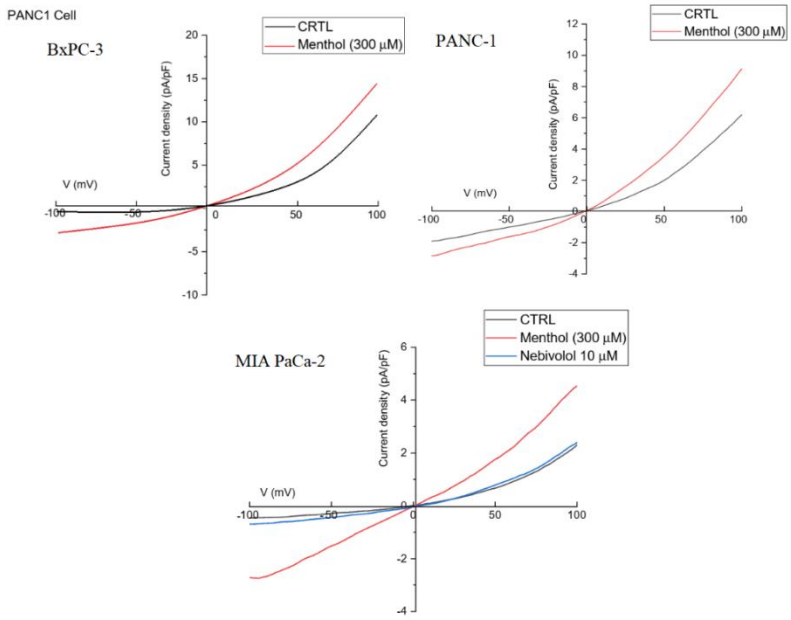

Figure 34. Effect of 300 µM menthol on outward current of pancreatic cancer cells evoked by ramp voltage.

Functionality of TRPM8 ion channels in MIA-PaCa 2, PANC-1, and BxPC-3 were examined by activating them with 300 µM menthol while recording via whole cell patch clamp

electrophysiology. The cancer cells show increase in the outward current made by ramp protocol while treated with 300 μM menthol.

3.6 Western blot

We also evaluated expression of TRPM8 ion channels via western blot assay. All three cancer cell lines were expressing detectable amount of TRPM8 ion channel. Expression of TPRM8 was confirmed in all three cancer cell lines. Higher expression of TRPM8 is noticeable in BxPC-3 cell line.

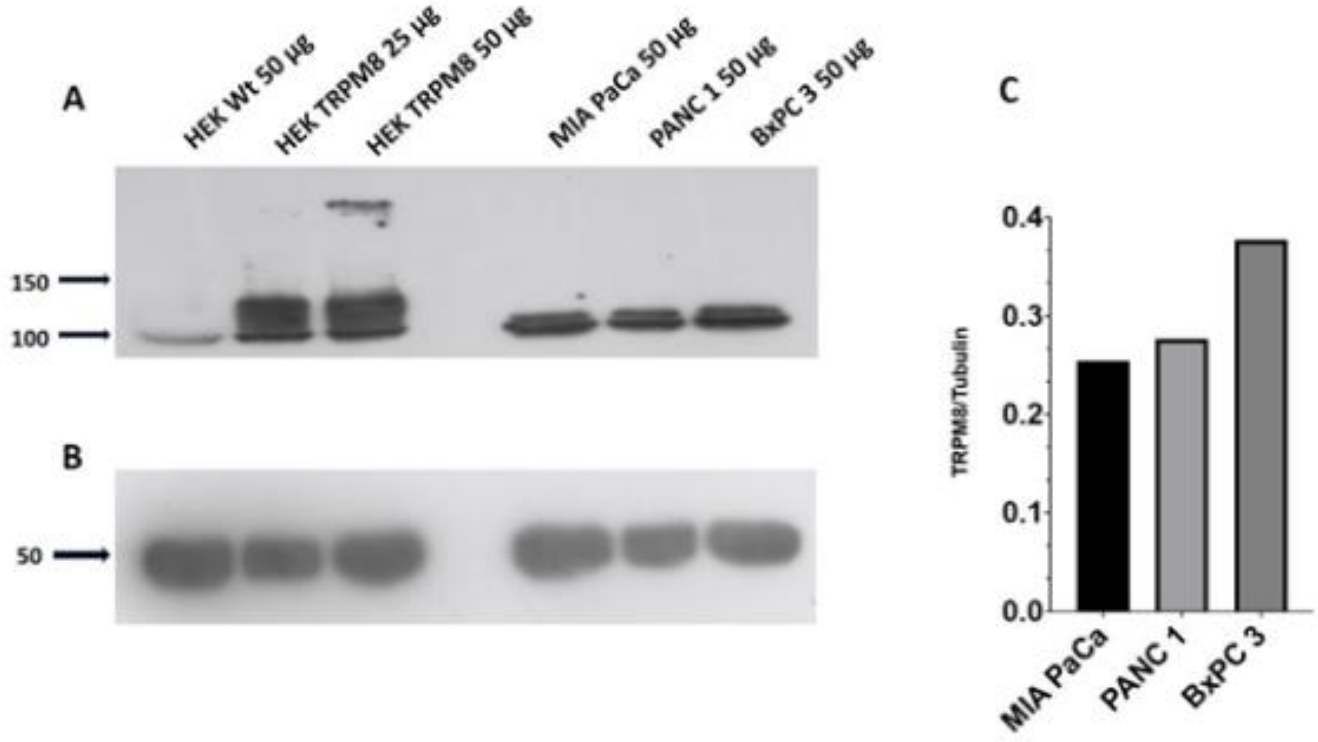

Figure 35. TRPM8 expression in pancreatic cancer cells. Western Blot was performed loading 50 ug of total lysates. HEK-293 cells (HEK-WT) and HEK-293 TRPM8 transfected cells (HEK TRPM8) were used as negative and positive control, respectively. A: antiTRPM8 antibody (Abcam); B: anti-α Tubulin antibody (Sigma); C: densitometric analysis performed using ImageJ software.

3.7 WST-1 Cell Cytotoxicity Assay

From drugs we identified propafenone and propranolol didn't have cytotoxicity on any of cells at up to 50 µM concentration. In correlation with potency of drugs, nebivolol had highest cytotoxicity against cancer cells, it was also toxic on wild type HEK-293 and TRPM8 expressing HEK- 293 cells.

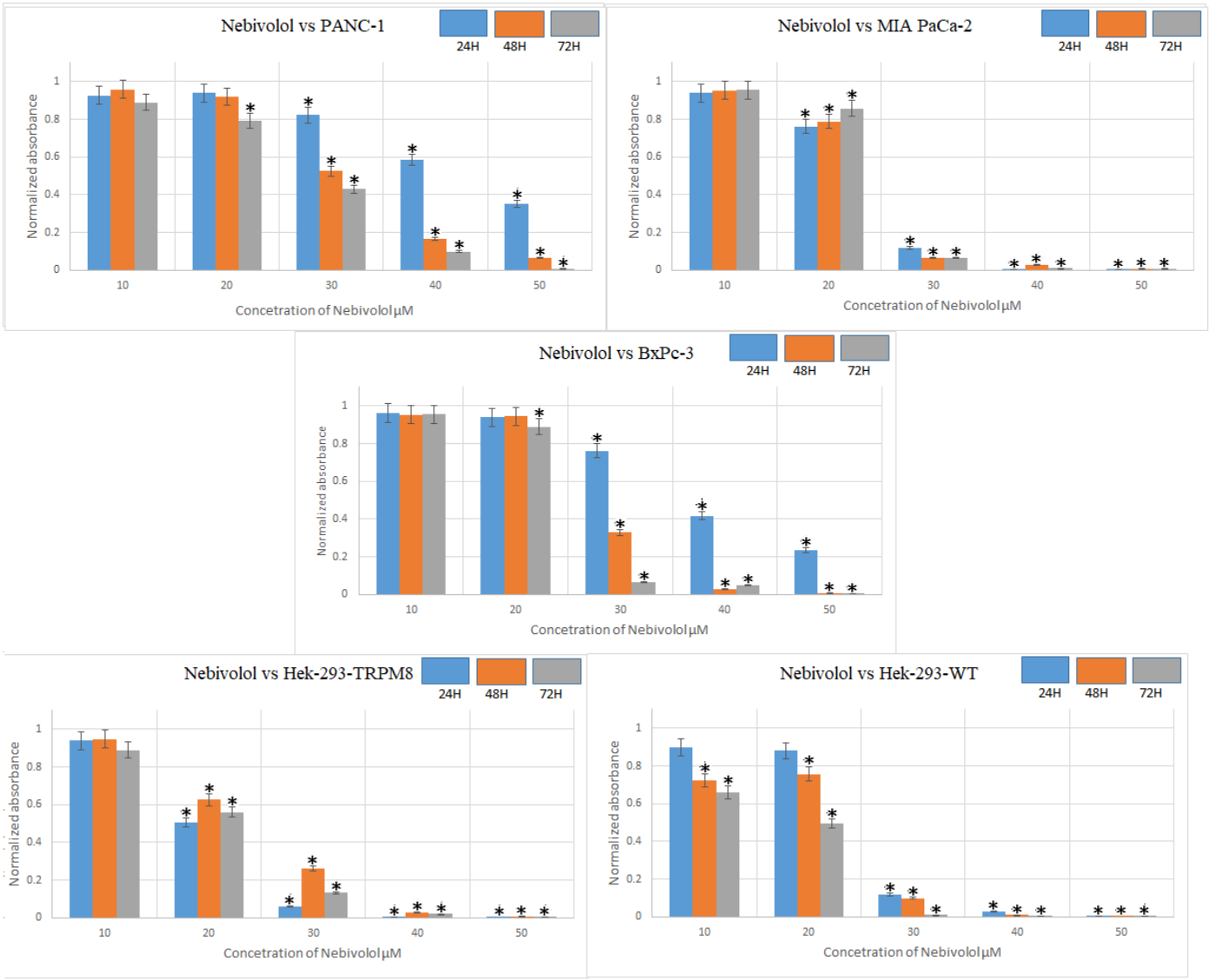

Figure 36. Concentration and time dependant changes in viability of different cell lines after treating with different concentrations of nebivolol. Three independent experiments performed in triplicate and all data are expressed as means ± SD. ∗$p<0.05$

Results

Carvedilol was less cytotoxic against cancer cells, but it also didn't show significant cytotoxicity on wild type HEK-293 up to 40 µM concentration.

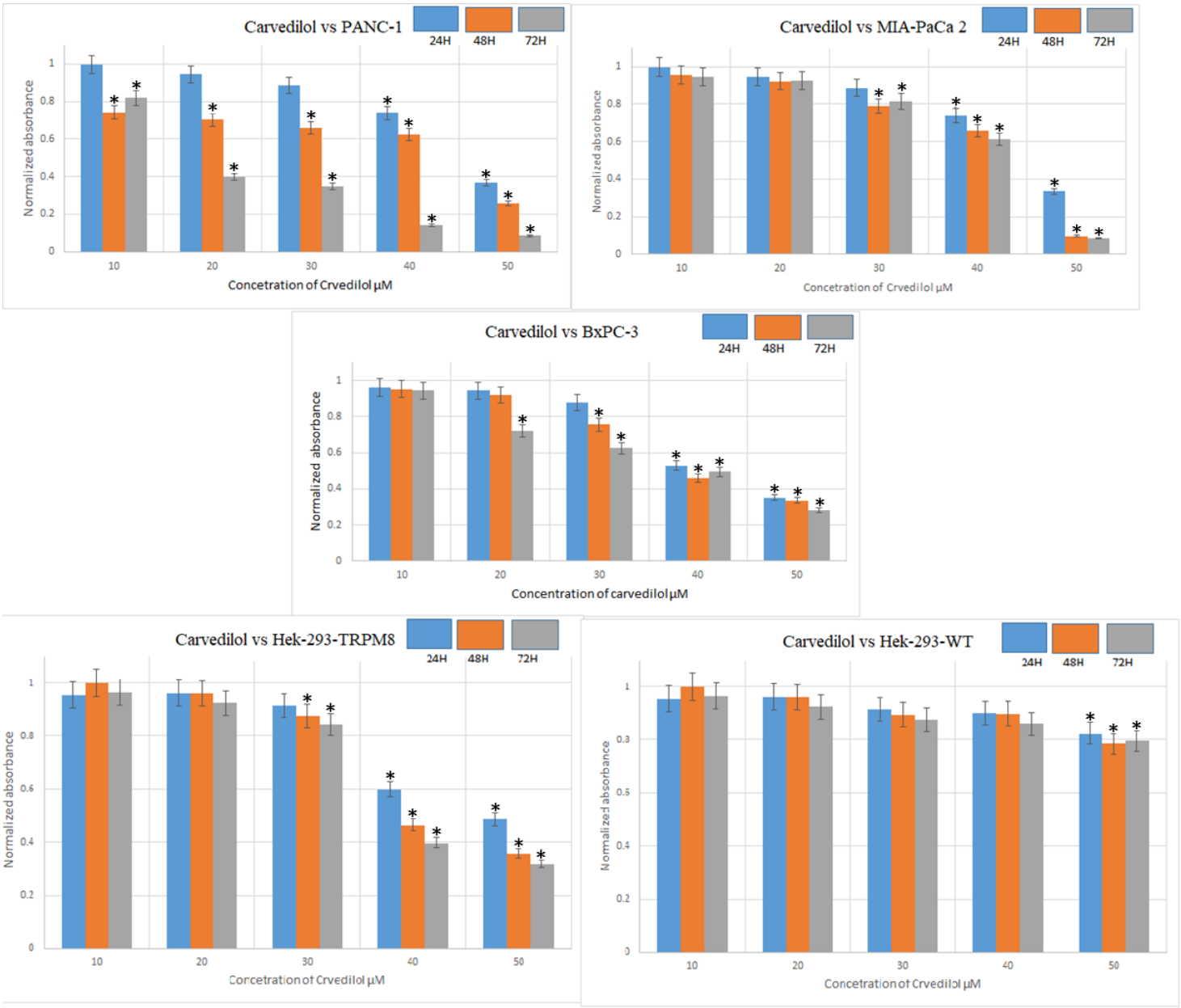

Figure 37. Concentration and time dependant changes in viability of different cell lines after treating with different concentrations of carvedilol. Three independent experiments performed in triplicate and all data are expressed as means±SD. ∗p<0.05

3.8 Molecular docking

3.8.1 Autodock vina

The docking results by Autodock vina predicted likely interactions with the antagonist binding site in the transmembrane region between S1, S2, S3 and S4 (Figure 38. a, c). For each docking experiment 9 different binding modes were predicted by Autodock vina, we selected the binding mode with minimum binding energy. The minimum binding energy for nebivolol, carvedilol, propafenone and propranolol was -11.4, -13.3, -9.1, and -10.4 kcal/mol respectively.

As it shown in 2D plot nebivolol has 5 different possibility of hydrogen bonds with Gln776, Asn790, Glu773, and Asp793 in the binding site of TRPM8. Additionally, two π–π stacking interactions are identifiable in the binding site, a face-to-face interaction with Tyr736 and T-shaped interaction with Tyr995. Other residues (Phe729, Arg998, Phe1003, Val733, Ile836, Arg832) are involved in hydrophobic interactions. (Figure 38)

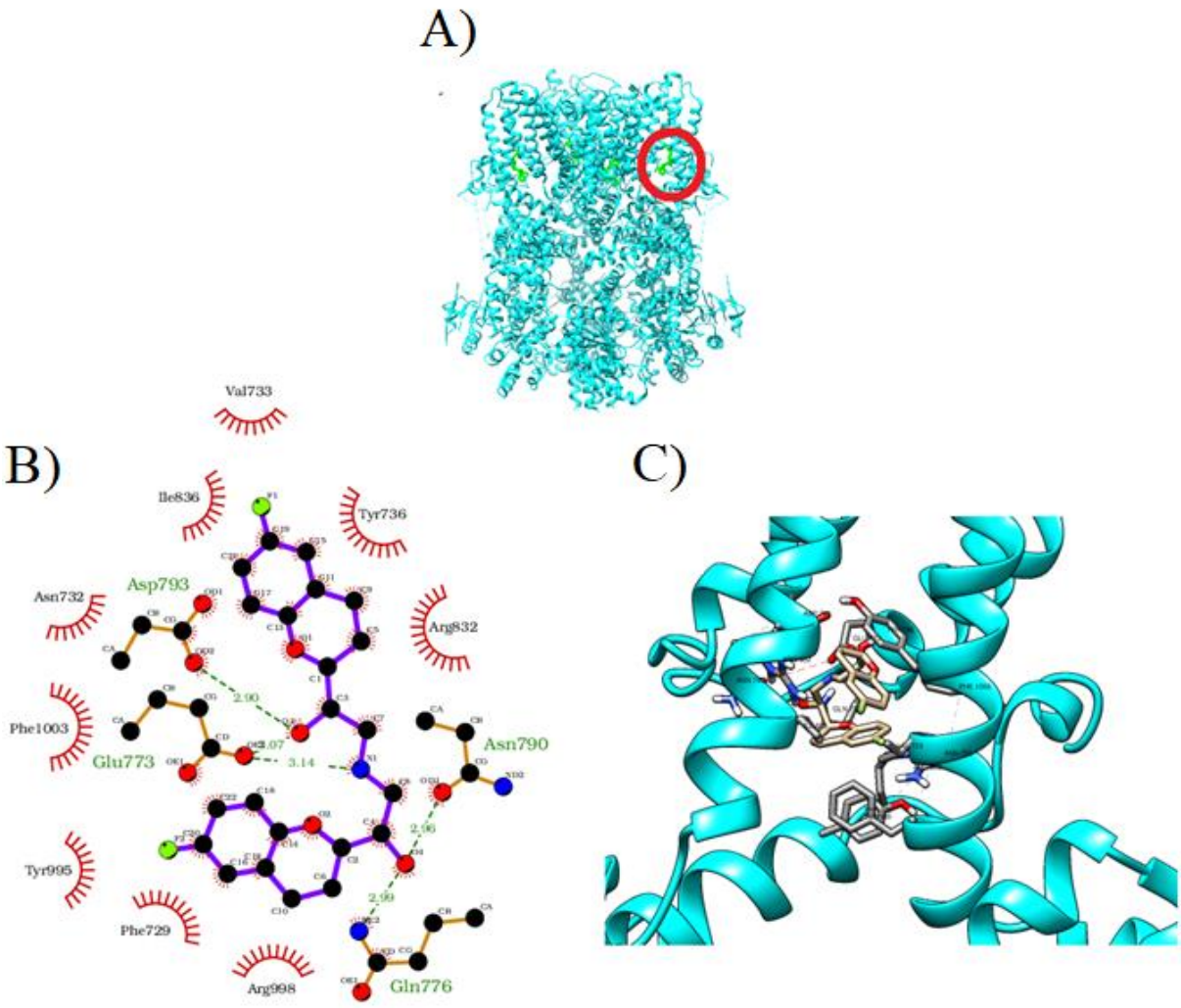

Figure 38. A) 3D structure of TRPM8, black circle shows one of four antagonist binding sites on TRPM8. B) 2D depiction of the intermolecular interactions of ligand-protein for the same binding mode of nebivolol C) 3D Binding mode of nebivolol in binding site of TRPM8. The 2D plot was generated by LigPlot+. Hydrogen bonds are shown as green dotted lines, while the red spoked arcs represent hydrophobic contacts of residues with drug. In the structure Carbon, Oxygen, Flour, and Nitrogen are black, red, green, blue respectively.

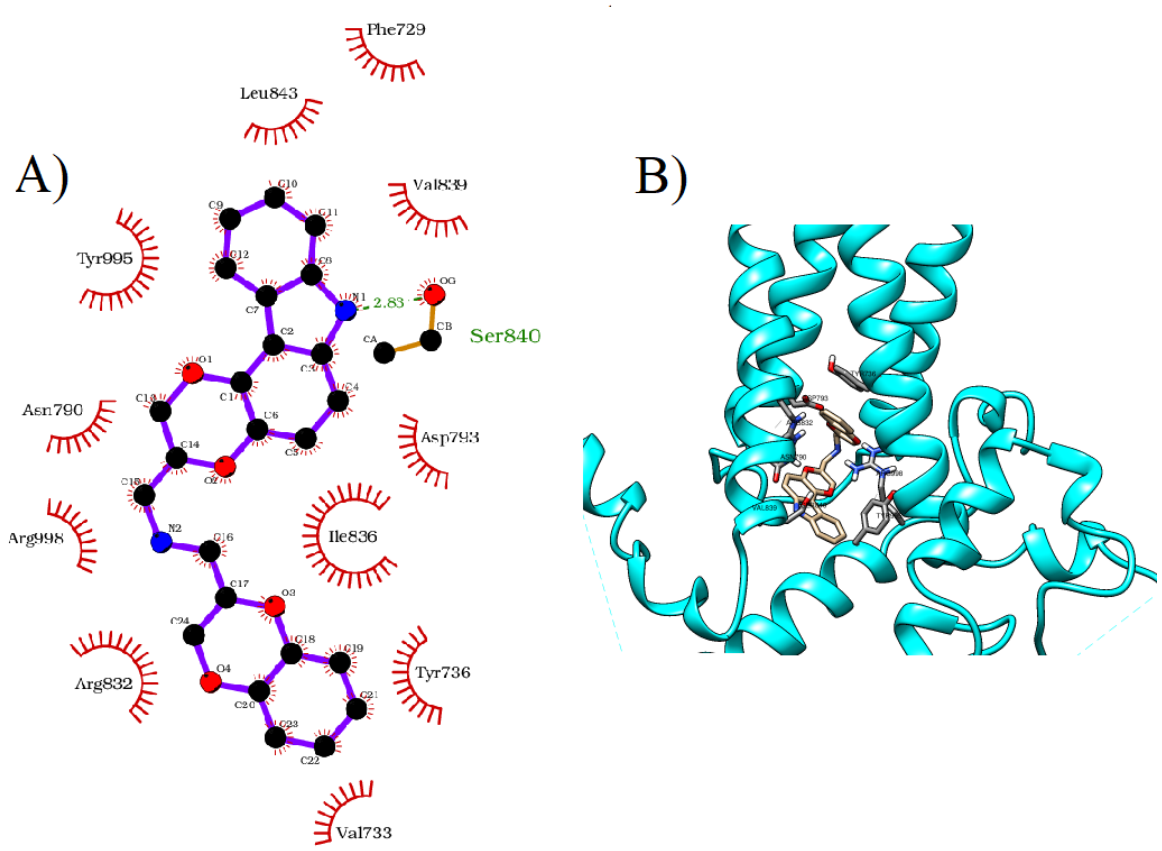

Figure 39. A) 2D depiction of the intermolecular interactions for carvedilol in the binding site. The 2D plots were generated by LigPlot+. Hydrogen bonds are shown as green dotted lines, while the red spoked arcs represent hydrophobic contacts of residues with drug. In the structure Carbon, Oxygen, Flour, and Nitrogen are black, red, green, blue respectively. B) 3D binding mode of carvedilol in binding site of TRPM8.

However, for Carvedilol there is only one hydrogen bond with Serine840, and two face-to-face π–π stacking one with Phen729 other with Tyr736. (Figure 39)

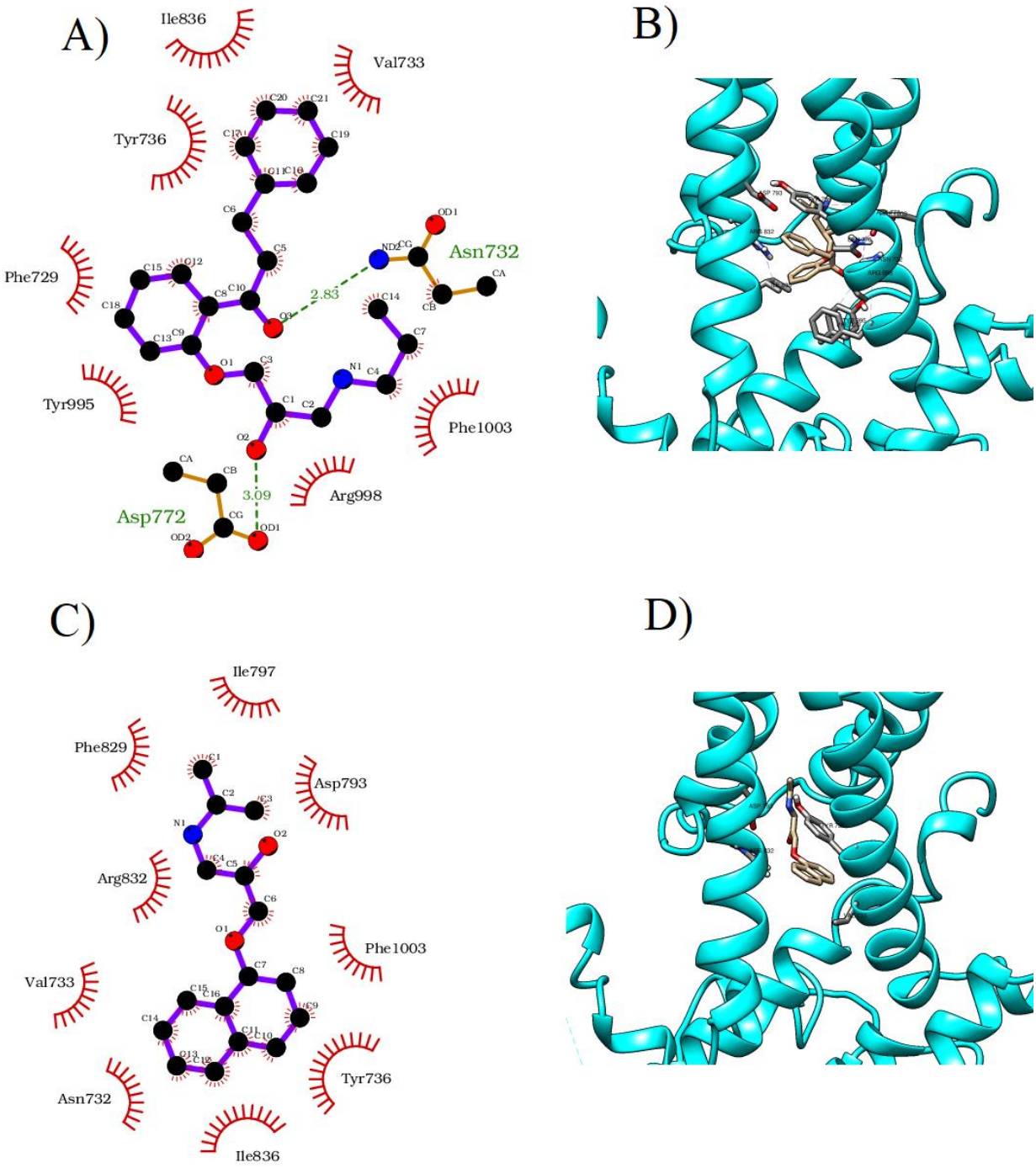

Figure 40**.** 2D depiction of the intermolecular interactions for A) Propafenone and C) Propranolol in the binding site. The 2D plots were generated by LigPlot+. Hydrogen bonds are shown as green dotted lines, while the red spoked arcs represent hydrophobic contacts of residues with drug. In the structure Carbon, Oxygen, Flour, and Nitrogen are black, red, green, blue respectively. B) and D) are 3D binding modes of propafenone and propranolol in the binding site of TRPM8.

And Propafenone has two hydrogen bonds with Asn732 and Asp772 and one face to face π–π stacking with Tyr736. Propranolol had no hydrogen bond and only one face to face π–π stacking with Tyr736.

3.8.2 SwissDock

The docking results by SwissDock also predicted possible interactions of ligand with the antagonist binding site in the transmembrane region between S1, S2, S3 and S4. For each docking experiment 250 different binding modes were predicted by SwissDock, we selected the binding mode with minimum binding energy. The minimum binding energy for nebivolol, carvedilol, propafenone and propranolol was -10.3, -10.2, -10.5, and -9.6 kcal/mol respectively.

Three possible hydrogen bind was predicted for nebivolol, 2 with Glu 773 and another with Leu769. Additionally, three π–π stacking interactions is identifiable in the binding site, a face-to-face interaction with Tyr736, and two T-shaped interaction with Tyr995 and Phe729. For carvedilol no hydrogen bind was identified, one parallel-displaced π–π stacking interaction with Tyr736 was noticeable. Also, other hydrophobic interactions with binding site residues.

Two possible hydrogen bonds were predicted for propafenone with Asp793 and Glu773, and one T-shaped π–π stacking with Phe1003. No hydrogen bond for propranolol was identified with that binding site, but T-shaped π–π stacking is noticeable with Tyr736.

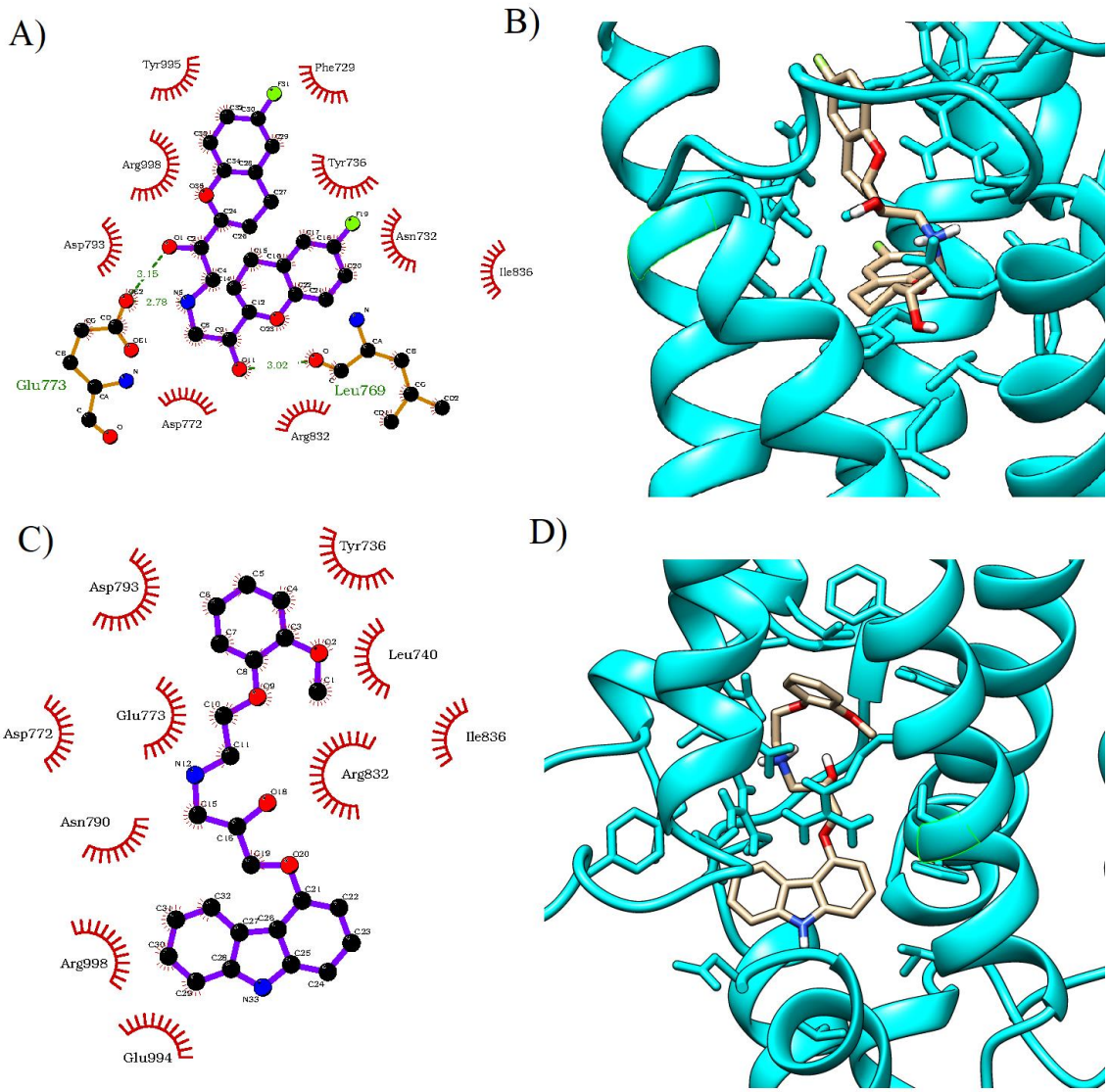

Figure 41. Docking results from SwissDock for nebvolol and carvedilol. A) 2D depiction of the intermolecular interactions of Ligand-protein between the binding site and nebivolol. B) 3D Binding mode of nebivolol in binding site of TRPM8. C) 2D depiction of the intermolecular interactions for carvedilol in the binding site. The 2D plots were generated by LigPlot+. Hydrogen bonds are shown as green dotted lines, while the red spoked arcs represent hydrophobic contacts of residues with drug. In the structure Carbon, Oxygen, Flour, and Nitrogen are black, red, green, blue respectively. D) 3D binding mode of carvedilol in binding site of TRPM8.

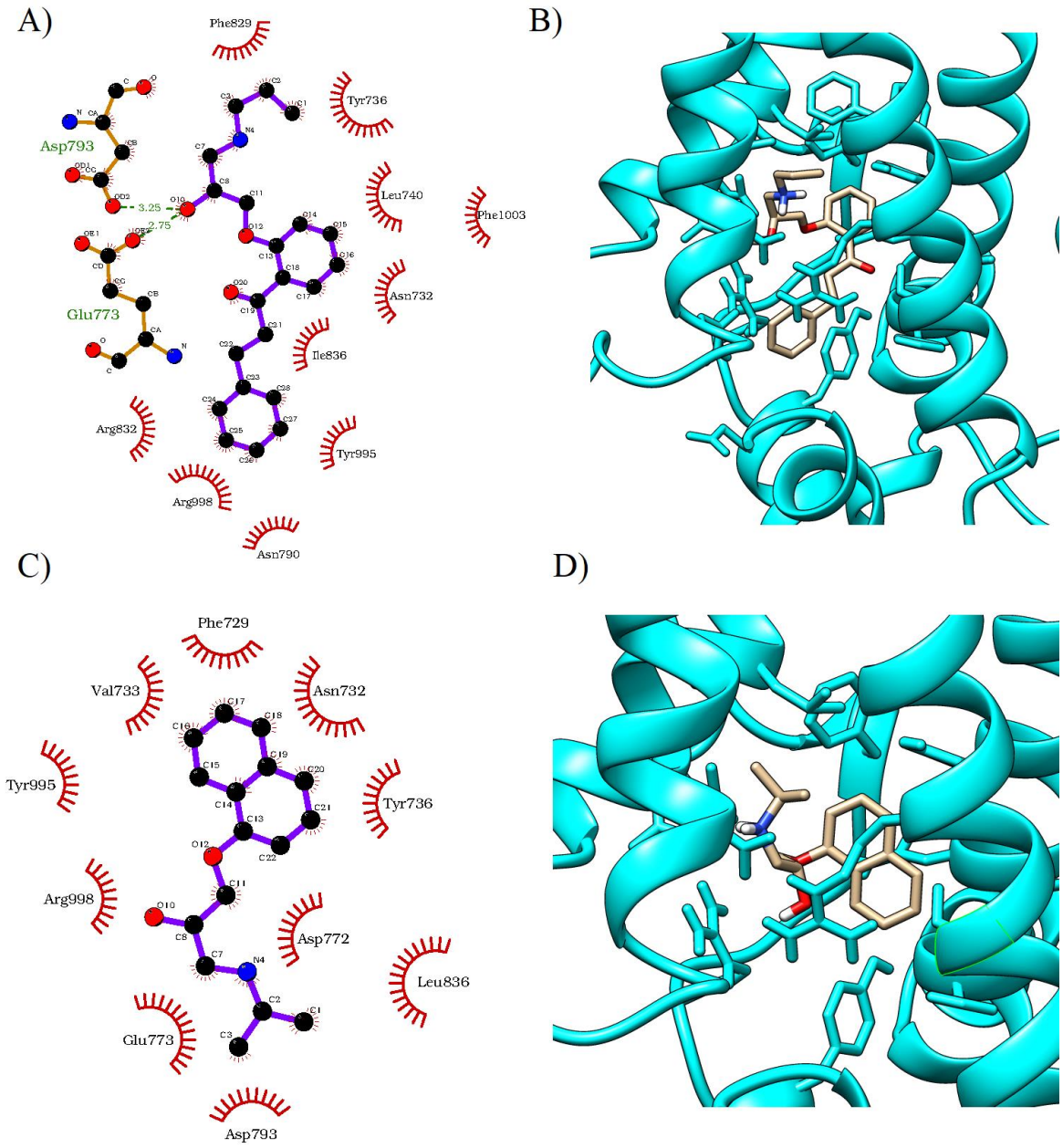

Figure 42. Docking results from SwissDock for propafenone and propranolol, A) 2D depiction of the intermolecular interactions of Ligand-protein between the binding site and propafenone. B) 3D Binding mode of propafenone in binding site of TRPM8. C) 2D depiction of the intermolecular interactions for propranolol in the binding site. The 2D plots were generated by LigPlot+. Hydrogen bonds are shown as green dotted lines, while the red spoked arcs represent hydrophobic contacts of

residues with drug. In the structure Carbon, Oxygen, Flour, and Nitrogen are black, red, green, blue respectively. D) 3D binding mode of propranolol in binding site of TRPM8.

Discussion

4.1 Automated patch clamp vs manual patch clamp

This was the first study of TRPM8 ion channel by IonFlux 16 automated patch clamp device. However TRPM8 was studied before by other automated patch clamp systems, like QPatch HT developed by sophion (Beck et al. 2010), and semi-automated planar patch-clamp setup developed by nanion (Lucius et al. 2016). With this study we must first develop and validate the automatic patch clamp electrophysiology assay for screening compounds on TRPM8 ion channel via IonFlux 16.

The pharmacology and function of TRPM8 were in general agreement between the automated and manual patch clamp. However, there was a tendency to left shift in the potency of compounds tested on IonFlux 16, which was relatively small shift for most of the compounds. Also, the order of potency for different compounds were similar between the methods. We also were able to record stable currents from TRPM8 transfected HEK-293 cell lines for long duration. The overall quality of results obtained by the IonFlux 16 was similar to the results from manual patch clamp.

Because IonFlux 16 select cells at random way in trap phase, it is generally important to have or generate stable cell lines where all cells have homogeneous and high-level expression of target ion channel for robust recording of currents. Other properties like size of cells in the single cell suspension for efficient cell trapping, quality of membrane of cells to easier whole cell confirmation with long time and stable recording should be considered in performing automated patch clamp electrophysiology. Such demands might be considered as limitation for IonFlux system. For instance, having cells with high level expression of target ion channel might not be possible for non-transfected cell lines like different cancer cells, which is limitation for using on automated patch clamp device.

Two of compounds menthol and AMTB were previously reported, menthol as agonist and AMTB as antagonist. The EC_{50} for menthol and IC_{50} for AMTB determined by automated patch clamp were in the range of the previous reports. Based on different methods, reported EC_{50} and IC_{50} varies from 101 to 196 μM for menthol(Andersson, Chase, and Bevan 2004)(Andersson, Chase, and Bevan 2004) and from 160 to 589 nM for AMTB(Andersson, Chase, and Bevan 2004)(Lashinger et al. 2008). Overall, the results have reasonable agreement with reported values in the literatures for these compounds.

Both manual and automated systems use continues perfusion system, except in automated patch clamp due to microfluidic design of plates cells were submerged with solutions faster and efficiently than manual patch clamp which results in quicker response to changes in solutions in comparison to manual patch clamp, hence effect of agonist and antagonist reach steady state faster than manual patch clamp. Which makes IonFlux better choice in studying ligand gated ion channels like TRPM8.

The volume of solution used in automated patch clamp is extremely lower in comparison to manual patch clamp electrophysiology, which is 0.2 ml in automated patch clamp compared to at least 2 ml in manual patch clamp, this could be highly beneficial in testing expensive or hazardous compounds.

4.2 Impact of virtual screening

The workflow included virtual screening as strong tool to generate virtual drug candidates for screening with automated patch clamp. We searched for drugs with similar structure to propafenone, based on idea that similar molecules share similar biological activities.

SwissSimilartity utilizes 2D and 3D screening methods, for 2D method FP2 fingerprints is a option for screening, this method is relatively faster from other ones. For 3D screening Eelctroshape-5D and Spectrophores are nonsuperposirional shape-based methods. Also Align-IT and Shape-IT are superpositional 3D pharmacophore and shape-based approaches, the recent two methods are most time consuming and they restricted to small libraries. All 3D consider conformational flexibility of molecules and 3D similarities were calculated to 20 different conformations of each molecule in the libraries. There is also combined method using both 2D and 3D approaches using combined scores of FP2 fingerprint and Electorshape methods (Zoete et al. 2016).

In our virtual screening Align-IT and Shape-IT didn't have result. And among results of other methods β-blockers were ligands with highest similarity score to propafenone. In comparison, screening β-blockers had 3 hits out of 7 drugs while sodium channel blockers had 1 hit out of 12 drugs at screening concentration of 50 μM. One limitation we noticed for this platform was poor or no result for complex structures, for this reason we couldn't use AMTB as input ligand.

4.3 Identified drugs

4.3.1 Nebivolol

Nebivolol is the most potent inhibitor we Identified with IC_{50} in the sub micromolar range. Sub micromolar range for IC_{50} is considered promising in drug discovery(Hughes et al. 2011). Nebivolol used to treat hypertension and aid in the management of heart failure. It is a third generation β-adrenergic receptor antagonist and highly selective to β1-adrenergic receptor. Additionally, it exhibits nitric oxide mediated vasodilation via stimulating β3-adrenergic receptor(Van de Water et al. 1988).

This dual mechanism of nebivolol causes many of the haemodynamic properties of this drug, which include heart rate and blood pressure reductions, and enhancements in systolic and diastolic function(Dessy et al. 2005). Nebivolol also shows improvement in peripheral and coronary blood flow, reversal of endothelial dysfunction, and anti-inflammatory activity with antioxidant effect(Refaie, El-Hussieny, and Zenhom 2018).

Nebivolol may represent a promising lead compound for further evaluation and modification. It could be used as starting structure for drug discovery, this approach increases the likelihoods of identifying new compounds with druglike properties. This strategy to discovering a new drug by increasing the side effect of an available drug, and reducing its main effect, has been introduced as Selective Optimization of Side Activities or SOSA approach(Wermuth 2006).

4.3.2 Carvedilol

Carvedilol is a nonselective β-blocker and α_1-blocker. Carvedilol inhibits tachycardia induced by exercise through its inhibition of β-adrenoceptors. Carvedilol's effect on α_1-adrenergic receptors relaxes smooth muscle in vasculature and reduces peripheral vascular resistance with overall reduction of blood pressure(Dulin and Abraham 2004).

At higher doses of carvedilol, blockade of calcium channel and antioxidant activity can be seen. The antioxidant aspect of carvedilol inhibits oxidation of low-density lipoproteins and prevents its uptake into coronary circulation(Dandona, Ghanim, and Brooks 2007). Carvedilol is used in treatment of high blood pressure and mild to severe chronic heart failure. In addition, it is used after a heart attack to increase the chance of survival if the heart is not pumping well. Studies suggests that carvedilol might have a protective effect against myocardial injuries. This protection is possibly due to the antioxidant properties and following carvedilol protection against free radicals(Yue et al. 1992). Carvedilol also shown to be beneficial for chemotherapy-related cardiotoxicity(Avila et al. 2018).

4.3.3 Propafenone

Propafenone is a Class 1C antiarrhythmic drug used for managing ventricular arrhythmias and paroxysmal atrial fibrillation/flutter. This drug shows a noticeable inhibitory effect on the sodium channel with weak beta blocking activity. Propafenone cause reduction on the fast inward current by blocking sodium ion channel, which is responsible for the drugs antiarrhythmic effect(Stoschitzky et al. 2016). At very high concentrations of propafenone in vitro, it can block the slow inward current of calcium ion channel(Hancox and Mitcheson 1997).

4.3.4 Propranolol

Propranolol is a non-selective β-adrenergic antagonist, it was developed more than 50 years ago primarily for the treatment of angina pectoris, after a while it was found effective and repurposed for several other conditions like hypertension, angina, atrial fibrillation, migraine, myocardial infarction, essential tremor, hypertrophic subaortic stenosis, and pheochromocytoma(Al-Majed et al. 2017).

4.4 Possible mechanism for blocking effect

4.4.1 Direct binding to antagonist binding site

Drugs in blind docking method had lower binding energy in the known binding site and in both methods showed higher amount of non-covalent interaction for nebivolol in comparison to other drugs. However, binding energies in both methods shouldn't considered as level of potency, and it could be misleading. In the results of SwissDock propafenone had lower binding energy (-10.5 kcal/mol) than nebivolol (-10.3 kcal/mol) and carvedilol (-10.2 kcal/mol) which clearly wasn't in agreement with experimental data, and in the results of Autodock vina, carvedilol had lower binding energy (-13.3 kcal/mol) in comparison to the nebivolol (-11.4 kcal/mol).

These inconsistency shows docking results are not directly comparable with experimental results. Such issue was reported previously for Autodock vina, but it also mentioned Autodock vina adopts much accurate binding poses(Nguyen et al. 2019). And in agreement with experimental results, in both methods nebivolol had higher number of hydrophobic interactions in comparison to other compounds. Hence analysing binding interactions is more accurate.

Table 3. Comparing docking results from two methods with calculated IC_{50}s

Ligand	IC_{50} (μM)	Binding energy calculated by Autodock vina (kcal/mol)	Binding energy calculated by SwissDock (kcal/mol)
Nebivolol	0.97 ± 0.15	-11.4	-10.3
Carvedilol	9.1 ± 0.6	-13.3	-10.2
Propafenone	16.8 ± 5	-9.1	-10.5
Propranolol	45 ± 7	-10.4	-9.6

Docking studies represented possible interactions of nebivolol and other drugs with the binding site within S1, S2, S3 and S4. This binding site is known as ligand hub for both agonists and antagonists(Xu et al. 2020). According to best binding pose from docking study via Autodock vina, nebivolol has possibility of five different hydrogen bonds. Furthermore, two π-π stacking connections stabilize the ligand-protein complex. Other additional hydrophobic interactions contribute to the enhanced affinity of nebivolol to the binding site.

These interactions could induce conformational rearrangements and result in blocking of TRPM8 or could inhibit binding of menthol to this binding site. In comparison to other drugs nebivolol is able to have more noncovalent interaction with the binding site, these results correlate with calculated IC_{50} of drugs. The results suggest observed blocking effect of drugs, mainly Nebivolol might be by direct binding to the antagonist binding site of TRPM8 ion channel.

4.4.2 Drug membrane interactions

Another possible mechanism for blocking TRPM8 ion channel might be by interactions of membrane lipid bilayer with drugs. Membranes are comprised of many proteins and lipids, and through their interactions many cellular activities occur. Although binding of drug to proteins regulates their activity, the interactions of membrane lipid is not less important.

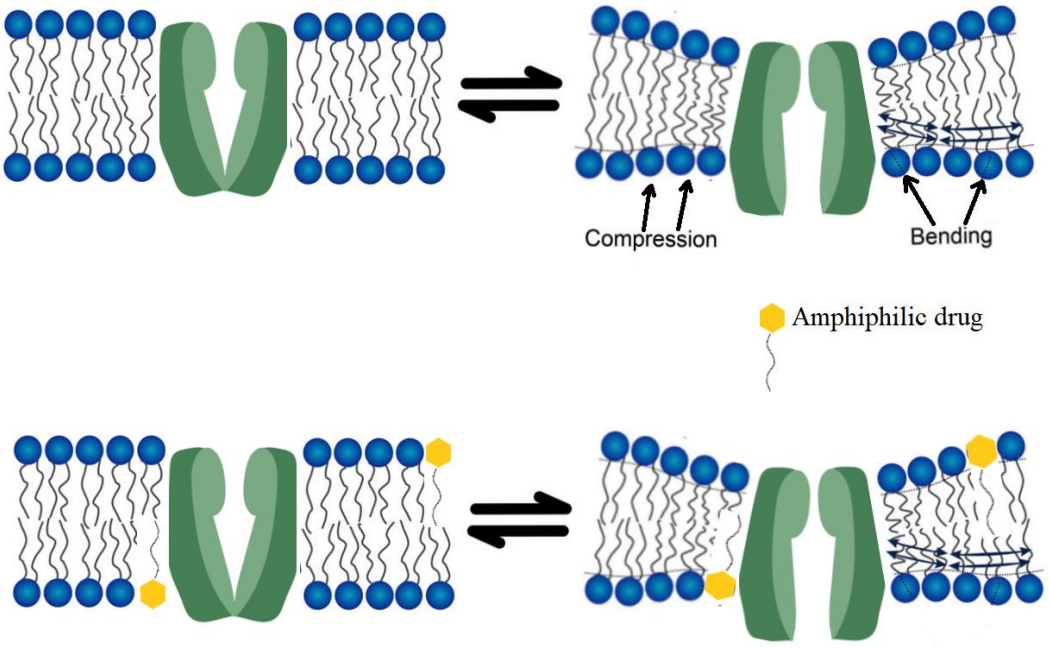

Figure 43. Membrane proteins like ion channels require certain physical properties of the lipid bilayer in which they are surrounded. Some molecules like amphiphilic drugs could perturb lipid bilayer interaction with protein or change the physical properties of lipid bilayer, which could affect membrane protein function.

Drugs we tested were amphiphilic, these drugs have both hydrophilic and lipophilic properties. They could alter the function of many diverse proteins as well as ion channels in membrane. Proteins in the Membrane of cell are energetically coupled to the lipids in membrane bilayer, and amphiphilic drugs like propafenone, propranolol, carvedilol and nebivolol could change the function of various membrane proteins by partitioning into cell membrane and altering the bilayer contribution to the energetics of membrane protein and conformational changes(Lundbæk 2008).

Such a mechanism was reported for variety of drugs as well as propranolol. Propranolol interacts with phospholipid bilayer in a concentration dependant manner and could alter the

interactions between ion channel and the lipid bilayer. It is reported that propranolol could increase the fluidity of membrane bilayer (Pereira-Leite et al. 2013). However, it should be considered not all amphiphilic drugs in our list had effect on TRPM8 ion channel.

TRPM8 is more susceptible to be affected by drug-membrane interactions since TRPM8 has several interactions with membrane lipid bilayer, for instance TRPM8 ion channel localized in cholesterol rich membrane domains, and decrease in cholesterol disrupts lipid rafts and causes a significant increase of TRPM8 response to cold and menthol(Morenilla-Palao et al. 2009).

Phospholipid phosphatidylinositol 4,5-bisphosphate (PIP_2) is known to be the main regulator of TRPM8. PIP_2 activates TRPM8 channel even without chemical and thermal stimulation, plus it enhances sensitivity of TRPM8 to cold temperature and menthol(Sarria et al. 2011). The inhibitory effect of ethanol is known to be caused by weakening the interaction of PIP_2 with TRPM8(Benedikt et al. 2007).

It has been reported carvedilol inhibits $Kir_{2.3}$ ion channel through interfering the interaction of PIP_2 with $kir_{2.3}$(Ferrer et al. 2011). This might be also possible mechanism for blocking effect of carvedilol on TRPM8 ion channel. It is also reported neutralization of positive charges in the TRP domain of C-terminus, weakens interaction with the head group of PIP_2 which is negatively charged, and it prevents channel activation(Brauchi et al. 2007). Interestingly, such effect was reported for Propafenone on blocking cardiac $Kir_{2.x}$ channels by reducing negative charges in their cytoplasmic pore and it results in the decrease of affinity for those ion channels to PIP_2(Amorós et al. 2013). Same mechanism might be the possible way propafenone blocks TRPM8 ion channel.

We cannot totally exclude the possibility that the identified drugs interact directly with TRPM8 ion channels, however the drug-membrane interactions could explain complex polypharmacology or promiscuity of identified drugs.

4.5 Effect of drugs on cells viability

TRPM8 is reported to be overexpressed in pancreatic cancer cells and its cell lines. This over expression was associated with maintaining the proliferation, and invasive ability of cancer cells(Yee et al. 2014). It is also reported that targeting TRPM8 could improve effect of gemcitabine on these cells(JieFeng Liu et al. 2018). However, the underlying mechanisms for these processes have yet to be explained. Our western blot results confirmed the expression of TRPM8 in PANC-1, MIAPaCa-2, and BxPC-3, and manual patch clamp results show the TRPM8 ion channels are functional in these cells as reported before (Ulăreanu et al. 2017)(Yee et al. 2014).

In corelation with drugs affinity to TRPM8, Propafenone and propranolol didn't have any effect on cells proliferation up to 50 μM concentration. But nebivolol was the drug with high cytotoxicity. Its effect was the most significant on MIAPaCa-2 cell lines. However, it was also toxic for both wild type HEK-293 and TRPM8 expressing HEK-293 cells. These results show cytotoxicity of nebivolol is independent to level of TRPM8. While Carvedilol was less potent in comparison to nebivolol, remarkably carvedilol was less cytotoxic against both wild type HEK-293 and TRPM8 expressing HEK-293 cells.

It also should be considered that glycosylation status of TRPM8 found to be different between pancreatic cancer cells and HEK-293 cells. Glycosylated form has expression in HEK-293 cells while non-glycosylated form of TRPM8 was detected in pancreatic cancer cells like PANC-1(Ulăreanu et al. 2017).

Nebivolol and carvedilol were reported to have anticancer properties. One study found nebivolol could inhibit complex I and ATP synthase activities which results in hindering oxidative phosphorylation in colon and breast carcinoma(Nuevo-Tapioles et al. 2020). Another study also suggests nebivolol could stop proliferation in oral squamous cell carcinoma by endoplasmic reticulum stress and mitochondria dysfunction(Chen et al. 2021).

Carvedilol could suppress invasion and migration of malignant breast cancer cells. By inactivation of Src involved in cAMP/PKA and PKCδ and suppressing invasive behaviour of breast cancer(Dezong et al. 2014). Another study revealed It can inhibit ROS- mediated PI3K/AKT signalling pathway(Ma et al. 2019).

Expression of different isoforms of TRPM8 was detected in prostate cancer cells. 4 transmembrane TRPM8 or 4TM-TRPM8 is a short isoform of TRPM8 which regulates mitochondrial Ca^{2+} (Bidaux et al. 2018). It was reported suppression of this isoform could induce endoplasmic reticulum stress, p21 expression, oxidative stress, and apoptosis in those cancer cells (Bidaux et al. 2016). However, the expression of this isoform was not reported for other cancer cells like pancreatic cancer cells.

In fact, carvedilol and nebivolol were known as drugs with high number of targets and off targets (Peters 2013). And their overall effect is result of network of interactions.

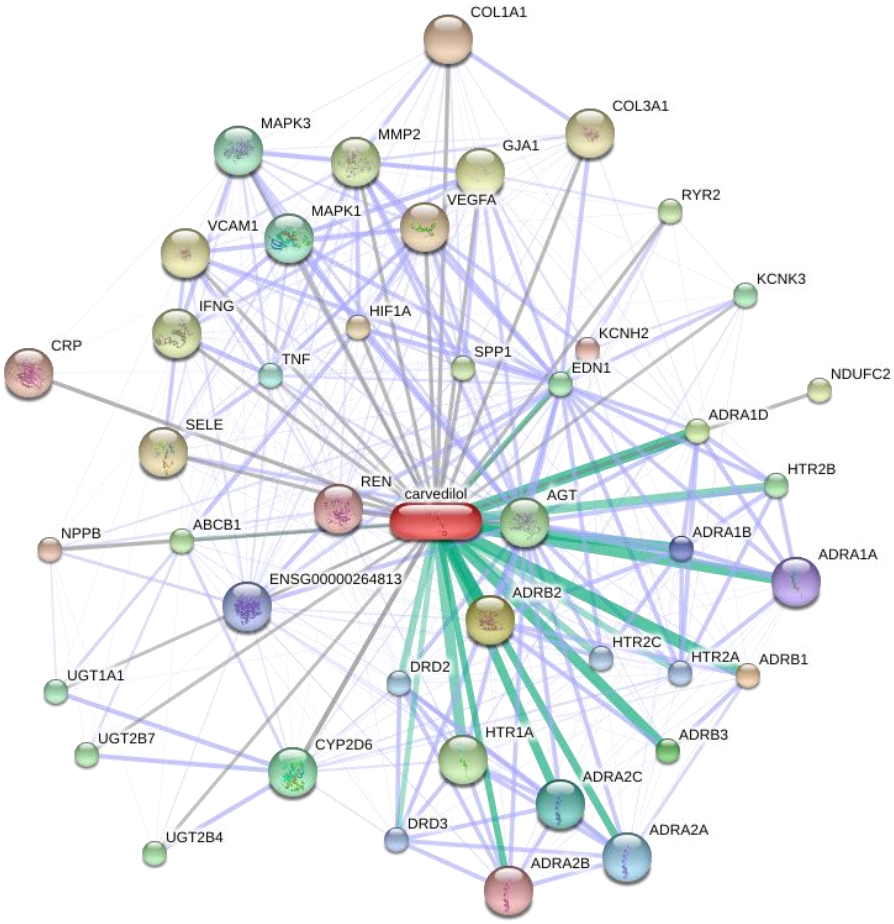

Figure 44. The drug-target networks for carvedilol constructed by the STITCH database

Obviously, these drugs are not selective and TRPM8 is just another target we identified for nebivolol and carvedilol. Hence, it is tough to point out exact mechanism for anticancer effect of the multi-target drugs like carvedilol. While having several targets could be considered origin of unwanted side effects for drugs, but multi-target drugs also could be advantageous in treatment of complex illnesses and drug resistance conditions (Ramsay et al. 2018).

Although targeted drug delivery could be solution for enhancing anticancer effect of nebivolol against pancreatic cancer (Zhao et al. 2016). It should be noted beside pancreatic

cancer there are multiple other diseases associated with TRPM8 ion channel which effect of nebivolol and carvedilol could be investigated.

Conclusion

In summary, we developed and validated automated patch clamp electrophysiology assay for rapid identification of potent agonist or antagonists for TRPM8 ion channel with IonFlux 16. Automated patch clamp had acceptable results in comparison to manual patch clamp it was faster with much stability. By combining automated patch clamp electrophysiology with virtual screening, we were able to identify several blockers for TRPM8 ion channel efficiently without having need for high throughput screening. Such procedure is applicable for other ion channels. Other candidate drugs provided by virtual screening could be considered for further screenings.

Nebivolol was the most potent antagonist for TRPM8, which possibly blocks TRPM8 ion channel by direct binding to the antagonist binding site. Hence, nebivolol could be considered for further optimizations to discover new selective TRPM8 antagonists based on initial structure of nebivolol. In other hand we identified carvedilol as less potent blocker but with interesting anticancer effect, which demands more investigations to understand its mechanism. Both nebivolol and carvedilol are potential candidates for other TRPM8 associated diseases.

Acknowledgement

This work is funded by the European Union's Horizon 2020 research and innovation program under the Marie Sklodowska-Curie grant agreement No 721841. And is part of the PAIN-Net project, an Innovative Training Network (ITN) funded by the European Commission.

Most of project was performed in DI.V.A.L. (spin-off participated by University of Florence which operates in the field of research and experimental development in the field of biotechnology). And part of project was done at Department of Experimental and Clinical Medicine in University of Florence.

Research integrity

I, Farhad Jahanfar, declare that this thesis has been composed by myself and this work has not been submitted, in whole or in part, for any other degree or professional qualification. I confirm that this work is solely the result of my own work, except where it is stated by references or in text.

10/10/2021

References:

Abriel, Hugues, and Elena V Zaklyazminskaya. 2013. “Cardiac Channelopathies: Genetic and Molecular Mechanisms.” *Gene* 517(1): 1–11.

Al-Majed, Abdulrahman A et al. 2017. “Propranolol.” In *Profiles of Drug Substances, Excipients and Related Methodology*, Elsevier, 287–338.

Amorós, Irene et al. 2013. “Propafenone Blocks Human Cardiac Kir2. x Channels by Decreasing the Negative Electrostatic Charge in the Cytoplasmic Pore.” *Biochemical pharmacology* 86(2): 267–78.

Andersson, David A, Henry W N Chase, and Stuart Bevan. 2004. “TRPM8 Activation by Menthol, Icilin, and Cold Is Differentially Modulated by Intracellular PH.” *Journal of Neuroscience* 24(23): 5364–69.

Andersson, David A, Mark Nash, and Stuart Bevan. 2007. “Modulation of the Cold-Activated Channel TRPM8 by Lysophospholipids and Polyunsaturated Fatty Acids.” *Journal of Neuroscience* 27(12): 3347–55.

Arcas, José Miguel et al. 2019. “The Immunosuppressant Macrolide Tacrolimus Activates Cold-Sensing TRPM8 Channels.” *Journal of Neuroscience* 39(6): 949–69.

Asuthkar, Swapna et al. 2015. “The TRPM8 Protein Is a Testosterone Receptor: II. Functional Evidence for an Ionotropic Effect of Testosterone on TRPM8.” *Journal of Biological Chemistry* 290(5): 2670–88.

Atukorala, Inoshi, and David J Hunter. 2013. “Valdecoxib: The Rise and Fall of a COX-2

Inhibitor." *Expert opinion on pharmacotherapy* 14(8): 1077–86.

Avila, Mônica Samuel et al. 2018. "Carvedilol for Prevention of Chemotherapy-Related Cardiotoxicity: The CECCY Trial." *Journal of the American College of Cardiology* 71(20): 2281–90.

Babes, Ramona-Madalina, Tudor Selescu, Dan Domocos, and Alexandru Babes. 2017. "The Anthelminthic Drug Praziquantel Is a Selective Agonist of the Sensory Transient Receptor Potential Melastatin Type 8 Channel." *Toxicology and applied pharmacology* 336: 55–65.

Bai, V Uma et al. 2010. "Androgen Regulated TRPM8 Expression: A Potential MRNA Marker for Metastatic Prostate Cancer Detection in Body Fluids." *International journal of oncology* 36(2): 443–50.

Bandell, Michael et al. 2006. "High-Throughput Random Mutagenesis Screen Reveals TRPM8 Residues Specifically Required for Activation by Menthol." *Nature neuroscience* 9(4): 493–500.

Bavencoffe, Alexis et al. 2011. "Complex Regulation of the TRPM8 Cold Receptor Channel: Role of Arachidonic Acid Release Following M3 Muscarinic Receptor Stimulation." *Journal of Biological Chemistry* 286(11): 9849–55.

Beccari, Andrea R et al. 2017. "Novel Selective, Potent Naphthyl TRPM8 Antagonists Identified through a Combined Ligand-and Structure-Based Virtual Screening Approach." *Scientific reports* 7(1): 1–15.

Beck, Edward J et al. 2010. "Development and Validation of a Secondary Screening Assay for TRPM8 Antagonists Using QPatch HT." *Assay and drug development technologies* 8(1): 63–72.

References

Behr, Elijah R et al. 2008. “Sudden Arrhythmic Death Syndrome: Familial Evaluation Identifies Inheritable Heart Disease in the Majority of Families.” *European heart journal* 29(13): 1670–80.

Behrendt, H-J et al. 2004. “Characterization of the Mouse Cold-menthol Receptor TRPM8 and Vanilloid Receptor Type-1 VR1 Using a Fluorometric Imaging Plate Reader (FLIPR) Assay.” *British journal of pharmacology* 141(4): 737–45.

Bell, Damian C, and Mark L Dallas. 2018. “Using Automated Patch Clamp Electrophysiology Platforms in Pain-related Ion Channel Research: Insights from Industry and Academia.” *British journal of pharmacology* 175(12): 2312–21.

Benedikt, Jan, Jan Teisinger, Ladislav Vyklicky, and Viktorie Vlachova. 2007. “Ethanol Inhibits Cold-menthol Receptor TRPM8 by Modulating Its Interaction with Membrane Phosphatidylinositol 4, 5-bisphosphate.” *Journal of neurochemistry* 100(1): 211–24.

Benemei, Silvia et al. 2013. “TRPA1 and Other TRP Channels in Migraine.” *The journal of headache and pain* 14(1): 1–8.

Bertamino, Alessia et al. 2018. “Identification of a Potent Tryptophan-Based TRPM8 Antagonist with in Vivo Analgesic Activity.” *Journal of medicinal chemistry* 61(14): 6140–52.

Bidaux, Gabriel et al. 2005. “Evidence for Specific TRPM8 Expression in Human Prostate Secretory Epithelial Cells: Functional Androgen Receptor Requirement.” *Endocrine-related cancer* 12(2): 367–82.

———. 2016. “Targeting of Short TRPM8 Isoforms Induces 4TM-TRPM8-Dependent Apoptosis in Prostate Cancer Cells.” *Oncotarget* 7(20): 29063.

———. 2018. “4TM-TRPM8 Channels Are New Gatekeepers of the ER-Mitochondria Ca2+

Transfer." *Biochimica et Biophysica Acta (BBA)-Molecular Cell Research* 1865(7): 981–94.

De Blas, Gerardo A et al. 2009. "TRPM8, a Versatile Channel in Human Sperm." *PLoS One* 4(6): e6095.

Brackenbury, William J. 2012. "Voltage-Gated Sodium Channels and Metastatic Disease." *Channels* 6(5): 352–61.

Brauchi, Sebastian et al. 2007. "Dissection of the Components for PIP2 Activation and Thermosensation in TRP Channels." *Proceedings of the National Academy of Sciences* 104(24): 10246–51.

Bugan, Ilknur et al. 2019. "Anti-Metastatic Effect of Ranolazine in an in Vivo Rat Model of Prostate Cancer, and Expression of Voltage-Gated Sodium Channel Protein in Human Prostate." *Prostate cancer and prostatic diseases* 22(4): 569–79.

Caceres, Ana I et al. 2017. "Transient Receptor Potential Cation Channel Subfamily M Member 8 Channels Mediate the Anti-inflammatory Effects of Eucalyptol." *British journal of pharmacology* 174(9): 867–79.

Camerino, Diana Conte, Domenico Tricarico, and Jean-François Desaphy. 2007. "Ion Channel Pharmacology." *Neurotherapeutics* 4(2): 184–98.

Cao, Chike et al. 2013. "Polyester Modification of the Mammalian TRPM8 Channel Protein: Implications for Structure and Function." *Cell reports* 4(2): 302–15.

de Castro, Sonia, and María-José Camarasa. 2018. "Polypharmacology in HIV Inhibition: Can a Drug with Simultaneous Action against Two Relevant Targets Be an Alternative to Combination Therapy?" *European journal of medicinal chemistry* 150: 206–27.

Chahl, Loris A. 2011. "TRP Channels and Psychiatric Disorders." *Transient Receptor*

Potential Channels: 987–1009.

Chasman, Daniel I et al. 2011. "Genome-Wide Association Study Reveals Three Susceptibility Loci for Common Migraine in the General Population." *Nature genetics* 43(7): 695–98.

Chen, Qian et al. 2021. "Adrenergic Blockade by Nebivolol to Suppress Oral Squamous Cell Carcinoma Growth via Endoplasmic Reticulum Stress and Mitochondria Dysfunction." *Frontiers in pharmacology* 12.

Coderre, T J, N Kumar, C D Lefebvre, and J S C Yu. 2007. "A Comparison of the Glutamate Release Inhibition and Anti-allodynic Effects of Gabapentin, Lamotrigine, and Riluzole in a Model of Neuropathic Pain." *Journal of neurochemistry* 100(5): 1289–99.

Colburn, Raymond W et al. 2007. "Attenuated Cold Sensitivity in TRPM8 Null Mice." *Neuron* 54(3): 379–86.

Cuddapah, Vishnu Anand, Kathryn L Turner, and Harald Sontheimer. 2013. "Calcium Entry via TRPC1 Channels Activates Chloride Currents in Human Glioma Cells." *Cell Calcium* 53(3): 187–94.

Curtis, Howard J, and Kenneth S Cole. 1938. "Transverse Electric Impedance of the Squid Giant Axon." *The Journal of general physiology* 21(6): 757–65.

Dandona, Paresh, Husam Ghanim, and David P Brooks. 2007. "Antioxidant Activity of Carvedilol in Cardiovascular Disease." *Journal of hypertension* 25(4): 731–41.

Dessy, Chantal et al. 2005. "Endothelial B3-Adrenoreceptors Mediate Nitric Oxide–Dependent Vasorelaxation of Coronary Microvessels in Response to the Third-Generation β-Blocker Nebivolol." *Circulation* 112(8): 1198–1205.

Dezong, Gao, Ma Zhongbing, Fu Qinye, and Yu Zhigang. 2014. "Carvedilol Suppresses

Migration and Invasion of Malignant Breast Cells by Inactivating Src Involving CAMP/PKA and PKCδ Signaling Pathway." *Journal of cancer research and therapeutics* 10(4): 991.

Dhaka, Ajay et al. 2007. "TRPM8 Is Required for Cold Sensation in Mice." *Neuron* 54(3): 371–78.

Diver, Melinda M, Yifan Cheng, and David Julius. 2019. "Structural Insights into TRPM8 Inhibition and Desensitization." *Science* 365(6460): 1434–40.

Dong, Xian-Ping et al. 2008. "The Type IV Mucolipidosis-Associated Protein TRPML1 Is an Endolysosomal Iron Release Channel." *Nature* 455(7215): 992–96.

Dulin, Brian, and William T Abraham. 2004. "Pharmacology of Carvedilol." *The American journal of cardiology* 93(9): 3–6.

Fernández-Falgueras, Anna et al. 2017. "Cardiac Channelopathies and Sudden Death: Recent Clinical and Genetic Advances." *Biology* 6(1): 7.

Fernández-Peña, Carlos, and Felix Viana. 2013. "Targeting TRPM8 for Pain Relief." *The Open Pain Journal* 6(1).

Ferrer, Tania et al. 2011. "Carvedilol Inhibits Kir2. 3 Channels by Interference with PIP2-Channel Interaction." *European journal of pharmacology* 668(1–2): 72–77.

Forouhan, Mitra, Stephan Sonntag, and Raymond P Boot-Handford. 2018. "Carbamazepine Reduces Disease Severity in a Mouse Model of Metaphyseal Chondrodysplasia Type Schmid Caused by a Premature Stop Codon (Y632X) in the Col10a1 Gene." *Human molecular genetics* 27(22): 3840–53.

Freilinger, Tobias et al. 2012. "Genome-Wide Association Analysis Identifies Susceptibility Loci for Migraine without Aura." *Nature genetics* 44(7): 777–82.

Gaston, Tyler E, and Daniel Friedman. 2017. “Pharmacology of Cannabinoids in the Treatment of Epilepsy.” *Epilepsy & Behavior* 70: 313–18.

Gauchan, Punam, Tsugunobu Andoh, Atsushi Kato, and Yasushi Kuraishi. 2009. “Involvement of Increased Expression of Transient Receptor Potential Melastatin 8 in Oxaliplatin-Induced Cold Allodynia in Mice.” *Neuroscience letters* 458(2): 93–95.

Gavva, Narender R et al. 2008. “Pharmacological Blockade of the Vanilloid Receptor TRPV1 Elicits Marked Hyperthermia in Humans.” *Pain* 136(1–2): 202–10.

Golden, Andrew P et al. 2011. “IonFlux: A Microfluidic Patch Clamp System Evaluated with Human Ether-à-Go-Go Related Gene Channel Physiology and Pharmacology.” *Assay and drug development technologies* 9(6): 608–19.

González-Muñiz, Rosario, M Bonache, Cristina Martín-Escura, and Isabel Gómez-Monterrey. 2019. “Recent Progress in TRPM8 Modulation: An Update.” *International journal of molecular sciences* 20(11): 2618.

Grace, M S et al. 2014. “Transient Receptor Potential (TRP) Channels in the Airway: Role in Airway Disease.” *British journal of pharmacology* 171(10): 2593–2607.

Greil, W et al. 1997. “Lithium versus Carbamazepine in the Maintenance Treatment of Bipolar Disorders–a Randomised Study.” *Journal of Affective Disorders* 43(2): 151–61.

Grosdidier, Aurelien, Vincent Zoete, and Olivier Michielin. 2011. “SwissDock, a Protein-Small Molecule Docking Web Service Based on EADock DSS.” *Nucleic acids research* 39(suppl_2): W270–77.

Guo, Huazhang, John Andrew Carlson, and Andrzej Slominski. 2012. “Role of TRPM in Melanocytes and Melanoma.” *Experimental dermatology* 21(9): 650–54.

Hancox, Jules C, and John S Mitcheson. 1997. “Inhibition of L-type Calcium Current by

Propafenone in Single Myocytes Isolated from the Rabbit Atrioventricular Node." *British journal of pharmacology* 121(1): 7–14.

Harrison, Joel L K, and Karen D Davis. 1999. "Cold-Evoked Pain Varies with Skin Type and Cooling Rate: A Psychophysical Study in Humans." *Pain* 83(2): 123–35.

Hensel, Herbert, and Yngve Zotterman. 1951. "The Response of the Cold Receptors to Constant Cooling." *Acta physiologica Scandinavica* 22(2-3): 96–105.

Hodgkin, Alan L, Andrew F Huxley, and Bernard Katz. 1952. "Measurement of Current-voltage Relations in the Membrane of the Giant Axon of Loligo." *The Journal of physiology* 116(4): 424–48.

Hossain, Mohammad Zakir et al. 2018. "Activation of TRPV1 and TRPM8 Channels in the Larynx and Associated Laryngopharyngeal Regions Facilitates the Swallowing Reflex." *International journal of molecular sciences* 19(12): 4113.

Hughes, James P, Stephen Rees, S Barrett Kalindjian, and Karen L Philpott. 2011. "Principles of Early Drug Discovery." *British journal of pharmacology* 162(6): 1239–49.

Inoue, Ryuji et al. 2006. "Transient Receptor Potential Channels in Cardiovascular Function and Disease." *Circulation research* 99(2): 119–31.

Ito, Hiroki et al. 2016. "Functional Role of the Transient Receptor Potential Melastatin 8 (TRPM 8) Ion Channel in the Urinary Bladder Assessed by Conscious Cystometry and Ex Vivo Measurements of Single-unit Mechanosensitive Bladder Afferent Activities in the Rat." *BJU international* 117(3): 484–94.

Jones, Kenneth A, Nicoletta Garbati, Hong Zhang, and Charles H Large. 2009. "Automated Patch Clamping Using the QPatch." In *High Throughput Screening*, Springer, 209–23.

Jourdan, Jean-Pierre, Ronan Bureau, Christophe Rochais, and Patrick Dallemagne. 2020. "Drug Repositioning: A Brief Overview." *Journal of Pharmacy and Pharmacology* 72(9): 1145–51.

Kaczorowski, Gregory J, Owen B McManus, Birgit T Priest, and Maria L Garcia. 2008. "Ion Channels as Drug Targets: The next GPCRs." *The Journal of general physiology* 131(5): 399–405.

Kaneko, Yosuke, and Arpad Szallasi. 2014. "Transient Receptor Potential (TRP) Channels: A Clinical Perspective." *British journal of pharmacology* 171(10): 2474–2507.

Kawashiri, Takehiro et al. 2012. "L Type Ca2+ Channel Blockers Prevent Oxaliplatin-Induced Cold Hyperalgesia and TRPM8 Overexpression in Rats." *Molecular Pain* 8: 1744–8069.

Keh, Siew M et al. 2011. "The Menthol and Cold Sensation Receptor TRPM8 in Normal Human Nasal Mucosa and Rhinitis." *Rhinology* 49(4): 453–57.

Khalil, M et al. 2016. "Transient Receptor Potential Melastatin 8 Ion Channel in Macrophages Modulates Colitis through a Balance-Shift in TNF-Alpha and Interleukin-10 Production." *Mucosal immunology* 9(6): 1500–1513.

Kim, June-Bum. 2014. "Channelopathies." *Korean journal of pediatrics* 57(1): 1.

Knowlton, Wendy M et al. 2011. "Pharmacological Blockade of TRPM8 Ion Channels Alters Cold and Cold Pain Responses in Mice." *PloS one* 6(9): e25894.

Kodandaramaiah, Suhasa B et al. 2012. "Automated Whole-Cell Patch-Clamp Electrophysiology of Neurons in Vivo." *Nature methods* 9(6): 585–87.

Kremeyer, Barbara et al. 2010. "A Gain-of-Function Mutation in TRPA1 Causes Familial Episodic Pain Syndrome." *Neuron* 66(5): 671–80.

Kullmann, Dimitri M. 2010. "Neurological Channelopathies." *Annual review of neuroscience* 33: 151–72.

de la Torre-Martínez, Roberto et al. 2017. "Synthesis, High-Throughput Screening and Pharmacological Characterization of β–Lactam Derivatives as TRPM8 Antagonists." *Scientific reports* 7(1): 1–13.

Lashinger, Erin S R et al. 2008. "AMTB, a TRPM8 Channel Blocker: Evidence in Rats for Activity in Overactive Bladder and Painful Bladder Syndrome." *American Journal of Physiology-Renal Physiology* 295(3): F803–10.

Laskowski, Roman A, and Mark B Swindells. 2011. "LigPlot+: Multiple Ligand–Protein Interaction Diagrams for Drug Discovery."

Li, MinChao et al. 2011. "Cold Temperature Induces Mucin Hypersecretion from Normal Human Bronchial Epithelial Cells in Vitro through a Transient Receptor Potential Melastatin 8 (TRPM8)–Mediated Mechanism." *Journal of Allergy and Clinical Immunology* 128(3): 626–34.

Liu, G et al. 2003. "Differential Interactions of Lamotrigine and Related Drugs with Transmembrane Segment IVS6 of Voltage-Gated Sodium Channels." *Neuropharmacology* 44(3): 413–22.

Liu, JieFeng et al. 2018. "Silencing of TRPM8 Inhibits Aggressive Tumor Phenotypes and Enhances Gemcitabine Sensitivity in Pancreatic Cancer." *Pancreatology* 18(8): 935–44.

Liu, Jinxin et al. 2014. "TRPM8 Promotes Aggressiveness of Breast Cancer Cells by Regulating EMT via Activating AKT/GSK-3β Pathway." *Tumor Biology* 35(9): 8969–77.

Lucius, Alexander et al. 2016. "3-Iodothyronamine Increases Transient Receptor Potential

Melastatin Channel 8 (TRPM8) Activity in Immortalized Human Corneal Epithelial Cells." *Cellular signalling* 28(3): 136–47.

Lundbæk, Jens A. 2008. "Lipid Bilayer–Mediated Regulation of Ion Channel Function by Amphiphilic Drugs." *The Journal of general physiology* 131(5): 421–29.

M Knowlton, Wendy, and David D McKemy. 2011. "TRPM8: From Cold to Cancer, Peppermint to Pain." *Current pharmaceutical biotechnology* 12(1): 68–77.

Ma, Zhongbing et al. 2019. "Carvedilol Suppresses Malignant Proliferation of Mammary Epithelial Cells through Inhibition of the ROS-mediated PI3K/AKT Signaling Pathway." *Oncology reports* 41(2): 811–18.

Madrid, Rodolfo et al. 2006. "Contribution of TRPM8 Channels to Cold Transduction in Primary Sensory Neurons and Peripheral Nerve Terminals." *Journal of Neuroscience* 26(48): 12512–25.

Malkia, Annika, Cruz Morenilla-Palao, and Felix Viana. 2011. "The Emerging Pharmacology of TRPM8 Channels: Hidden Therapeutic Potential underneath a Cold Surface." *Current pharmaceutical biotechnology* 12(1): 54–67.

Martinez, Dolores et al. 2010. "High-Fidelity Patch-Clamp Recordings from Neurons Cultured on a Polymer Microchip." *Biomedical microdevices* 12(6): 977–85.

Masamoto, Yukiko, Fuminori Kawabata, and Tohru Fushiki. 2009. "Intragastric Administration of TRPV1, TRPV3, TRPM8, and TRPA1 Agonists Modulates Autonomic Thermoregulation in Different Manners in Mice." *Bioscience, biotechnology, and biochemistry* 73(5): 1021–27.

Matthews, E, and M G Hanna. 2014. "Repurposing of Sodium Channel Antagonists as Potential New Anti-Myotonic Drugs." *Experimental neurology* 261: 812–15.

McBride, William Griffith. 1961. “Thalidomide and Congenital Abnormalities.” *Lancet* 2(1358): 90927–28.

McCoy, Daniel D et al. 2013. “Enhanced Insulin Clearance in Mice Lacking TRPM8 Channels.” *American Journal of Physiology-Endocrinology and Metabolism* 305(1): E78–88.

McKemy, David D, Werner M Neuhausser, and David Julius. 2002. “Identification of a Cold Receptor Reveals a General Role for TRP Channels in Thermosensation.” *Nature* 416(6876): 52–58.

Michelini, Elisa et al. 2010. “Cell-Based Assays: Fuelling Drug Discovery.” *Analytical and bioanalytical chemistry* 398(1): 227–38.

Miller, Robert G, J Douglas Mitchell, and Dan H Moore. 2012. “Riluzole for Amyotrophic Lateral Sclerosis (ALS)/Motor Neuron Disease (MND).” *Cochrane database of systematic reviews* (3).

Morenilla-Palao, Cruz et al. 2009. “Lipid Raft Segregation Modulates TRPM8 Channel Activity.” *Journal of Biological Chemistry* 284(14): 9215–24.

Morgan, Steve et al. 2011. “The Cost of Drug Development: A Systematic Review.” *Health policy* 100(1): 4–17.

Moridani, Majid, and Sam Harirforoosh. 2014. “Drug Development and Discovery: Challenges and Opportunities.” *Drug Discov Today* 19(11): 1679.

Mueller-Tribbensee, Sonja M et al. 2015. “Differential Contribution of TRPA1, TRPV4 and TRPM8 to Colonic Nociception in Mice.” *PLoS One* 10(7): e0128242.

Mukerji, Gaurav et al. 2006. “Cool and Menthol Receptor TRPM8 in Human Urinary Bladder Disorders and Clinical Correlations.” *BMC urology* 6(1): 1–11.

Naumov, Denis E et al. 2015. “Transient Receptor Potential Melastatin 8 Gene Polymorphism Is Associated with Cold-induced Airway Hyperresponsiveness in Bronchial Asthma.” *Respirology* 20(8): 1192–97.

Neher, Erwin, Bert Sakmann, and Joe Henry Steinbach. 1978. “The Extracellular Patch Clamp: A Method for Resolving Currents through Individual Open Channels in Biological Membranes.” *Pflügers Archiv* 375(2): 219–28.

Nguyen, Nguyen Thanh et al. 2019. “Autodock Vina Adopts More Accurate Binding Poses but Autodock4 Forms Better Binding Affinity.” *Journal of Chemical Information and Modeling* 60(1): 204–11.

Nilius, Bernd, and Grzegorz Owsianik. 2010. “Transient Receptor Potential Channelopathies.” *Pflügers Archiv-European Journal of Physiology* 460(2): 437–50.

Nuevo-Tapioles, Cristina et al. 2020. “Coordinate β-Adrenergic Inhibition of Mitochondrial Activity and Angiogenesis Arrest Tumor Growth.” *Nature communications* 11(1): 1–18.

O’Donnell, Patricio et al. 2019. “Strategies to Address Challenges in Neuroscience Drug Discovery and Development.” *International Journal of Neuropsychopharmacology* 22(7): 445–48.

Palumbo, Antonio et al. 2008. “Thalidomide for Treatment of Multiple Myeloma: 10 Years Later.” *Blood* 111(8): 3968–77.

Palve, Vinayak, Yi Liao, Lily L Remsing Rix, and Uwe Rix. 2020. “Turning Liabilities into Opportunities: Off-Target Based Drug Repurposing in Cancer.” In *Seminars in Cancer Biology*, Elsevier.

Parra, Andrés et al. 2010. “Ocular Surface Wetness Is Regulated by TRPM8-Dependent Cold Thermoreceptors of the Cornea.” *Nature medicine* 16(12): 1396–99.

Parvathaneni, Vineela, Nishant S Kulkarni, Aaron Muth, and Vivek Gupta. 2019. "Drug Repurposing: A Promising Tool to Accelerate the Drug Discovery Process." *Drug discovery today* 24(10): 2076–85.

Pereira-Leite, Catarina et al. 2013. "Biophysical Characterization of the Drug–Membrane Interactions: The Case of Propranolol and Acebutolol." *European journal of pharmaceutics and biopharmaceutics* 84(1): 183–91.

Pertusa, María et al. 2012. "N-Glycosylation of TRPM8 Ion Channels Modulates Temperature Sensitivity of Cold Thermoreceptor Neurons." *Journal of Biological Chemistry* 287(22): 18218–29.

Peters, Jens-Uwe. 2013. "Polypharmacology–Foe or Friend?" *Journal of medicinal chemistry* 56(22): 8955–71.

De Petrocellis, Luciano et al. 2007. "Regulation of Transient Receptor Potential Channels of Melastatin Type 8 (TRPM8): Effect of CAMP, Cannabinoid CB1 Receptors and Endovanilloids." *Experimental cell research* 313(9): 1911–20.

———. 2008. "Plant-Derived Cannabinoids Modulate the Activity of Transient Receptor Potential Channels of Ankyrin Type-1 and Melastatin Type-8." *Journal of Pharmacology and Experimental Therapeutics* 325(3): 1007–15.

Pettersen, Eric F et al. 2004. "UCSF Chimera—a Visualization System for Exploratory Research and Analysis." *Journal of computational chemistry* 25(13): 1605–12.

Piñero, Janet et al. 2016. "DisGeNET: A Comprehensive Platform Integrating Information on Human Disease-Associated Genes and Variants." *Nucleic acids research*: gkw943.

Planells-Cases, Rosa, and Thomas J Jentsch. 2009. "Chloride Channelopathies." *Biochimica et Biophysica Acta (BBA)-Molecular Basis of Disease* 1792(3): 173–89.

Posner, Bruce A. 2005. “High-Throughput Screening-Driven Lead Discovery: Meeting the Challenges of Finding New Therapeutics.” *Current opinion in drug discovery & development* 8(4): 487–94.

Premkumar, Louis S et al. 2005. “Downregulation of Transient Receptor Potential Melastatin 8 by Protein Kinase C-Mediated Dephosphorylation.” *Journal of Neuroscience* 25(49): 11322–29.

Prevarskaya, Natalia, Roman Skryma, and Yaroslav Shuba. 2010. “Ion Channels and the Hallmarks of Cancer.” *Trends in molecular medicine* 16(3): 107–21.

Prevarskaya, Natalia, Lei Zhang, and Greg Barritt. 2007. “TRP Channels in Cancer.” *Biochimica et Biophysica Acta (BBA)-Molecular Basis of Disease* 1772(8): 937–46.

Prince, Patricia B et al. 2004. “The Effect of Weather on Headache.” *Headache: The Journal of Head and Face Pain* 44(6): 596–602.

Proudfoot, Clare J et al. 2006. “Analgesia Mediated by the TRPM8 Cold Receptor in Chronic Neuropathic Pain.” *Current Biology* 16(16): 1591–1605.

Pushpakom, Sudeep et al. 2019. “Drug Repurposing: Progress, Challenges and Recommendations.” *Nature reviews Drug discovery* 18(1): 41–58.

Ramsay, Rona R et al. 2018. “A Perspective on Multi-Target Drug Discovery and Design for Complex Diseases.” *Clinical and translational medicine* 7(1): 1–14.

Refaie, Marwa M M, Maram El-Hussieny, and Nagwa M Zenhom. 2018. “Protective Role of Nebivolol in Cadmium-Induced Hepatotoxicity via Downregulation of Oxidative Stress, Apoptosis and Inflammatory Pathways.” *Environmental toxicology and pharmacology* 58: 212–19.

Restrepo-Angulo, Ivan, Carmen Sanchez-Torres, and Javier Camacho. 2011. “Human EAG1

Potassium Channels in the Epithelial-to-Mesenchymal Transition in Lung Cancer Cells." *Anticancer research* 31(4): 1265–70.

Rohács, Tibor, Coeli M B Lopes, Ioannis Michailidis, and Diomedes E Logothetis. 2005. "PI (4, 5) P 2 Regulates the Activation and Desensitization of TRPM8 Channels through the TRP Domain." *Nature neuroscience* 8(5): 626–34.

Rolim, Ana Luiza R et al. 2010. "Ion Channelopathies in Endocrinology: Recent Genetic Findings and Pathophysiological Insights." *Arquivos Brasileiros de Endocrinologia & Metabologia* 54(8): 673–81.

Saito, Rintaro et al. 2012. "A Travel Guide to Cytoscape Plugins." *Nature methods* 9(11): 1069.

Sarria, Ignacio, Jennifer Ling, Michael X Zhu, and Jianguo G Gu. 2011. "TRPM8 Acute Desensitization Is Mediated by Calmodulin and Requires PIP2: Distinction from Tachyphylaxis." *Journal of neurophysiology* 106(6): 3056–66.

Selescu, Tudor et al. 2013. "Camphor Activates and Sensitizes Transient Receptor Potential Melastatin 8 (TRPM8) to Cooling and Icilin." *Chemical senses* 38(7): 563–75.

Shapovalov, George et al. 2013. "Opiates Modulate Thermosensation by Internalizing Cold Receptor TRPM8." *Cell reports* 4(3): 504–15.

Silva, Darizy Flavia et al. 2015. "TRPM8 Channel Activation Induced by Monoterpenoid Rotundifolone Underlies Mesenteric Artery Relaxation." *PloS one* 10(11): e0143171.

Singhal, Seema et al. 1999. "Antitumor Activity of Thalidomide in Refractory Multiple Myeloma." *New England Journal of Medicine* 341(21): 1565–71.

Sleigh, Sara H, and Cheryl L Barton. 2010. "Repurposing Strategies for Therapeutics." *Pharmaceutical Medicine* 24(3): 151–59.

Stein, Robert J et al. 2004. “Cool (TRPM8) and Hot (TRPV1) Receptors in the Bladder and Male Genital Tract.” *The Journal of urology* 172(3): 1175–78.

Stoschitzky, Kurt et al. 2016. “Propafenone Shows Class Ic and Class II Antiarrhythmic Effects.” *Europace* 18(4): 568–71.

Szklarczyk, Damian et al. 2016. “STITCH 5: Augmenting Protein–Chemical Interaction Networks with Tissue and Affinity Data.” *Nucleic acids research* 44(D1): D380–84.

Tabur, S et al. 2015. “Role of the Transient Receptor Potential (TRP) Channel Gene Expressions and TRP Melastatin (TRPM) Channel Gene Polymorphisms in Obesity-Related Metabolic Syndrome.” *Eur Rev Med Pharmacol Sci* 19(8): 1388–97.

Tang, Zongxiang et al. 2013. “Pirt Functions as an Endogenous Regulator of TRPM8.” *Nature communications* 4(1): 1–9.

Tanoli, Ziaurrehman et al. 2021. “Exploration of Databases and Methods Supporting Drug Repurposing: A Comprehensive Survey.” *Briefings in bioinformatics* 22(2): 1656–78.

Taylor, J C, S Brauer, and M L Espir. 1981. “Long-Term Treatment of Trigeminal Neuralgia with Carbamazepine.” *Postgraduate Medical Journal* 57(663): 16–18.

Taylor, James T et al. 2008. “Calcium Signaling and T-Type Calcium Channels in Cancer Cell Cycling.” *World journal of gastroenterology: WJG* 14(32): 4984.

Thippegowda, Prabhakar B et al. 2010. “Ca2+ Influx via TRPC Channels Induces NF-KB-Dependent A20 Expression to Prevent Thrombin-Induced Apoptosis in Endothelial Cells.” *American Journal of Physiology-Cell Physiology* 298(3): C656–64.

Tikhonov, Denis B, and Boris S Zhorov. 2017. “Mechanism of Sodium Channel Block by Local Anesthetics, Antiarrhythmics, and Anticonvulsants.” *Journal of General Physiology* 149(4): 465–81.

Tran, Tu-Anh. 2017. "Muckle–Wells Syndrome: Clinical Perspectives." *Open access rheumatology: research and reviews* 9: 123.

Trott, Oleg, and Arthur J Olson. 2010. "AutoDock Vina: Improving the Speed and Accuracy of Docking with a New Scoring Function, Efficient Optimization, and Multithreading." *Journal of computational chemistry* 31(2): 455–61.

Tsavaler, Larisa, Michael H Shapero, Stan Morkowski, and Reiner Laus. 2001. "Trp-P8, a Novel Prostate-Specific Gene, Is up-Regulated in Prostate Cancer and Other Malignancies and Shares High Homology with Transient Receptor Potential Calcium Channel Proteins." *Cancer research* 61(9): 3760–69.

Ulăreanu, Roxana et al. 2017. "N-Glycosylation of the Transient Receptor Potential Melastatin 8 Channel Is Altered in Pancreatic Cancer Cells." *Tumor Biology* 39(10): 1010428317720940.

Vaeth, Martin, and Stefan Feske. 2018. "Ion Channelopathies of the Immune System." *Current opinion in immunology* 52: 39–50.

Vahabi, Bahareh et al. 2013. "TRPM8 Agonists Modulate Contraction of the Pig Urinary Bladder." *Canadian journal of physiology and pharmacology* 91(7): 503–9.

Valero, Maria, Cruz Morenilla-Palao, Carlos Belmonte, and Felix Viana. 2011. "Pharmacological and Functional Properties of TRPM8 Channels in Prostate Tumor Cells." *Pflügers Archiv-European Journal of Physiology* 461(1): 99–114.

Veliz, Luis A et al. 2010. "Near-Membrane Dynamics and Capture of TRPM8 Channels within Transient Confinement Domains." *PLoS One* 5(10): e13290.

Venkatachalam, Kartik, and Craig Montell. 2007. "TRP Channels." *Annu. Rev. Biochem.* 76: 387–417.

Vetter, Irina, and Richard J Lewis. 2011. "Natural Product Ligands of TRP Channels." *Transient receptor potential channels*: 41–85.

Viana, Félix. 2011. "Chemosensory Properties of the Trigeminal System." *ACS chemical neuroscience* 2(1): 38–50.

Vinuela-Fernandez, Ignacio et al. 2014. "The TRPM8 Channel Forms a Complex with the 5-HT1B Receptor and Phospholipase D That Amplifies Its Reversal of Pain Hypersensitivity." *Neuropharmacology* 79: 136–51.

Wakap, Stéphanie Nguengang et al. 2020. "Estimating Cumulative Point Prevalence of Rare Diseases: Analysis of the Orphanet Database." *European Journal of Human Genetics* 28(2): 165–73.

Wang, Zhiguo. 2004. "Roles of K+ Channels in Regulating Tumour Cell Proliferation and Apoptosis." *Pflügers Archiv* 448(3): 274–86.

Van de Water, A et al. 1988. "Pharmacological and Hemodynamic Profile of Nebivolol, a Chemically Novel, Potent, and Selective Beta 1-Adrenergic Antagonist." *Journal of cardiovascular pharmacology* 11(5): 552–63.

Weil, Annette et al. 2005. "Conservation of Functional and Pharmacological Properties in the Distantly Related Temperature Sensors TRPV1 and TRPM8." *Molecular pharmacology* 68(2): 518–27.

Wermuth, Camille G. 2006. "Selective Optimization of Side Activities: The SOSA Approach." *Drug discovery today* 11(3–4): 160–64.

Wishart, David S et al. 2018. "DrugBank 5.0: A Major Update to the DrugBank Database for 2018." *Nucleic acids research* 46(D1): D1074–82.

Wondergem, Robert et al. 2008. "HGF/SF and Menthol Increase Human Glioblastoma Cell

Calcium and Migration." *Biochemical and biophysical research communications* 372(1): 210–15.

Wondergem, Robert, and Jeremy W Bartley. 2009. "Menthol Increases Human Glioblastoma Intracellular Ca 2+, BK Channel Activity and Cell Migration." *Journal of biomedical science* 16(1): 1–7.

Xing, Hong et al. 2007. "TRPM8 Mechanism of Cold Allodynia after Chronic Nerve Injury." *Journal of Neuroscience* 27(50): 13680–90.

Xiong, Mingmei et al. 2016. "TRPM8 Genetic Variations Associated with COPD Risk in the Chinese Han Population." *International journal of chronic obstructive pulmonary disease* 11: 2563.

Xu, Lizhen et al. 2020. "Molecular Mechanisms Underlying Menthol Binding and Activation of TRPM8 Ion Channel." *Nature communications* 11(1): 1–13.

Yajuan, Xiao, Liang Xin, and Li Zhiyuan. 2012. "A Comparison of the Performance and Application Differences between Manual and Automated Patch-Clamp Techniques." *Current chemical genomics* 6: 87.

Yamamoto, Shota, Nobuaki Egashira, Makoto Tsuda, and Satohiro Masuda. 2018. "Riluzole Prevents Oxaliplatin-Induced Cold Allodynia via Inhibition of Overexpression of Transient Receptor Potential Melastatin 8 in Rats." *Journal of pharmacological sciences* 138(3): 214–17.

Yamamura, Hisao et al. 2008. "TRPM8 Activation Suppresses Cellular Viability in Human Melanoma." *American Journal of Physiology-Cell Physiology* 295(2): C296–301.

Yee, Nelson S et al. 2014. "Aberrantly Over-Expressed TRPM8 Channels in Pancreatic Adenocarcinoma: Correlation with Tumor Size/Stage and Requirement for Cancer Cells

Invasion." *Cells* 3(2): 500–516.

———. 2016. "TRPM8 Ion Channels as Potential Cancer Biomarker and Target in Pancreatic Cancer." *Advances in protein chemistry and structural biology* 104: 127–55.

Yue, Tian-Li et al. 1992. "Carvedilol, a New Vasodilator and Beta Adrenoceptor Antagonist, Is an Antioxidant and Free Radical Scavenger." *Journal of Pharmacology and Experimental Therapeutics* 263(1): 92–98.

Zhang, Jing-Jing, Qin-Ming Zhou, Sheng Chen, and Wei-Dong Le. 2018. "Repurposing Carbamazepine for the Treatment of Amyotrophic Lateral Sclerosis in SOD1-G93A Mouse Model." *CNS neuroscience & therapeutics* 24(12): 1163–74.

Zhang, Lei, and Gregory John Barritt. 2004. "Evidence That TRPM8 Is an Androgen-Dependent Ca2+ Channel Required for the Survival of Prostate Cancer Cells." *Cancer research* 64(22): 8365–73.

Zhang, Xuming et al. 2012. "Direct Inhibition of the Cold-Activated TRPM8 Ion Channel by Gα Q." *Nature cell biology* 14(8): 851–58.

Zhao, Xiao et al. 2016. "Inducing Enhanced Immunogenic Cell Death with Nanocarrier-Based Drug Delivery Systems for Pancreatic Cancer Therapy." *Biomaterials* 102: 187–97.

Zoete, Vincent, Antoine Daina, Christophe Bovigny, and Olivier Michielin. 2016. "SwissSimilarity: A Web Tool for Low to Ultra High Throughput Ligand-Based Virtual Screening."

Zuo, Xiaozhuo, Jennifer X Ling, Guang-Yin Xu, and Jianguo G Gu. 2013. "Operant Behavioral Responses to Orofacial Cold Stimuli in Rats with Chronic Constrictive Trigeminal Nerve Injury: Effects of Menthol and Capsazepine." *Molecular pain* 9:

1744–8069.